5-29-2020 10:30 AM

Investigating the Role of Carbon Stress in the Mortality of Tamarack Seedlings Under a Warming Environment

Bridget K. Murphy, *The University of Western Ontario*

Supervisor: Way, Danielle A., *The University of Western Ontario*

A thesis submitted in partial fulfillment of the requirements for the Master of Science degree in Biology

Abstract

Climate warming is increasing the frequency of climate-induced tree mortality events. While drought combined with heat is considered the primary cause of this tree mortality, little is known about whether high temperatures alone can induce mortality, or whether rising CO_2 will increase survival. I grew tamarack in two experiments combining warming (0-8 ˚C above ambient) and CO_2 (400-750 ppm) to investigate whether high growth temperatures led to carbon limitations and mortality. Using glasshouses, +8 ˚C warming with ambient CO_2 (8TAC) led to 40% mortality despite thermal acclimation of respiration. Dying 8TAC seedlings had lower needle carbon concentrations and lower ratios of photosynthesis to respiration, indicating carbon limitation. Using growth chambers, no seedlings died, and carbon flux results contradicted those of the glasshouses. Overall, environmental conditions in the glasshouses were more representative of the field than growth chamber conditions, and my work highlights that warming can directly induce mortality.

Keywords

Climate change, tree mortality, *Larix laricina*, carbon starvation, acclimation, photosynthesis, respiration, temperature

Summary for Lay Audience

Trees will be negatively impacted by warming caused by climate change and may be less able to fix enough carbon from the atmosphere to maintain growth or even survive. Previous studies have found that plants can adjust their physiology (i.e. acclimation) to respond to long-term changes in temperature and CO_2. Under ideal circumstances, acclimation helps plants deal with climate stress by maximizing carbon gain and minimizing carbon loss, thereby maintaining growth and tree health. However, the number of climate-induced tree mortality events has been increasing as the climate warms. Tree die-offs have been linked to a combination of drought and heat stress, but whether heat stress alone can result in mortality has received little attention. I investigated whether high growth temperatures would cause carbon stress and mortality in tamarack, a common tree in Canada's northern forests. I grew tamarack in two experiments (using either glasshouses or growth chambers) with warming (of up to 8 ˚C) and high CO_2 (up to 750 ppm) to simulate future climate scenarios. In the glasshouses, seedlings reduced carbon losses through acclimation, but carbon gain was unresponsive to warming. The +8 ˚C warming with ambient CO_2 led to 40% mortality, which correlated with low needle carbon concentrations and low ratios of carbon gain to carbon loss. The growth chamber experiment was designed as a follow-up to measure a greater number of seedlings, but surprisingly there was no mortality in this study. As well, growth chamber seedlings increased carbon gain with warming, but carbon losses were unaffected, the opposite of what I saw in the glasshouse. For both experiments, high CO_2 stimulated carbon gain, which offset mortality in the glasshouses. The glasshouse experiment was more similar to conditions experienced in the field (e.g. natural light and daily temperature changes). I therefore argue that tamarack will have strong acclimation to warming (resulting in lower carbon loss) paired with stimulated carbon gain under high CO_2. While warming alone induced carbon limitations and subsequent mortality in seedlings, carbon gain associated with high CO_2 will likely offset carbon stress in the future.

Co-Authorship Statement

Chapter 2 is a version of a manuscript that has been submitted. I am the first author and Danielle A. Way (DAW) is the co-author. DAW designed the experiment, DAW and I discussed the best method of data collection, I collected and analyzed the data, I wrote the manuscript with input and editing from DAW.

Chapter 3 is exclusively a chapter for my thesis. DAW and I designed the experiment, DAW and I discussed the best method of data collection, Andre G. Duarte (AGD) and I collected the data, I analyzed the data, and I wrote the chapter with input and editing from DAW.

Acknowledgments

First of all, I thank my supervisor Dr. Danielle Way, who has given me all the opportunities I could have asked for. She was endlessly supportive as I navigated most of my Masters either pregnant or with a baby at home. When I grow up, I want to be you.

I also thank my husband, Nick Boehler, for giving me constant encouragement, emotional support, and taking such good care of our son while also completing his Masters. Thanks also go to my son, who was my sidekick in utero throughout my growth chamber experiment, and always reminds me why climate change research is so important. I am also very grateful for the endless support from my parents and my mother-in-law.

I was very lucky to start my academic journey in a lab with so many kind individuals who taught me the ins and outs of experimental design, gas exchange measurements and statistical analyses. Thank you to: Dr. Joseph Stinziano, who has always been both a mentor and a friend to me; Dr. Eric Dusenge, who brought me along on my first field campaign and taught me everything I know about LICORs; Dr. Andre Duarte, who showed me the beauty of graphing with R and always makes me laugh; and Joshua Frank-Webb, who taught me all about fungi and heat shock proteins. I also need to thank the volunteers who were always happy to lend a hand: Kristyn Bennett, Julianne Radford, and Andrew Cook.

Special thanks go to my advisory committee members, Dr. Mark Bernards and Dr. Brent Sinclair, for their guidance in designing my experiment and for always asking the tough (but important) questions.

Lastly, I am grateful to all the funding sources of Dr. Danielle Way's research program and the Ontario Graduate Scholarship for financially supporting me through my MSc.

Table of Contents

List of Tables

List of Figures

List of Abbreviations

AC = Ambient CO_2

A_{25} = Net CO_2 assimilation rates measured at 400 ppm CO_2 and 25 ˚C

A_{400} = Net CO_2 assimilation rates measured at 400 ppm CO_2

A_c = Photosynthesis limited by Rubisco carboxylation

Acetyl-CoA = Acetyl coenzyme A

A_{growth} = Net CO_2 assimilation rates at growth conditions

$A_{growth\text{-}seedling\text{-}day}$ = Daily net CO_2 assimilation rates at growth conditions per seedling

A_j = Photosynthesis limited by RuBP regeneration

A_{net} = Net CO_2 assimilation rates

A_p = Photosynthesis limited by triose-phosphate availability

A/R_{25} = Ratio of photosynthesis to respiration at 400 ppm CO_2 and 25 ˚C

A/R_{growth} = Ratio of photosynthesis to respiration at growth conditions

$A_{seedling}$ = Net CO_2 assimilation rates at growth conditions per seedling

ATP = Adenosine triphosphate

$Biomass_{root}$ = Root biomass of a seedling

$Biomass_{root/shoot}$ = Ratio of root to shoot biomass

$Biomass_{total}$ = Total biomass of a seedling

C = Carbon

C_a = Atmospheric CO_2 concentration

CH_4 = Methane

C_i = Intracellular CO_2 concentration

C_i/C_a = Ratio of intracellular to atmospheric CO_2

$C_i/C_{a\text{-}25}$ = Ratio of intracellular to atmospheric CO_2 at 400 ppm CO_2 and 25 ˚C

$C_i/C_{a\text{-}growth}$ = Ratio of intracellular to atmospheric CO_2 at growth conditions

CO_2 = Carbon dioxide

$C_{seedling}$ = Whole plant carbon uptake

e^- = Electron

E = Transpiration rates

E_{25} = Transpiration rates measured at 400 ppm CO_2 and 25 ˚C

E_{growth} = Transpiration rates measured at growth conditions

EC = Elevated CO_2

ETC = Electron transport chain

$FADH_2$ = Flavin adenine dinucleotide

Fd = Ferredoxin

GHG = Greenhouse gases

g_s = Stomatal conductance

$g_{s\text{-}25}$ = Stomatal conductance measured at 400 ppm CO_2 and 25 ˚C

$g_{s\text{-}400}$ = Stomatal conductance measured at 400 ppm CO_2

$g_{s\text{-}growth}$ = Stomatal conductance measured under growth conditions

G3P = Glyceraldehyde-3-phosphate

H^+ = Proton

IPCC = Intergovernmental Panel on Climate Change

J_{max} = Maximum rate of electron transport

$J_{max\text{-}growth}$ = Maximum rate of electron transport at growth conditions

$J_{max\text{-}growth}/V_{cmax\text{-}growth}$ = Ratio of the maximum rate of electron transport to the maximum rate of Rubisco carboxylation at growth conditions

$J_{max\text{-}25}$ = Maximum rate of electron transport at 400 ppm CO_2 and 25 ˚C

$J_{max\text{-}25}/V_{cmax\text{-}25}$ = Ratio of the maximum rate of electron transport to the maximum rate of Rubisco carboxylation at 400 ppm CO_2 and 25 ˚C

LA = Leaf area

$LA_{seedling}$ = Total leaf area for a whole seedling

LMA = Leaf mass per unit area (LMA)

N = Nitrogen

NADH = Nicotinamide adenosine diphosphate hydrogen

NADPH = Nicotinamide adenine dinucleotide phosphate hydrogen

$NADP^+$ = Nicotinamide adenine dinucleotide phosphate

NPP = Net primary production

NSC = Non-structural carbohydrates

N_2O = Nitrous oxide

O_2 = Oxygen

PSI = Photosystem I

PSII = Photosystem II

Q_{10} = Proportional change in respiration per 10 ˚C change in temperature

$Q_{10\text{-}shoot}$ = Proportional change in shoot respiration per 10 ˚C change in temperature

R = Replicate

RCP = Representative concentration pathways

R_{dark} = Dark respiration rate

R_{growth} = Dark respiration rate measured under growth conditions

RH = Relative humidity

R_{root} = Dark respiration rate of root tissue

R_{shoot} = Dark respiration rate of shoot tissue

$R_{shoot-25}$ = Dark respiration rate at 25 ˚C

$R_{shoot-growth}$ = Dark respiration rate of shoots at growth temperature

$R_{shoot-seedling}$ = Dark respiration rate of shoots at growth temperature per seedling

$R_{shoot-seedling-day}$ = Daily dark respiration rate of shoots at growth temperature per seedling

$R_{root-growth}$ = Dark respiration rate of roots at growth temperature

$R_{root-seedling}$ = Dark respiration rate of roots at growth temperature per seedling

$R_{root-seedling-day}$ = Daily dark respiration rate of roots at growth temperature per seedling

Rubisco = Ribulose-1,5-bisphosphate carboxylase/oxygenase

RuBP = Ribulose-1,5-bisphosphate

T_m = Measurement temperature

T_{opt} = Temperature optimum of photosynthesis

$T_{opt-400}$ = Temperature optimum of photosynthesis measured at 400 ppm CO_2

$T_{opt-growth}$ = Temperature optimum of photosynthesis measured at growth conditions

TPU = Triose-phosphate utilization

V_{cmax} = Maximum rate of Rubisco carboxylation

$V_{cmax-25}$ = Maximum rate of Rubisco carboxylation at 400 ppm CO_2 and 25 ˚C

$V_{cmax-growth}$ = Maximum rate of Rubisco carboxylation at growth conditions

VPD = Vapour pressure deficit

%C = Needle percent carbon

%N = Needle percent nitrogen

0T = Ambient temperature

4T = +4 ˚C warming above 0T

8T = +8 ˚C warming above 0T

Chapter 1

1 General Introduction

1.1 Climate Change

Despite the warnings of scientists, greenhouse gas (GHG) emissions continue to increase and contribute to global warming. The main GHG emissions include carbon dioxide (CO_2), methane (CH_4) and nitrous oxide (N_2O). Since the pre-Industrial era, there have been significant increases in GHGs due to fossil fuel burning and land use change (IPCC, 2014). Pre-Industrial CO_2 concentrations have been estimated at ~280 ppm, while the highest CO_2 values seen in the past 420,000 years have reached only ~300 ppm (Petit et al., 2013). But atmospheric CO_2 is currently rising at a rate of 2.0 ppm/year, leading to a current CO_2 concentration of 413 ppm (NOAA, 2020). If GHG emissions continue at current rates, we will see substantially higher CO_2 concentrations and significant warming in the decades to come.

The Fifth Assessment report by the Intergovernmental Panel on Climate Change (IPCC) outlined four future scenarios depending on socioeconomic trajectory and mitigation of GHG emissions, referred to as Representative Concentration Pathways (RCPs) (IPCC, 2014). We are currently on the "business as usual" trajectory, i.e. if GHG emissions continue at current rates. The "business as usual" trajectory is referred to as RCP8.5 and represents very high GHG emissions. Under RCP8.5, the IPCC has predicted mean global temperatures will rise 2.6-4.8 ˚C by the years 2081-2100. However, it is important to note that this warming will not be uniform across all latitudes. Higher latitudes are expected to experience greater warming than the tropics (IPCC, 2014; Serreze et al., 2000). Northern latitudes, which encompass the North American boreal forest, can expect to see warming of mean annual temperatures up to 8 ˚C by 2100. The faster warming rate projected in high northern latitudes has been hypothesized to be due to shifts in atmospheric circulation, the large-scale movement of air, and therefore heat, around the earth (Serreze et al., 2000). Disproportionate movement of air to higher latitudes coupled with atmospheric warming is thus driving a more severe temperature shift near the poles

(Byrne & Schneider, 2018). Warming will also not be uniform seasonally or diurnally. Warming is projected to be more pronounced in the winter than the summer and at night than during the day, which could affect boreal productivity year-round (IPCC, 2014; Kreyling et al. 2019).

There have already been observable changes in plants living in northern latitudes in response to on-going climate change. For example, terrestrial net primary production (NPP) of these latitudes has increased as moderate warming has resulted in longer growing seasons due to earlier spring thaw (Barichivich et al., 2013; Danielewska, Urbaniak, & Olejnik, 2015; Randerson, Field, Fung, & Tans, 1999). While small increases in temperature can be beneficial to plants, we must also consider how larger increases can be detrimental to vegetation and how this will impact our biomes.

1.2 The Boreal Forest

The boreal forest biome is the largest land-based biome in the world, spanning the high latitudes of North America, northern Europe and Asia. The boreal biome provides many ecological and economic services. The forest industry contributes billions of dollars every year to the Canadian economy through wood and paper production, making it of great economic importance (Gauthier, Bernier, Kuuluvainen, Shvidenko, & Schepaschenko, 2015). The boreal forest also acts as a habitat for many animals. Arguably, the most important ecosystem service of this biome is carbon (C) sequestration. The entire boreal biome stores ~800 Gt C in biomass, soil, peat and detritus C pools (Apps et al., 1993). The Canadian boreal forest alone stores 186 Gt C and takes up 62 Mt of atmospheric CO_2 each year (Kurz et al., 2013). Carbon sequestration by vegetation mitigates the amount of CO_2 added to the atmosphere annually from anthropogenic sources, and therefore slows down climate change (Dusenge, Duarte, & Way, 2019). For boreal forests to continue to serve as sinks for atmospheric C, boreal trees will need to maintain positive C balances by taking up more CO_2 for photosynthesis than the amount of CO_2 they release through respiration as temperatures increase.

The boreal region is primarily composed of forests, wetlands and lakes (Apps et al., 1993). The boreal forest of North America is mainly dominated by cold-tolerant

coniferous (cone-bearing) trees, such as *Picea glauca, Picea mariana, Larix larcina, Abies balsamea,* and *Pinus banksiana* (Brandt, 2009). Deciduous broad-leaved trees, such as *Populus tremuloides* and *Betula papyrifera,* also co-occur with these conifers. Boreal biomes experience high seasonal temperature variation and relatively low annual rainfall compared to other forest regions (Bonan & Shugart, 1989). Low soil temperatures limit nutrient availability, as mineralization of bound nutrients is dictated by microbial activity, which increases with warming (Nedwell, 1999). Permafrost, which underlays 40-50% of Canada, can also limit nutrient uptake by restricting the rooting zones of trees (Lawrence & Oechel, 1983; Yuan & Chen, 2010). Variable soil moisture drives community composition of different sites across Canada, as boreal species prefer different levels of soil moisture (Bonan & Shugart, 1989). For example, *Picea mariana* (black spruce) and *Larix laricina* (tamarack) favour wetter sites, whereas *Picea glauca* (white spruce) favours drier sites. While the *Larix* genus (Larch) is distributed across the boreal biome, tamarack is found only in North America's boreal forests.

1.2.1 Tamarack, a Deciduous Conifer

Tamarack is a deciduous conifer native to North America, widely distributed in the boreal forest from the northern United States to northern Canada (Brandt, 2009). Across the boreal forest, tamarack dominates wetlands, disturbed forest edges and woodland zones north of evergreen-dense areas (Gower & Richards, 1990). Overall, conifers are well suited for the boreal biome as they are cold-tolerant and efficient in their use of nutrients and water (Gower & Richards, 1990), important traits in a place where nutrient availability is low. Evergreen conifers are well equipped for harsh conditions because of their early investment into needle longevity, ultimately resulting in lower C and nutrient requirements later (Reich, Rich, Lu, Wang, & Oleksyn, 2014). So, what makes a deciduous conifer such as tamarack widespread across the North American boreal forest?

With the rapid rate of global warming, northern trees are unlikely to be able to adapt to future climates, but phenotypic plasticity could facilitate their survival (Kramer, 1995). Phenotypic plasticity is defined as "the range of phenotypes a single genotype can express as a function of its environment" (Nicotra et al., 2010). Deciduous conifers are considered to be more phenotypically plastic than evergreens, as they produce new

needles each spring. This allows them to utilize the “live fast, die hard” strategy of producing larger, cheaper needles that do not need to withstand winter desiccation (Gower & Richards, 1990). Greater investment in larger needles leads to higher rates of C uptake in larch species than in co-occurring evergreen conifers (Gowin, Lourtioux, & Mousseau, 1980; Kloeppel, Gower, Vogel, & Reich, 2000; Reich, Kloeppel, Ellsworth, & Walters, 1995). Larch species also have higher nitrogen-use-efficiency than evergreen species and have 25-49% greater leaf nitrogen (N) concentrations in their needles compared to evergreen needles (Gower & Richards, 1990). The trade-off of having higher rates of C uptake and leaf N are that deciduous species also have higher rates of C losses through shoot respiration (Reich et al., 1998), findings which have been supported in tamarack (Tjoelker, Oleksyn, & Reich, 1998; Tjoelker, Oleksyn, & Reich, 1999a; Islam & Macdonald, 2005). Larch species also have lower water-use-efficiency than evergreens, which is why they favour wetlands (Gower & Richards, 1990). Tree C, water and N relations will be affected by climate change and the phenotypic plasticity of larch could be advantageous for survival of this species in a changing climate. Understanding the response of tamarack to increasing temperatures and CO_2 will help to predict the future growth and C sequestration potential of a major component of the Canadian boreal forest.

1.2.2 Future Canadian Boreal Forest: C Sink or C Source?

A major question is whether boreal forests will shift from being C sinks, as they currently are, to C sources with global warming. A large proportion of Canadian boreal C is accumulated in peatlands, soil, and permafrost deposits, with the rest residing in living plant biomass (Bradshaw & Warkentin, 2015). With warming, permafrost loss and subsequent soil respiration rates are increasing, leading to greater amounts of C being released into the atmosphere (Bond-Lamberty & Thomson, 2010). Through modelling of mean C flux estimates, it is predicted that the Canadian boreal forest will shift from a C sink to C source by the end of 2100 (Bradshaw & Warkentin, 2015; Metsaranta, Kurz, Neilson, & Stinson, 2010; Miquelajauregui, Cumming, & Gauthier, 2019). Global vegetation models expect decreases in forest productivity and increases in soil decomposition, leading to overall greater C losses from the boreal ecosystem with

increases in temperature. However, the response of modelled boreal C gains to climate change could be positive or negative depending on the severity of warming considered.

Small shifts in temperature can increase the length of the growing season and therefore increase net primary production (Beck et al., 2011; Danielewska et al., 2015; Richardson et al., 2018), but large shifts in temperature make plants more susceptible to mortality (Allen et al., 2010). There is already evidence of decreasing C uptake in boreal trees with a mean temperature increase of 1.5 ˚C (IPCC, 2014). The Canadian boreal forest C sink was reduced by half from 1990-1997 to 2000-2007, largely due to high tree mortality rates driven by climate change (Pan et al., 2011). Additionally, increases in temperature will not be equally matched with increases in precipitation, leading to greater vapour pressure deficits (VPD; IPCC 2014) and more frequent droughts (McDowell et al., 2016), both of which lead to greater water stress on forests.

1.3 Tree Mortality

In 2010, there were 88 large-scale documented cases of mortality linked to climate change globally (Allen et al., 2010) and this number has only increased since then (Aleixo et al., 2019; Allen, Breshears, & McDowell, 2015; Zhang, Shao, Jia, & Wei, 2017). Climatic stresses, such as warming and high VPD, make trees susceptible to forest fires and insect outbreaks, which are often the final cause of death (Adams et al., 2017). It has been estimated that 12% of global biomass C losses were caused by tree death from the years 2001-2014 (Pugh, Arneth, Kautz, Poulter, & Smith, 2019). Tree mortality will have large effects on terrestrial C pools over time. The boreal forest of Canada, as described above, has already seen reductions in overall C pools, as well as increases in the mortality rates of four common tree species (*Populus tremuloides*, trembling aspen; *Pinus banksiana*, jack pine; black spruce; and white spruce; Peng et al., 2011). A meta-analysis by Zhang et al. (2017) found that gymnosperms, including conifers, have higher mortality (7.1%) compared to angiosperms (4.8%) due to climate change stressors, with the differences in mortality deriving from the relative abilities of these two plant groups to mitigate climatic stress.

1.3.1 Main Abiotic Causes of Mortality

The two main hypotheses for climate change-related abiotic tree mortality are hydraulic failure and C starvation (Anderegg, Berry, & Field, 2012; Wiley, Hoch, & Landhäusser, 2017; Sevanto et al., 2014; Zhang et al., 2017; Adams et al., 2017; Meir, Mencuccini, & Dewar, 2015). Hydraulic failure and C starvation are both hypothesized to occur as a result of water stress driven by global warming. Elevated temperatures in the spring and summer increase VPD and decrease soil moisture, creating water demands that plants cannot meet, leading to mortality via a loss of xylem conductivity (hydraulic failure) or a depletion of internal C pools (C starvation; Williams et al., 2013).

1.3.2 Hydraulic Failure

Hydraulic failure occurs when rates of transpiration are greater than root water uptake rates, leading to xylem cavitation (Sevanto et al., 2014). Drought-induced tree death is therefore caused by irreparable damage to xylem and phloem transport (Anderegg et al., 2012). As such, hydraulic failure can be characterized by rapid declines in leaf water potential and low hydraulic conductivity at the point of death. Before this point, cavitation of the xylem is repairable if soil moisture is restored, transpiration is reduced, and/or available carbohydrates are used to lower the osmotic potential of xylem cells (Anderegg et al., 2012). Coordination between xylem and phloem tissues is critical for the movement of hormones, water, and carbohydrates throughout the tree. Hydraulic failure is the main cause of drought-induced die-offs of trembling aspen and woodland conifers in the USA (Gitlin et al., 2006; Worrall et al., 2008). However, water conservation strategies that can decrease the chance of hydraulic failure can negatively impact survivability by diminishing carbohydrate pools required for repairs.

1.3.3 Carbon Starvation: An Overview

Carbon starvation occurs when plants close their stomata under high VPD and drought stress to conserve water, reducing C gain through photosynthesis. Because respiratory losses remain high, especially under elevated temperatures, this creates a negative C balance where plants use more C than they gain. Under stress, plants will use stored C pools to buffer negative C balances and fuel metabolism (Sala, Woodruff, & Meinzer,

2012). Carbon starvation is therefore characterized by low carbohydrate reserves with minimal changes to leaf and xylem water potentials (Sevanto et al., 2014). Under climatic stress, trees with high C reserves are therefore more likely to survive (Dietze et al., 2014; Sala et al., 2012). However, negative C balances can be sustained by stored C for only short durations.

Allen et al. (2015) characterized the cause of recorded tree mortality events related to climate change as a combination of both hydraulic failure and C starvation. While C starvation is often in response to water stress, temperature alone may also be able to drive a C budget imbalance. Carbon fluxes are temperature-sensitive: photosynthetic C gain has a unimodal response to changes in leaf temperature, whereas respiration increases exponentially with increasing leaf temperatures (Sage & Kubien, 2007; Atkin, Millar, & Day, 2000). The high respiratory costs of warming can be observed through decreased C pools in plants that cannot replenish these C pools effectively. All tissue types (e.g. leaves, stems and roots) respire, but photosynthesis is limited to foliar and stem tissue, and the ratio of leaves to other tissues often decreases as plants grow (Dietze et al., 2014). Seedlings are also more vulnerable to C budget imbalances due to relatively small soluble C pools (Dietze et al., 2014).

In studies that aim to study C stress, seedlings are often grown under shade to reduce C gain and photosynthetic rates are not measured (Wiley et al., 2017). Wiley et al. (2017) found that the survival times of aspen seedlings decreased with increasingly opaque shade treatments (lower C gain) and increased warming treatments (from 20 ˚C to 28 ˚C; higher C losses). Shoot respiration rates were 41% higher under warming and C pools were depleted, leading to shorter survival times (Wiley et al., 2017). Although some researchers have used shade to induce C stress, there is a lack of studies on C starvation under ecologically relevant experimental designs where C gains are also being considered.

Most of the current research done on boreal tree species has been conducted on either evergreen conifers or deciduous broad-leaved trees, leaving a gap in our knowledge of deciduous conifers (Hartmann, Ziegler, & Trumbore, 2013; Mantgem et al., 2009; Peng

et al., 2011; Wiley et al., 2017). Compared to other deciduous trees, larch species have small C pools, similar to evergreen conifers (Hoch, Richter, & Korner, 2003). However, larch species also have lower water use efficiency than evergreen conifers, which, when combined with low C storage, may put them at a disadvantage for combating C stress compared to other Canadian boreal tree species (Gower & Richards, 1990). Understanding the vulnerability of tamarack to climatic stressors will help predict the future community composition of the boreal forest.

1.4 Carbon Fluxes

The sugars available for plant development and metabolism are ultimately determined by the C balance of plants, specifically the relative rates of photosynthesis and respiration. A positive C balance refers to when the amount of sugars produced through photosynthesis is greater than the use of these sugars for metabolism and growth, resulting in storage of unused sugars (Sala et al., 2012). The opposite is a negative C balance, when the use of sugars for metabolism is greater than the production by photosynthesis and stored C pools are depleted. If a positive C balance cannot be reached and all stored sugars are used, C starvation will occur. To understand how warming can affect the C balances of plants, we first need to understand the fundamentals of photosynthesis, specifically C_3 photosynthesis.

1.4.1 C_3 Photosynthesis

Photosynthesis is the process by which plants convert light energy into sugars using CO_2 and water (Atkin et al., 2000). Photosynthesis can be broken down into two main components: light-dependent reactions, also referred to as the photosynthetic electron transport chain (ETC), and light-independent reactions, referred to as the Calvin-Benson cycle (Taiz & Zeiger, 2010; Figure 1.1). Both processes take place in chloroplasts, with the ETC operating in the thylakoid membrane. The light-dependent reactions start when photosystem II (PSII) absorbs a 680 nm wavelength photon and uses it to excite chlorophyll in the reaction center of PSII. When excited, PSII becomes unstable and transfers an electron (e^-) to oxidized pheophytin through a process known as charge separation. The oxygen evolving complex (OEC) oxidizes water into oxygen (O_2)

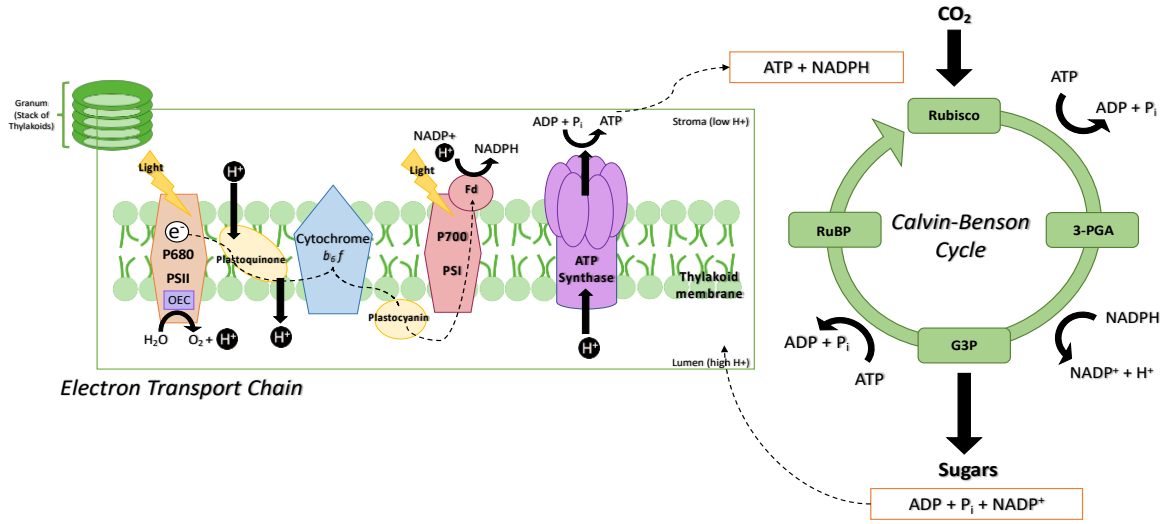

Figure 1.1. Simplified schematic of photosynthesis. Light energy is absorbed by photosystem II (PSII) and used to excite chlorophyll in the reaction center. An electron (e^-) is lost from PSII to a close-by electron acceptor, pheophytin. The e^- moves through the electron transport chain along a decreasing redox potential until it is reenergized at photosystem I (PSI) to create NADPH (nicotinamide adenine dinucleotide phosphate hydrogen). ATP (adenosine triphosphate) is also produced by ATP synthase using an electrochemical gradient produced by the H^+ gradient across the thylakoid membrane. This e^- is replaced with an e^- from the oxidation of water at the OEC. The products of the electron transport chain are then used by the Calvin-Benson cycle to fix CO_2, produce sugars and regenerate RuBP. P680, primary electron donor for PSII; P700, primary electron donor for PSI; H^+, proton; ADP, adenosine diphosphate; P_i, inorganic phosphate; NADP+, nicotinamide adenine dinucleotide phosphate; Rubisco, Ribulose-1,5-bisphosphate carboxylase/oxygenase; 3-PGA, 3-phosphoglycerate; G3P, glyceraldehyde-3-phosphate; RuBP, Ribulose-1,5-bisphosphate. Redrawn and modified from Taiz and Zeiger (2010).

replacing the electron in chlorophyll, and also generates a proton (H^+). The e^- initially transferred from chlorophyll is then transferred along the ETC through a series of oxidation-reductions involving plastoquinone, cytochrome b_6f, and plastocyanin, until it reaches photosystem I (PSI). PSI absorbs a 700 nm photon, creating the redox potential needed to reduce $NADP^+$ (nicotinamide adenine dinucleotide phosphate) to NADPH (nicotinamide adenine dinucleotide phosphate hydrogen) by the action of ferredoxin (Fd). The oxidation of water and the transfer of e^-s from plastoquinone to cytochrome b_6f transports H^+ molecules into the thylakoid lumen. This acidification of the thylakoid lumen creates an electrochemical potential gradient which drives an ATP (adenosine triphosphate) synthase, producing ATP in the stroma. The products from the light-dependent reactions, ATP and NADPH, are then utilized by the Calvin-Benson cycle.

In the Calvin-Benson cycle, CO_2 is fixed by the enzyme Ribulose-1,5-bisphosphate carboxylase/oxygenase (Rubisco) to ribulose-1,5-bisphosphate (RuBP), forming 3-phosphoglycerate (3-PGA). The 3-PGA molecules are first phosphorylated using ATP, and then undergoes a reduction using NADPH to form two molecules of glyceraldehyde-3-phosphate (G3P). The G3P molecules are then utilized in two ways: to make glucose (which requires two G3P molecules per glucose) and to regenerate RuBP to continue the Calvin-Benson cycle (which requires ten G3P molecules). The regeneration of RuBP also requires additional ATP.

The Calvin-Benson cycle relies on the enzyme Rubisco for the initial carboxylation step. Rubisco is a dual function enzyme capable of both carboxylation (the fixation of CO_2 to RuBP) or oxygenation (the fixation of O_2 to RuBP) depending on which molecule the active site binds. The process of RuBP oxygenation is referred to as photorespiration (Miziorko & Lorimer, 1983). In the photorespiratory pathway, RuBP is oxygenated to form one 2-phosphoglycolate molecule and one molecule of 3-PGA (Peterhansel et al., 2010). The 2-phosphoglycolate is then converted back into 3-PGA through a series of steps that require ATP and NADPH, with the 3-PGA finally being utilized by the Calvin-Benson cycle. The photorespiratory pathway is often considered wasteful since the pathway requires reductants and ATP, and it releases previously fixed CO_2.

The balance between photosynthesis and photorespiration depends on temperature and the relative concentrations of CO_2 and O_2 within the cell. Under increasing temperatures, the solubility of CO_2 decreases more than that of O_2, resulting in a decreased ratio of [CO_2] to [O_2] and an increase in photorespiration (Tenhunen, Weber, Yocum, & Gates, 1979). Under warming, the kinetic properties of Rubisco also result in higher specificity for O_2 to the active site of RuBP than CO_2 (Tcherkez, 2016). On the contrary, under elevated CO_2 (EC) conditions, higher CO_2 substrate availability increases photosynthesis and suppress photorespiration. With climate change, there will be increases in both temperature and CO_2, which will affect the balance between photorespiration and photosynthesis, and therefore the C balance of C_3 plants.

1.4.2 Plant Respiration

Respiration, like photorespiration, is heavily influenced by temperature and determines plant C balance. Mitochondrial respiration occurs in all aerobic organisms, consuming sugars to fuel metabolism, growth and reproduction. Plant respiration can be broken down into three steps (Figure 1.2). The first step is glycolysis, where sugars, such as fructose and sucrose, are converted into pyruvate, resulting in a net production of ATP (Plaxton & Podestá, 2006; Atkin, Millar, & Day, 2000). Pyruvate is converted into acetyl coenzyme A (Acetyl-CoA) before entering a mitochondrion, which releases CO_2. The second step involves the citric acid cycle, which uses the C molecules from Acetyl-CoA to produce CO_2, reductants and ATP. These reductants include nicotinamide adenosine diphosphate hydrogen, NADH, and flavin adenine dinucleotide, $FADH_2$. Lastly, the mitochondrial electron transport chain uses these reductants to make more ATP through an ATP synthase by utilizing a proton gradient. For every molecule of glucose, respiration produces six CO_2, six H_2O, and ~38 ATP molecules.

1.4.3 Acclimation of Photosynthesis

Thermal acclimation of photosynthesis will be critical for the survival of C_3 plants under future warming. Leaf C uptake can be measured as the net CO_2 assimilation rate (A_{net}), which is the gross rate of photosynthesis minus CO_2 losses from respiration and photorespiration. It is not usually practicable to separate out measurements of respiration

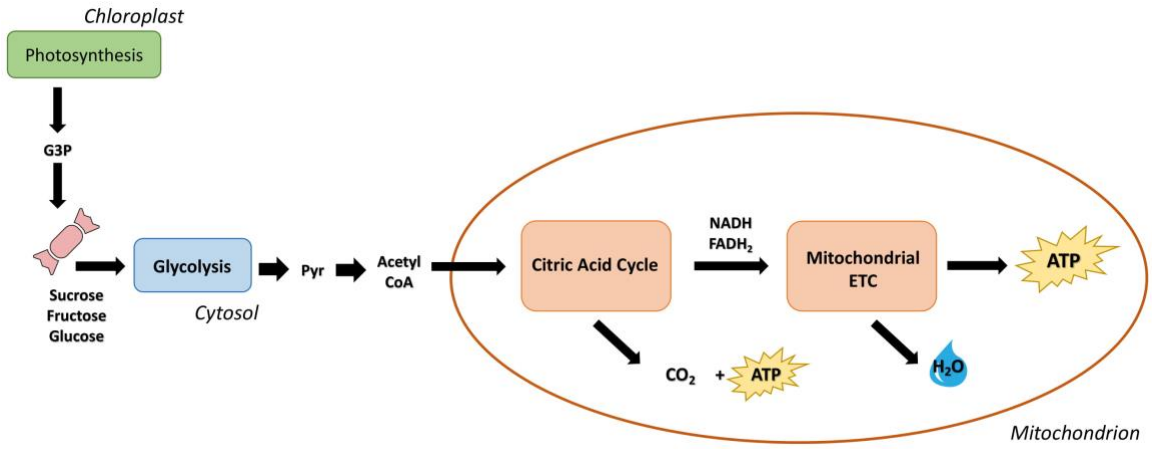

Figure 1.2. Simplified schematic of plant respiration. Triose phosphates made by photosynthesis are used in mitochondrial respiration to produce energy in the form of ATP (adenosine triphosphate) and by-products (CO_2 and H_2O). G3P, glyceraldehyde-3-phosphate; Pyr, pyruvate; Acetyl-CoA, acetyl coenzyme A; CO_2, carbon dioxide; NADH, nicotinamide adenosine diphosphate hydrogen; $FADH_2$, flavin adenine dinucleotide; ATP, adenosine triphosphate; ETC, electron transport chain. Redrawn and modified from Atkin and Tjoelker (2003).

or photorespiration from CO_2 uptake in the light, which is why A_{net} is frequently used in the literature.

A_{net} can function between ~0 ˚C and 30 ˚C in cold-tolerant plants, such as boreal conifers (Sage & Kubien, 2007). The temperature optimum (T_{opt}) of photosynthesis represents the temperature where A_{net} is highest (Figure 1.3). There are three main outcomes of acclimation to warming in terms of how A_{net} is affected by temperature: a) an increase in $T_{opt,}$ resulting in an increase in A_{net} at the new growth temperature (A_{growth}); b) an increase in T_{opt}, resulting in a decrease in A_{growth}; and, c) an increase in T_{opt} resulting in a similar A_{growth} between cool- and warm-grown plants (Way & Yamori, 2014). Acclimation can therefore be characterized by a shift in T_{opt} and subsequent changes to A_{net}.

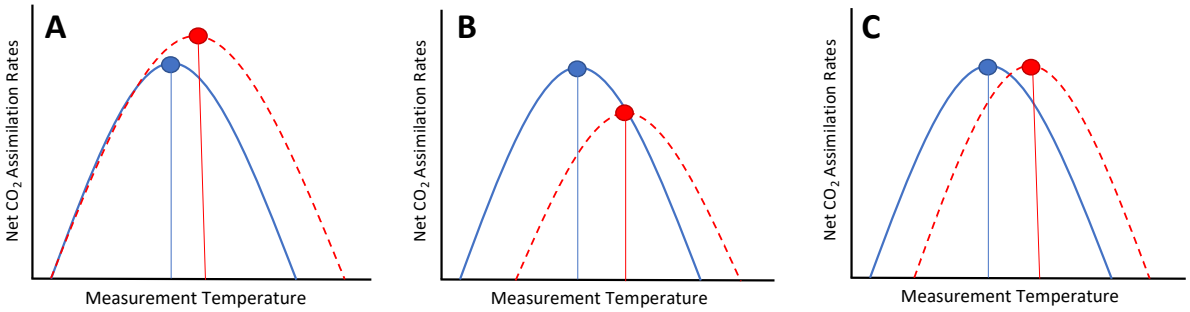

Figure 1.3. Conceptual temperature response curves for photosynthetic acclimation. Net CO_2 assimilation rates of plants grown at a cool growth temperature (blue solid lines) and at a warm growth temperature (red dashed lines). Blue circles indicate the photosynthetic temperature optimum (T_{opt}) of the cool-grown plants and red circles indicate T_{opt} of the warm-grown plants. Photosynthetic thermal acclimation can result in a range of changes (A: increase, B: decrease and C: similar) in net CO_2 assimilation rates at the new growth condition, even if T_{opt} increases in each scenario. Redrawn from Way and Yamori (2014).

Photosynthetic capacity, a measure of the maximum capacity of a leaf to fix CO_2, can also be used to quantify photosynthetic thermal acclimation (Way & Yamori, 2014). Photosynthetic capacity consists of both the maximum rate of electron transport, J_{max}, and the maximum rate of Rubisco carboxylation, V_{cmax}. Both V_{cmax} and J_{max} can be estimated by measuring A_{net} at a range of intracellular CO_2 (C_i) concentrations under saturating light (Figure 1.4), using the Farquhar-von Caemmerer-Berry model of C_3 photosynthesis (Farquhar, von Caemmerer, & Berry, 1980). This model is used to derive the biochemical limitations of photosynthesis, including Rubisco carboxylation, regeneration of RuBP, and triose-phosphate utilization (TPU) (Gu, Pallardy, Tu, Law, & Wullschleger, 2010; Sage & Kubien, 2007). Rubisco limitations are common under low CO_2 concentrations when there is not enough CO_2 substrate to saturate Rubisco carboxylation capacity. Therefore, V_{cmax} can be calculated using the initial slope of CO_2 consumption to rising C_i. Once C_i increases above ~400 ppm CO_2, the regeneration of RuBP using NADPH and ATP from the electron transport chain becomes limiting, and J_{max} can be calculated. Lastly, at very high CO_2 concentrations, inorganic phosphate availability begins to limit

A_{net}, as the ability to use triose phosphates to make sucrose and starch slows. This TPU limitation is observable when the A/C_i curve flattens out at high CO_2, since TPU-limited photosynthesis is CO_2-insensitive.

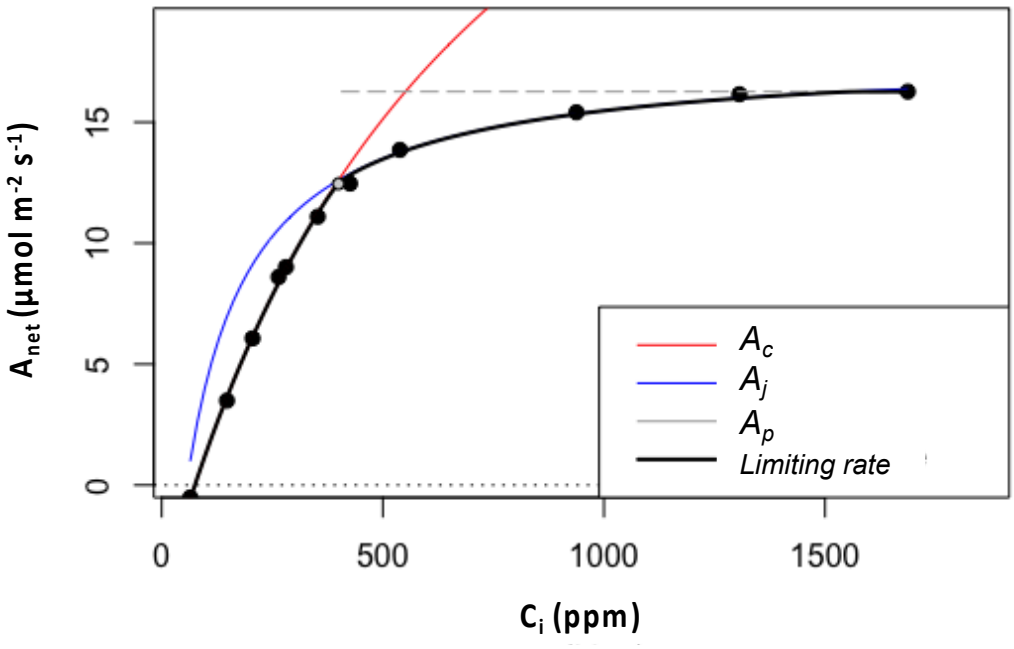

Figure 1.4. A representative A/Ci curve fitted using the Farquhar-Berry-von Caemmerer model of leaf photosynthesis. A/C_i curves are modeled using net CO_2 assimilation rate (A_{net}) measured over a range of intracellular CO_2 concentrations (C_i). Rubisco carboxylation is limiting net photosynthesis at low C_i (red line, A_c), RuBP regeneration becomes limiting above ~400 ppm (blue line, A_j), and triose phosphate regeneration is limiting at very high CO_2 concentrations (dashed grey line, A_p). The black line represents the limiting rate of the A/C_i curve, based on the minimum A_{net} of the three limitations. Data from Chapter Two of a *Larix larcina* seedling grown at ambient temperature.

Elevated growth temperature and CO_2 both affect J_{max} and V_{cmax}. Hypothetically, if all else remains equal, plants should decrease their photosynthetic capacity if it is advantageous to maintain the same A_{net} at a warmer temperature. In contrast, plants could increase their photosynthetic capacity to maximize A_{net} at warmer growth temperatures if water and nutrient availability are not limiting, which is often the case (Way & Yamori,

2014). Thus, any change (positive or negative) of V_{cmax} and J_{max} indicates an adjustment of photosynthetic capacity to warming, and may represent thermal acclimation (Way & Yamori, 2014). Photosynthetic capacity can also be affected by growth under EC. Long-term exposure of plants to EC often results in a decrease in photosynthetic capacity (Ainsworth & Rogers, 2007; Albert, Mikkelsen, Michelsen, Ro-Poulsen, & van der Linden, 2011; Moore, Cheng, Sims, & Seemann, 1999). Under EC, plants are able to maintain high photosynthetic rates with less investment in Rubisco, since CO_2 substrate availability is high. Leaf N can act as a proxy for Rubisco (Reich et al., 1998). Therefore, reported decreases in total leaf N are often indicative of decreases in photosynthetic capacity.

1.4.4 Acclimation of Respiration

Measurements of respiration rates in the dark (R_{dark}) can be made on dark-acclimated plants, eliminating the confounding presence of photosynthesis. Dark respiration is the parameter used in this thesis to quantify respiration. While respiration is relatively insensitive to short-term variation in CO_2, it is sensitive to temperature, and thus thermal acclimation is critical for minimizing future C losses from vegetation. The Q_{10}, defined as the proportional change in an enzyme's activity per 10 ˚C change in temperature, can be used to quantify this thermal sensitivity. Most enzymes have Q_{10} values between 2-3. However, the Q_{10} of respiration can vary with environmental conditions (Atkin & Tjoelker, 2003). Over a six month span, respiratory thermal acclimation in *Eucalyptus pauciflora* resulted in higher Q_{10} values in the winter compared to the summer (Atkin, Holly, & Ball, 2000). The Q_{10} and subsequent rates of respiration also vary across plant functional types, seasons, and biomes (Atkin & Tjoelker, 2003; Villar, Held, & Merino, 1995). For example, the mean Q_{10} of Arctic plants is 2.56, while the mean Q_{10} of tropical plants is 2.14 (Tjoelker, Oleksyn, & Reich, 2001). An Arctic plant will thus be more sensitive to short-term warming compared to a tropical plant with a lower Q_{10}. Comparisons of Q_{10} differences across seasons and biomes show how growth environments, in terms of both acclimation and adaptation, can have large impacts on respiration in response to shifts in temperature.

There are two main types of thermal acclimation of respiration (Figure 1.5; Atkin & Tjoelker, 2003). Type I acclimation refers to a change in the Q_{10}, e.g. a change in the temperature sensitivity of respiration (Covey-Crump, Attwood, & Atkin, 2002). Type II acclimation refers to a shift in the entire temperature response curve of respiration, resulting in a new Y intercept (Tjoelker et al., 1999a; Tjoelker, Oleksyn, & Reich, 1999b). Type II acclimation is thought to mitigate C losses more effectively than Type I acclimation by decreasing respiration rates under warming. However, Type I acclimation makes plants less sensitive to acute changes in temperature by decreasing the Q_{10}. All plant tissues respire, so it is also possible to compare shoot and root respiration to understand total plant C loss. Understanding how different plant species acclimate to changing temperatures and CO_2 concentrations will be necessary when considering how global C pools will be affected by climate change in the future.

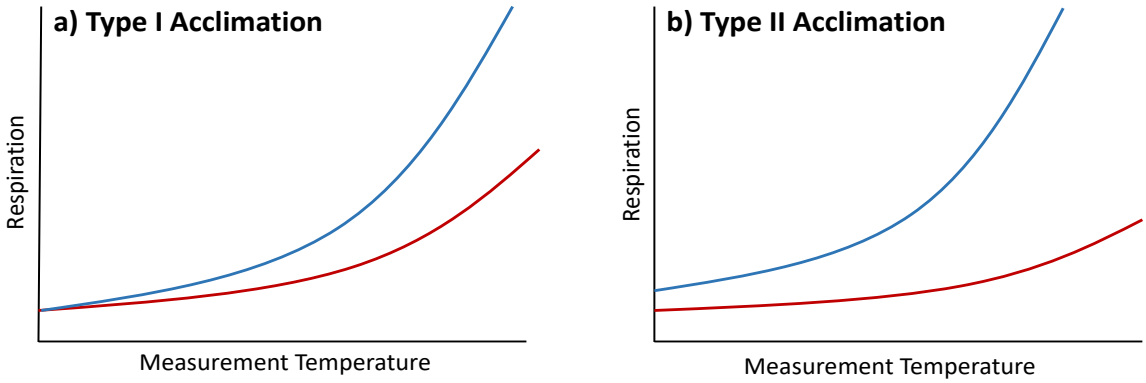

Figure 1.5. Type I and type II acclimation of respiration to temperature. Short-term response of respiration in a plant grown at a cool temperature (blue line) and the same plant exposed to long-term warming (red line). A) Type I acclimation, where warming results in a decrease in the Q_{10}; and B) Type II acclimation, where warming results in a complete downward shift in the respiration temperature response curve. Redrawn from Atkin and Tjoelker (2003).

In comparison to photosynthesis and photorespiration, which occur primarily in leaf tissue, respiration happens in all plant tissues. This means that, as plants grow, plant respiration costs increase (Loveys et al., 2003; Poorter et al., 1991). However, unlike photorespiration, plant respiration is relatively insensitive to short-term changes in CO_2

concentrations (Amthor, Koch, Willms, & Layzell, 2001). Acclimation to long-term shifts in warming may help plants reduce C losses under global warming.

1.4.5 Response of Tamarack to Elevated Temperature and CO_2

The responses of tamarack, specifically photosynthesis and respiration, to increasing growth temperature and CO_2 have not been well-studied. In a pioneering experiment, Tjoekler et al. (1998) found that tamarack seedlings grown in chambers had lower A_{net} after long-term exposure to EC (580 ppm), but there was no thermal acclimation of photosynthesis. Tamarack seedlings also displayed thermal acclimation of respiration by decreasing respiration rates under warming treatments (Tjoelker et al., 1999a). Despite this, slow-growing conifers in their study, including tamarack, had greater respiratory losses through shoots and roots compared to other plant functional types. But in a previous study conducted in the Way lab, Dusenge, Madhavji, and Way (2020) found contrasting acclimation photosynthesis responses of tamarack seedlings grown in glasshouses and exposed to warming (up to 8 ˚C above ambient) and CO_2 enrichment (up to 750 ppm). Photosynthetic capacity of tamarack was reduced in response to warming, resulting in similar A_{net} across the treatments, and the T_{opt} increased with warming. But similar to Tjoelker et al. (1998), tamarack seedlings thermally acclimated shoot respiration to warming (Dusenge et al., 2020). Overall, tamarack seedlings had higher biomass when grown under moderate warming but had decreased biomass and increased mortality under extreme warming with no CO_2 effect (Dusenge et al., 2020). Tjoelker et al. (1998) and Dusenge et al. (2020) both found that photosynthesis was stimulated by EC when measured under growth conditions.

The most surprising finding by Dusenge et al. (2020) was that tamarack seedlings had high mortality under ambient +8 ˚C warming in combination with AC (8TAC), but this mortality was offset by EC. The seedlings were well-watered, so water stress (i.e. hydraulic failure) was unlikely. The survival of ambient +8 ˚C seedlings supplemented with EC indicated that greater C gains prevented C stress. This led me to the question: are tamarack seedlings dying from C starvation under ambient +8 ˚C warming with ambient

CO_2? If so, this would be the first study to show that C starvation may be induced directly by warming without any water stress.

1.5 Rationale and Objectives

Tamarack is an important tree species in the Canadian boreal forest and contributes to the boreal forest's C sequestration potential. The overarching objective of my thesis was to investigate if C starvation in tamarack seedlings led to mortality under extreme warming. By examining the C fluxes of tamarack, I planned to model C balances to understand the responses of growth, performance and survival of seedlings under future climate conditions.

1.5.1 Chapter 2: Glasshouse Experiment

Using the same experimental design as Dusenge et al. (2020), tamarack was grown from seed in glasshouses under warming, with and without CO_2 enrichment. I planned to test the C starvation hypothesis by comparing C fluxes and percent foliar C of dying vs. healthy 8TAC seedlings. Under C starvation, dying seedlings would have decreased ratios of photosynthesis to respiration and lower foliar C concentrations compared to healthy seedlings. Carbon fluxes of healthy seedlings across all treatments would also be measured to evaluate acclimation, performance and growth of tamarack across the treatments. By modelling C balance across all treatments, I could test if healthy 8TAC seedlings had overall lower C balances than seedlings form other treatments and whether this made them more vulnerable to C stress.

1.5.2 Chapter 3: Follow-up Growth Chamber Experiment

Following the glasshouse experiment, the goal of my second experiment was to use growth chambers to measure a greater sample size of dying seedlings and to test C starvation with a C rescue (plants displaying signs of mortality would be moved into the EC treatment to test whether a recovery could be made). However, the growth chamber experiment resulted in zero mortality of 8TAC seedlings. The goal then became to investigate whether this greater survival in the growth chamber study (compared to the

glasshouses) was due to greater acclimation of C fluxes under constant temperature and light conditions.

1.6 References

Adams, H. D., Zeppel, M. J. B., Anderegg, W. R. L., Hartmann, H., Landhäusser, S. M., Tissue, D. T., … McDowell, N. G. (2017). A multi-species synthesis of physiological mechanisms in drought-induced tree mortality. *Nature Ecology and Evolution*, *1*(9), 1285–1291. https://doi.org/10.1038/s41559-017-0248-x

Ainsworth, E. A., & Rogers, A. (2007). The response of photosynthesis and stomatal conductance to rising [CO_2]: Mechanisms and environmental interactions. *Plant, Cell and Environment*, *30*(3), 258–270. https://doi.org/10.1111/j.1365-3040.2007.01641.x

Albert, K. R., Mikkelsen, T. N., Michelsen, A., Ro-Poulsen, H., & van der Linden, L. (2011). Interactive effects of drought, elevated CO_2 and warming on photosynthetic capacity and photosystem performance in temperate heath plants. *Journal of Plant Physiology*, *168*(13), 1550–1561. https://doi.org/10.1016/j.jplph.2011.02.011

Aleixo, I., Norris, D., Hemerik, L., Barbosa, A., Prata, E., Costa, F., & Poorter, L. (2019). Amazonian rainforest tree mortality driven by climate and functional traits. *Nature Climate Change*. *9*, 384–388. https://doi.org/10.1038/s41558-019-0458-0

Allen, C. D., Breshears, D. D., & McDowell, N. G. (2015). On underestimation of global vulnerability to tree mortality and forest die-off from hotter drought in the Anthropocene. *Ecosphere*, *6*(8), 1–55. https://doi.org/10.1890/ES15-00203.1

Allen, C. D., Macalady, A. K., Chenchouni, H., Bachelet, D., McDowell, N., Vennetier, M., … Cobb, N. (2010). A global overview of drought and heat-induced tree mortality reveals emerging climate change risks for forests. *Forest Ecology and Management*, *259*(4), 660–684. https://doi.org/10.1016/j.foreco.2009.09.001

Amthor, J. S., Koch, G. W., Willms, J. R., & Layzell, D. B. (2001). Leaf O_2 uptake in the dark is independent of coincident CO_2 partial pressure. *Journal of Experimental Botany*, *52*(364), 2235–2238. https://doi.org/10.1093/jexbot/52.364.2235

Anderegg, W. R. L., Berry, J. A., & Field, C. B. (2012). Linking definitions, mechanisms, and modeling of drought-induced tree death. *Trends in Plant Science*, *17*(12), 693–700. https://doi.org/10.1016/j.tplants.2012.09.006

Apps, M. J., Kurz, W. A., Luxmoore, R. J., Nilsson, L. O., Sedjo, R. A., Schmidt, R., … Vinson, T. S. (1993). Boreal forests and tundra. *Water, Air, & Soil Pollution*, *70*(1–4), 39–53. https://doi.org/10.1007/BF01104987

Atkin, O. K., Holly, C., & Ball, M. C. (2000). Acclimation of snow gum (*Eucalyptus pauciflora*) leaf respiration to seasonal and diurnal variations in temperature: The importance of changes in the capacity and temperature sensitivity of respiration. *Plant, Cell and Environment*, *23*(1), 15–26. https://doi.org/10.1046/j.1365-3040.2000.00511.x

Atkin, O. K., & Tjoelker, M. G. (2003). Thermal acclimation and the dynamic response of plant respiration to temperature. *Trends in Plant Science*, *8*(7), 343–351. https://doi.org/10.1016/S1360-1385(03)00136-5

Atkin, O., Millar, H. A., & Day, D. A. (2000). Photosynthesis, carbohydrate metabolism, and respiration in leaves of higher plants. In *Photosynthesis: Physiology and Metabolism* (Vol. 9, pp. 153–175). https://doi.org/10.1007/0-306-48137-5

Barichivich, J., Briffa, K. R., Myneni, R. B., Osborn, T. J., Melvin, T. M., Ciais, P., … Tucker, C. (2013). Large-scale variations in the vegetation growing season and annual cycle of atmospheric CO_2 at high northern latitudes from 1950 to 2011. *Global Change Biology*, *19*(10), 3167–3183. https://doi.org/10.1111/gcb.12283

Beck, P. S. A., Juday, G. P., Alix, C., Barber, V. A., Winslow, S. E., Sousa, E. E., … Goetz, S. J. (2011). Changes in forest productivity across Alaska consistent with biome shift. *Ecology Letters*, *14*(4), 373–379. https://doi.org/10.1111/j.1461-0248.2011.01598.x

Bonan, G. B., & Shugart, H. H. (1989). Environmental factors and ecological processes in boreal forests. *Annual Review of Ecology and Systematics*, *20*, 1–28. https://doi.org/10.1146/annurev.es.20.110189.000245

Bond-Lamberty, B., & Thomson, A. (2010). Temperature-associated increases in the global soil respiration record. *Nature*, *464*(7288), 579–582. https://doi.org/10.1038/nature08930

Bradshaw, C. J. A., & Warkentin, I. G. (2015). Global estimates of boreal forest carbon stocks and flux. *Global and Planetary Change*, *128*, 24–30. https://doi.org/10.1016/j.gloplacha.2015.02.004

Brandt, J. P. (2009). The extent of the North American boreal zone. *Environmental Reviews*, *17*, 101–161. https://doi.org/10.1139/A09-004

Byrne, M. P., & Schneider, T. (2018). Atmospheric dynamics feedback: Concept, simulations, and climate implications. *Journal of Climate*, *31*(8), 3249–3264. https://doi.org/10.1175/JCLI-D-17-0470.1

Covey-Crump, E. M., Attwood, R. G., & Atkin, O. K. (2002). Regulation of root respiration in two species of *Plantago* that differ in relative growth rate: The effect of short- and long-term changes in temperature. *Plant Cell and Environment*, *25*, 1501–1513.

Danielewska, A., Urbaniak, M., & Olejnik, J. (2015). Growing season length as a key factor of cumulative net ecosystem exchange over the pine forest ecosystems in Europe. *International Agrophysics*, *29*(2), 129–135. https://doi.org/10.1515/intag-2015-0026

Dietze, M. C., Sala, A., Carbone, M. S., Czimczik, C. I., Mantooth, J. A., Richardson, A. D., & Vargas, R. (2014). Nonstructural carbon in woody plants. *Annual Review of Plant Biology*, *65*(1), 667–687. https://doi.org/10.1146/annurev-arplant-050213-040054

Dusenge, M. E., Duarte, A. G., & Way, D. A. (2019). Plant carbon metabolism and climate change: Elevated CO_2 and temperature impacts on photosynthesis, photorespiration and respiration. *New Phytologist*, *221*(1), 32–49. https://doi.org/10.1111/nph.15283

Dusenge, M. E., Madhavji, S., & Way, D. A. (2020). Contrasting acclimation responses to elevated CO_2 and warming between an evergreen and a deciduous boreal conifer. *Global Change Biology*. https://doi.org/10.1111/gcb.15084

Farquhar, G. D., von Caemmerer, S., & Berry, J. A. (1980). A biochemical model of photosynthetic CO_2 assimilation in leaves of C_3 species. *Planta*, *149*(1), 78–90. https://doi.org/10.1007/BF00386231

Gauthier, S., Bernier, P., Kuuluvainen, T., Shvidenko, A. Z., & Schepaschenko, D. G. (2015). Boreal forest health and global change. *Science*, *349*(6250), 819–822. https://doi.org/10.1126/science.aaa9092

Gitlin, A. R., Sthultz, C. M., Bowker, M. A., Stumpf, S., Paxton, K. L., Kennedy, K., … Whitham, T. G. (2006). Mortality gradients within and among dominant plant populations as barometers of ecosystem change during extreme drought. *Conservation Biology*, *20*(5), 1477–1486. https://doi.org/10.1111/j.1523-1739.2006.00424.x

Gower, S. T., & Richards, J. H. (1990). Larches: Deciduous conifers in an evergreen world. *BioScience*, *40*(11), 818–826. https://doi.org/10.2307/1311484

Gowin, T., Lourtioux, A., & Mousseau, M. (1980). Influence of constant growth temperature upon the productivity and gas exchange of seedlings of Scots pine and European larch. *Forest Science*, *26*(2), 301–309. https://doi.org/10.1093/forestscience/26.2.301

Gu, L., Pallardy, S. G., Tu, K., Law, B. E., & Wullschleger, S. D. (2010). Reliable estimation of biochemical parameters from C_3 leaf photosynthesis-intercellular carbon dioxide response curves. *Plant, Cell and Environment*, *33*(11), 1852–1874. https://doi.org/10.1111/j.1365-3040.2010.02192.x

Hartmann, H., Ziegler, W., & Trumbore, S. (2013). Lethal drought leads to reduction in nonstructural carbohydrates in Norway spruce tree roots but not in the canopy. *Functional Ecology*, *27*(2), 413–427. https://doi.org/10.1111/1365-2435.12046

Hoch, G., Richter, A., & Korner, C. (2003). Non-structural carbon compounds in temperate forest trees. *Plant Cell and Environment*, *26*, 1067–1081. https://doi.org/10.1046/j.0016-8025.2003.01032.x

IPCC. (2014). *Summary for Policy Makers*. *Climate Change 2014: Synthesis Report. Contribution of Working Groups I, II and III to the Fifth Assessment Report of the Intergovernmental Panel on Climate Change*. https://doi.org/10.1017/CBO9781107415324

Islam, M. A., & Macdonald, S. E. (2005). Effects of variable nitrogen fertilization on growth, gas exchange, and biomass partitioning in black spruce and tamarack seedlings. *Canadian Journal of Botany*, *83*(12), 1574–1580. https://doi.org/10.1139/b05-123

Kerling, J., Grant, K., Hammerl, V., Arfin-Khan, M. A. S., Malyshev, A.V., Penuelas, J., … Beirekulnlein, C. (2019). Winter warming is ecologically more relevant than summer warming in a cool-temperature grassland. *Scientific Reports*, *9,* 14632.

Kloeppel, B. D., Gower, S. T., Vogel, J. G., & Reich, P. B. (2000). Leaf-level resource use for evergreen and deciduous conifers along a resource availability gradient. *Functional Ecology*, *14*(3), 281–292. https://doi.org/10.1046/j.1365-2435.2000.00439.x

Kramer, K. (1995). Phenotypic plasticity of the phenology of seven European tree species in relation to climatic warming. *Plant, Cell & Environment*, *18*(2), 93–104. https://doi.org/10.1111/j.1365-3040.1995.tb00356.x

Lawrence, W. T., & Oechel, W. C. (1983). Effects of soil temperature on the carbon exchange of taiga seedlings: Root respiration. *Canadian Journal of Forest Research*, *13*(5), 840–849. https://doi.org/10.1139/x83-114

Loveys, B. R., Atkinson, L. J., Sherlock, D. J., Roberts, R. L., Fitter, A. H., & Atkin, O. K. (2003). Thermal acclimation of leaf and root respiration: An investigation comparing inherently fast- and slow-growing plant species. *Global Change Biology*, *9*(6), 895–910. https://doi.org/10.1046/j.1365-2486.2003.00611.x

Mantgem, P. J. Van, Stephenson, N. L., Byrne, J. C., Daniels, L. D., Franklin, J. F., Fulé, P. Z., … Veblen, T. T. (2009). Widespread increase of tree mortality rates in the western United States. *Science*, *323*(5913), 521–524. https://doi.org/10.1126/science.1165000

Miziorko, H. M., & Lorimer, G. H. (1983). Ribulose-1,5-bisphosphate carboxylase-oxygenase. *Annual Review of Biochemistry*, *52*, 507-535. https://doi.org/10.1146/annualrev.bi.52.070183.002451

McDowell, N. G., Williams, A. P., Xu, C., Pockman, W. T., Dickman, L. T., Sevanto, S., … Koven, C. (2016). Multi-scale predictions of massive conifer mortality due to chronic temperature rise. *Nature Climate Change*, *6*(3), 295–300. https://doi.org/10.1038/nclimate2873

Meir, P., Mencuccini, M., & Dewar, R. C. (2015). Drought-related tree mortality: Addressing the gaps in understanding and prediction. *New Phytologist*, *207*(1), 28–33. https://doi.org/10.1111/nph.13382

Metsaranta, J. M., Kurz, W. A., Neilson, E. T., & Stinson, G. (2010). Implications of future disturbance regimes on the carbon balance of Canada's managed forest (2010-2100). *Tellus, Series B: Chemical and Physical Meteorology*, *62*(5), 719–728. https://doi.org/10.1111/j.1600-0889.2010.00487.x

Miquelajauregui, Y., Cumming, S. G., & Gauthier, S. (2019). Short-term responses of boreal carbon stocks to climate change: A simulation study of black spruce forests. *Ecological Modelling*, *409*, 108754. https://doi.org/10.1016/j.ecolmodel.2019.108754

Moore, B. D., Cheng, S. H., Sims, D., & Seemann, J. R. (1999). The biochemical and molecular basis for photosynthetic acclimation to elevated atmospheric CO_2. *Plant, Cell and Environment*, *22*(6), 567–582. https://doi.org/10.1046/j.1365-3040.1999.00432.x

Nedwell, D. B. (1999). Effect of low temperature on microbial growth: Lowered affinity for substrates limits growth at low temperature. *FEMS Microbiology Ecology*, *30*(2), 101–111. https://doi.org/10.1016/S0168-6496(99)00030-6

Nicotra, A. B., Atkin, O. K., Bonser, S. P., Davidson, A. M., Finnegan, E. ., Mathesius, U., … Van Kleunen, M. (2010). Plant phenotypic plasticity in a changing climate. *Trends in Plant Science*, *15*(12), 684–692. https://doi.org/10.1016/j.tplants.2010.09.008

NOAA (2020) Data provided by the Physical Sciences Division of NOAA/ESRL. URL:https://www.esrl.noaa.gov/gmd/ccgg/trends/monthly.html

Pan, Y., Birdsey, R. A., Fang, J., Houghton, R. A., Kauppi, P. E., Kurz, W. A., … Hayes, D. (2011). A large and persistent carbon sink in the world's forest. *Science*, *333*(6045), 988–993. https://doi.org/10.1126/science.1201609

Peng, C., Ma, Z., Lei, X., Zhu, Q., Chen, H., Wang, W., … Zhou, X. (2011). A drought-induced pervasive increase in tree mortality across Canada's boreal forests. *Nature Climate Change*, *1*(9), 467–471. https://doi.org/10.1038/nclimate1293

Peterhansel, C., Horst, I., Niessen, M., Blume, C., Kebeish, R., Kürkcüoglu, S., & Kreuzaler, F. (2010). Photorespiration. *The Arabidopsis Book*, *8*, e0130. https://doi.org/10.1199/tab.0130

Petit, J. R., Jouzel, J., Raynaud, D., Barnola, J. M., Basile, I., Bender, M., … Stievenard, M. (2013). Climate and atmospheric history of the past 420,000 years from the Vostok ice core, Antarctica. *Nature*, *399*, 348–358. https://doi.org/10.1038/20859

Plaxton, W. C., & Podestá, F. E. (2006). The functional organization and control of plant respiration. *Critical Reviews in Plant Sciences*, *25*(2), 159–198. https://doi.org/10.1080/07352680600563876

Poorter, H., van der Werf, A., Lambers Poorter, H., der Werf, V., Poorter, H., van der Werf, A., & Lambers, H. (1991). Respiratory energy requirements of roots vary with the potential growth rate of a plant spedes. *Physiologia Plantarum*, *83*, 469–475. https://doi.org/10.1111/j.399-3054.1991.tb00122.x

Pugh, T. A. M., Arneth, A., Kautz, M., Poulter, B., & Smith, B. (2019). Important role of forest disturbances in the global biomass turnover and carbon sinks. *Nature Geoscience*, *12*(9), 730–735. https://doi.org/10.1038/s41561-019-0427-2

Randerson, J. T., Field, C. B., Fung, I. Y., & Tans, P. P. (1999). Increases in early season ecosystem uptake explain recent changes in the seasonal cycle of atmospheric CO_2 at high northern latitudes. *Geophysical Research Letters*, *26*(17), 2765–2768. https://doi.org/10.1029/1999GL900500

Reich, P. B., Kloeppel, B. D., Ellsworth, D. S., & Walters, M. B. (1995). Different photosynthesis-nitrogen relations in deciduous hardwood and evergreen coniferous tree species. *Oecologia*, *104*, 24–30. https://doi.org/10.1007/BF00365558

Reich, P. B., Rich, R. L., Lu, X., Wang, Y. P., & Oleksyn, J. (2014). Biogeographic variation in evergreen conifer needle longevity and impacts on boreal forest carbon cycle projections. *Proceedings of the National Academy of Sciences of the United States of America*, *111*(38), 13703–13708. https://doi.org/10.1073/pnas.1216054110

Reich, P. B., Walters, M. B., Ellsworth, D. S., Vose, J. M., John, C., Gresham, C., & Bowman, W. D. (1998). Relationships of leaf dark respiration to leaf nitrogen , specific leaf Area and leaf life-span: A test across biomes and functional groups. *Oecologia*, *114*(4), 471–482. https://doi.org/10.1007/s004420050471

Richardson, A. D., Hufkens, K., Milliman, T., Aubrecht, D. M., Furze, M. E., Seyednasrollah, B., … Hanson, P. J. (2018). Ecosystem warming extends vegetation activity but heightens vulnerability to cold temperatures. *Nature*, *560*(7718), 368–371. https://doi.org/10.1038/s41586-018-0399-1

Sage, R. F., & Kubien, D. S. (2007). The temperature response of C_3 and C_4 photosynthesis. *Plant, Cell and Environment*, *30*(9), 1086–1106. https://doi.org/10.1111/j.1365-3040.2007.01682.x

Sala, A., Woodruff, D. R., & Meinzer, F. C. (2012). Carbon dynamics in trees: feast or famine? *Tree Physiology*, 32, 764–775. https://doi.org/10.1093/treephys/tpr143

Serreze, M. C., Walsh, J. E., Chapin, F. S. I., Osterkamp, T., Dyurgerov, M., Romanovsky, V., … Barry, R. G. (2000). Observational evidence of recent change in the northern high-latitude environment. *Climatic Change*, *46*(1–2), 159–207. https://doi.org/10.1023/A:1005504031923

Sevanto, S., Mcdowell, N. G., Dickman, L. T., Pangle, R., & Pockman, W. T. (2014). How do trees die? A test of the hydraulic failure and carbon starvation hypotheses. *Plant, Cell and Environment*, *37*(1), 153–161. https://doi.org/10.1111/pce.12141

Taiz, L. & Zeiger, E. (2010) Plant Physiology. 5th Edition, Sinauer Associates, Inc., Sunderland.

Tcherkez, G. (2016). The mechanism of Rubisco-catalysed oxygenation. *Plant Cell and Environment*, *39*(5), 983–997. https://doi.org/10.1111/pce.12629

Tenhunen, J. D., Weber, J. A., Yocum, C. S., & Gates, D. M. (1979). Solubility of gases and the temperature dependency of whole leaf affinities for carbon dioxide and oxygen. *Plant Physiology*, *63*(5), 916–923. https://doi.org/10.1104/pp.63.5.916

Tjoelker, M. G., Oleksyn, J., & Reich, P. B. (1998). Seedlings of five boreal tree species differ in acclimation of net photosynthesis to elevated CO_2 and temperature. *Tree Physiology*, *18*, 715–716. https://doi.org/10.1093/treephys/18.11.715

Tjoelker, M. G., Oleksyn, J., & Reich, P. (1999a). Acclimation of respiration to temperature and CO_2 in seedlings of boreal tree species in relation to plant size and relative growth rate. *Global Change Biology*, *49*(6), 679–691. https://doi.org/10.1046/j.1365-2486.1999.00257.xn

Tjoelker, M. G., Oleksyn, J., & Reich, P. B. (2001). Modelling respiration of vegetation: Evidence for a general temperature-dependent Q_{10}. *Global Change Biology*, *7*(2), 223–230. https://doi.org/10.1046/j.1365-2486.2001.00397.x

Tjoelker, M. G., Reich, P. B., & Oleksyn, J. (1999b). Changes in leaf nitrogen and carbohydrates underlie temperature and CO_2 acclimation of dark respiration in five boreal tree species. *Plant, Cell and Environment*, *22*(7), 767–778. https://doi.org/10.1046/j.1365-3040.1999.00435.x

Villar, R., Held, A. A., & Merino, J. (1995). Dark leaf respiration in light and darkness of an evergreen and a deciduous plant species. *Plant Physiology*, *107*(2), 421–427. https://doi.org/10.1104/pp.107.2.421

Way, D. A., & Yamori, W. (2014). Thermal acclimation of photosynthesis: On the importance of adjusting our definitions and accounting for thermal acclimation of respiration. *Photosynthesis Research*, *119*(1–2), 89–100. https://doi.org/10.1007/s11120-013-9873-7

Wiley, E., Hoch, G., & Landhäusser, S. M. (2017). Dying piece by piece: Carbohydrate dynamics in aspen (*Populus tremuloides*) seedlings under severe carbon stress. *Journal of Experimental Botany*, *68*(18), 5221–5232. https://doi.org/10.1093/jxb/erx342

Williams, A. P., Allen, C. D., Macalady, A. K., Griffin, D., Woodhouse, C. A., Meko, D. M., … Mcdowell, N. G. (2013). Temperature as a potent driver of regional forest drought stress and tree mortality. *Nature Climate Change*, *3*(3), 292–297. https://doi.org/10.1038/nclimate1693

Worrall, J. J., Egeland, L., Eager, T., Mask, R. A., Johnson, E. W., Kemp, P. A., & Shepperd, W. D. (2008). Rapid mortality of *Populus tremuloides* in southwestern Colorado, USA. *Forest Ecology and Management*, *255*(3–4), 686–696. https://doi.org/10.1016/j.foreco.2007.09.071

Yuan, Z. Y., & Chen, H. Y. H. (2010). Fine root biomass, production, turnover rates, and nutrient contents in boreal forest ecosystems in relation to species, climate, fertility, and stand age: Literature review and meta-analyses. *Critical Reviews in Plant Sciences*, *29*(4), 204–221. https://doi.org/10.1080/07352689.2010.483579

Zhang, Q., Shao, M., Jia, X., & Wei, X. (2017). Relationship of climatic and forest factors to drought- and heat-induced tree mortality. *Public Library of Science One*, *12*(1), e0169770. https://doi.org/10.1371/journal.pone.0169770

Chapter 2

2 Elevated CO_2 and Warming Effects on Plant C Fluxes, Growth, and Mortality: Evidence for Carbon Starvation at High Temperatures Without Water Stress

2.1 Introduction

With atmospheric CO_2 concentrations increasing at ~2.0 ppm per year, global temperatures are projected to increase 2.0-4.5 ˚C by the year 2100 (Cramer et al., 2014). Warming is predicted to be most extreme in northern latitudes, which could experience temperature increases of more than 8 ˚C by the end of the century (Oppenheimer et al., 2014; Serreze et al., 2000). This warming will directly impact the boreal forest, which accounts for 30% of global forests and acts as a significant carbon (C) sink (Brandt, 2009; Kurz et al., 2013). The ability of the boreal forest to continue sequestering C is largely dictated by both the growth and mortality of boreal plants and the balance between the C fluxes of boreal vegetation and soil organisms. Plant growth, mortality and physiological processes are sensitive to changes in temperature and CO_2, meaning that these processes will be affected by future climate conditions and could feed back on the C sink strength of the boreal forest.

Increased temperatures and atmospheric CO_2 concentrations have already intensified climatic stress on vegetation, leading to greater tree mortality globally. Since 1970, there have been over 88 documented large-scale tree mortality events, and tree mortality has been identified as a major contributor to future vegetation shifts (Allen et al., 2010; Allen et al., 2015). Many forest mortality events have been linked to global change-related droughts, where high temperatures and drought occur simultaneously. Tree die-offs have therefore been largely attributed to water stress causing either hydraulic failure (i.e. catastrophic xylem cavitation) or C starvation (where low stomatal conductance suppresses photosynthetic C gains, but respiratory C losses remain high) (Adams et al., 2017; Allen et al., 2010; Anderegg et al., 2012; Hartmann et al., 2018; Mcdowell & Sevanto, 2010; Sevanto et al., 2014). Regardless of the cause of mortality, tree die-offs are already proving to be detrimental to the boreal biome. High latitude regions in North

America are also experiencing increases in tree mortality rates associated with climate change, with boreal tree species experiencing increased mortality of up to 4.7% per year since 1963 (Peng et al., 2011). But while warming was positively correlated with mortality rates for all plots in their study, water deficits were positively correlated with mortality rates only in western Canada (Peng et al., 2011), indicating that temperature, and not drought was the main driver of mortality. This raises the question of whether warming may directly increase tree mortality risk through carbon starvation, an idea which has received little attention.

Photosynthesis is stimulated by short-term exposure to high CO_2 concentrations, as Rubisco is substrate-limited under current CO_2 concentrations (Ainsworth & Rogers, 2007). However, plants will often down-regulate net CO_2 assimilation rates (A_{net}) after long-term exposure to elevated CO_2 to cope with sink limitations, such as low nitrogen (N) availability (Ainsworth & Rogers, 2007; Tjoelker et al., 1998). Photosynthetic responses to elevated temperatures are more variable. The temperature response of net photosynthesis is curvilinear, with A_{net} peaking near the growth temperature experienced by the plant (Sage & Kubien, 2007). Above this thermal optimum, A_{net} declines. Plants acclimate to warming by shifting the photosynthetic temperature optimum towards higher temperatures (Way & Yamori, 2014). However, thermal acclimation can result in increased, similar or even lower rates of A_{net} at the new growth temperature compared to a control plant (Way & Yamori, 2014).

The other main determinant of plant C balance is respiration. Over minutes to hours, respiration increases exponentially with increasing temperatures, but respiration is relatively insensitive to short-term changes in CO_2 concentrations (Amthor et al., 2001). Under longer-term exposure to elevated temperatures, thermal acclimation of respiration often results in a decrease in respiration at a common measurement temperature, which mitigates plant C losses (Atkin & Tjoelker, 2003). Long-term exposure to elevated CO_2 can also actually increase respiration in both herbaceous and woody species (Way, Oren, & Kroner, 2015). If plants are unable to reach a sufficiently high ratio of photosynthesis to respiration under elevated growth temperatures and CO_2 concentrations, they will be at risk for growth reductions and mortality from C starvation in future climate conditions.

In this study, I grew tamarack at either ambient or elevated CO_2 concentrations combined with ambient temperatures or a +4 °C or +8 ˚C warming treatment to simulate future climate scenarios. Tamarack is a common deciduous conifer across the North American boreal forest (Islam & Macdonald, 2004). In a recent experiment, tamarack seedlings had 38% mortality under 8 ˚C warming when coupled with ambient CO_2 (Dusenge et al., 2020). I hypothesized that C starvation caused this high mortality in tamarack, since seedlings were well-watered, and seedlings grown under the same temperature regime, but with elevated CO_2, had minimal mortality. The main objectives of my study were therefore to evaluate: (i) C fluxes, growth and performance of healthy tamarack seedlings across all six treatments; and (ii) C fluxes, growth and performance of dying tamarack seedlings. The overarching goal was to determine if differences in whole plant C balance between dying and healthy seedlings grown under elevated temperatures and ample water imply that warming can directly induce C starvation.

2.2 Methods

2.2.1 Experimental Design

Tamarack seeds were sown on May 12, 2017 in 11.3 L pots filled with Promix HP mycorrhizal growing medium (Premier Tech Horticulture, Rivieire-du-Loup, QC, Canada) with slow-release fertilizer (Slow Release Plant Food, 12-4-8, Miracle Grow, The Scotts Company, Mississauga, ON, Canada). Seeds were ordered from the Canadian National Seed Tree Center (provenance from Finch Township, ON, 45.133 °N, 75.083 °W) to match the seed collection site with ambient growing season temperatures and photoperiods of London, ON where the experiment was performed.

Forty pots with five seeds per pot were assigned to one of six climate-controlled glasshouses at the University of Western Ontario's Biotron Experimental Climate Change Research Centre (N = 240 pots). Once seedlings were established, seedlings were thinned to one per pot. Each glasshouse had a different temperature × CO_2 treatment. Seedlings were grown under either ambient CO_2 (AC, 400 ppm) or elevated CO_2 (EC, 750 ppm) concentrations with either ambient (0T, ambient control temperatures), ambient +4 ˚C (4T) or ambient +8˚C (8T) temperatures. The 0T temperature regime was determined

from hourly temperature averages for each day of the growing season (using data from 2012-2016) from the London, ON airport meteorological station (Environment Canada; Figure 2.1). Carbon dioxide concentrations were measured in each glasshouse every 10 minutes with an infrared gas analyzer in the Argus control system (Argus Control Systems, Surrey, Canada) and were controlled by injecting pure CO_2 as needed to maintain the EC treatment. The growth irradiance matched outdoor light conditions, varying with naturally fluctuating sunlight. Humidity was controlled at 60% and seedlings were watered as needed to maintain a moist growth medium, as assessed by measurements of volumetric soil water content made in each pot every 14 days (HH2 Moisture Meter, Delta-T Devices, Cambridge, UK) (Figure 2.2).

Once the seedlings were established and thinned, stem height and health ratings were recorded on all seedlings every 14 days. Health was rated on a scale of 1-5 based on the percent of brown needles (Figure 2.3).

2.2.2 Physiological Measurements

Shoot gas exchange measurements were taken in August and September 2017 on fully-expanded needles using a portable photosynthesis system (Li-cor 6400XT, Li-cor Biosciences, Lincoln, NE). First, six healthy seedlings from each treatment were measured for gas exchange to establish treatment effects (N=36). Plants were sampled across the treatments to avoid potential phenological effects. Then, to compare gas exchange across trees of varying health, six healthy and six dying (health rating = 2-4) seedlings were measured in the 8TAC treatment.

For all seedlings, A_{net} was assessed at light saturation (1200 μmol photons m^{-2} s^{-1}) and a relative humidity (RH) of 30-65%. RH was held constant at ~65% at the 25 ˚C measurement temperature. However, it decreased with increasing growth temperature measurements despite use of a bubbler. The A_{net} was quantified at a range of intracellular

After the last A/C_i measurement was recorded at 2000 ppm, the cuvette CO_2 was set to 400 ppm and the sample was dark-acclimated for 20 minutes. Shoot dark respiration (R_{shoot}) was then measured at 400 ppm for all seedlings, as there is no short-term effect of

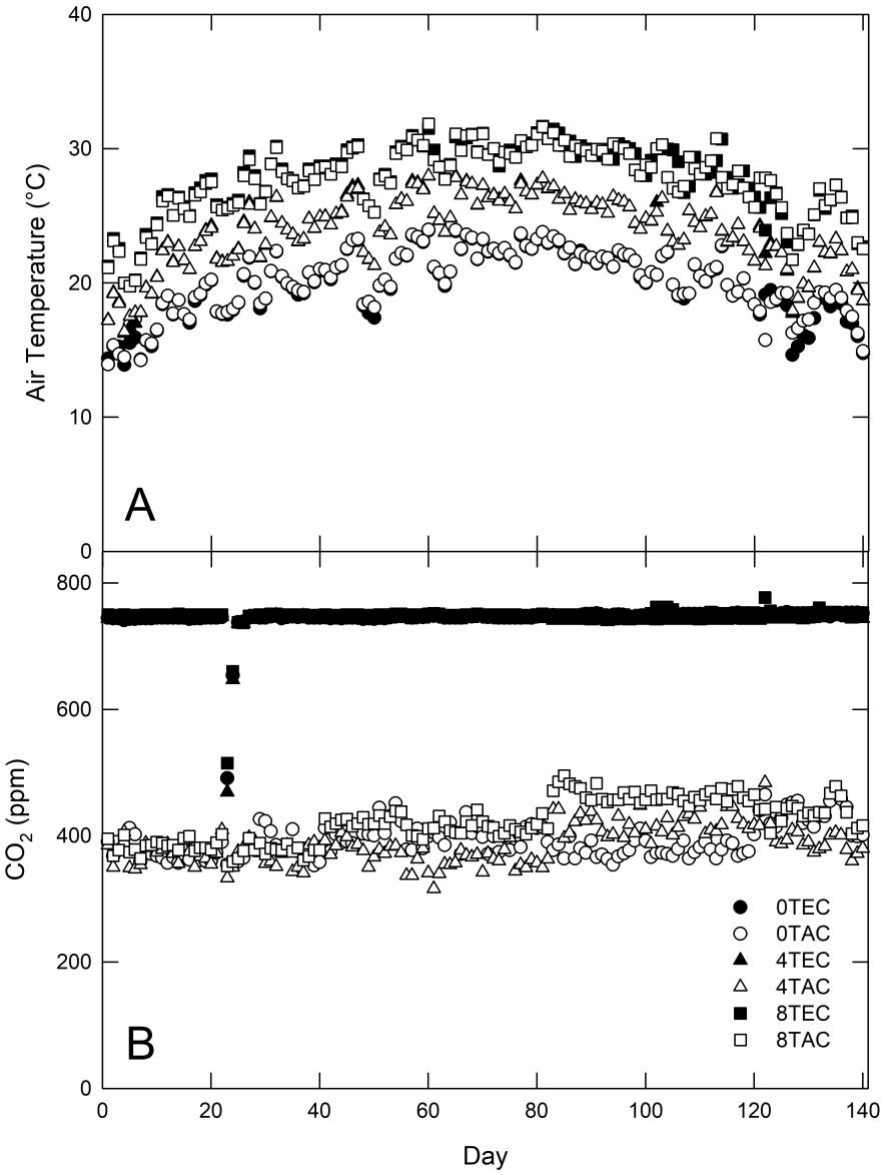

Figure 2.1. Daily temperature and CO_2 levels across all six biomes over the duration of the experiment. Day 0 indicates when seeds were potted (May 12th) and day 140 indicates when seedlings were harvested (Sept 28th). Temperature and CO_2 readings were taken daily. Circles, ambient temperature (0T); triangles, +4 ˚C warming (4T); squares, +8 ˚C warming (8T). White symbols, ambient growth CO_2 (AC); black symbols, elevated growth CO_2 (EC).

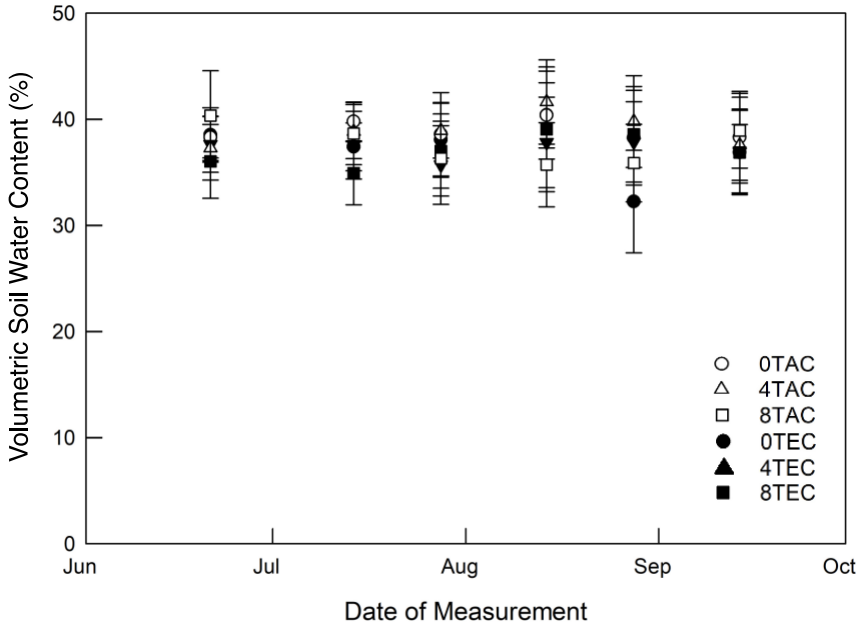

Figure 2.2. Volumetric soil water content (%) of tamarack seedlings grown under six climate treatments. Data are means ± SD, n = 40. Circles, ambient temperature (0T); triangles, +4 ˚C warming (4T); squares, +8 ˚C warming (8T). White symbols, ambient growth CO_2 (AC); black symbols, elevated growth CO_2 (EC).

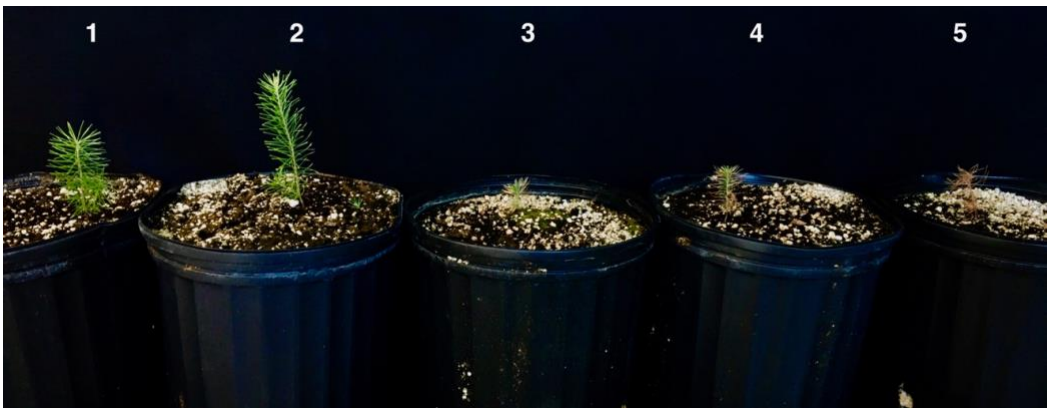

Figure 2.3. Representative seedlings showing the seedling health scale. (1) needles are 100% green; (2) seedling has <50% brown needle tissue; (3) seedling has approximately 1:1 brown to green leaf tissue; (4) seedling has >50% brown needle tissue; (5) seedling is 100% brown.

CO_2 on R_{shoot} (Amthor et al., 2001). The R_{shoot} was measured at 25 ˚C ($R_{shoot-25}$) and 35 ˚C ($R_{shoot-35}$) and these data were used to calculate Q_{10} values, defined as the temperature sensitivity of respiration rates over a 10 ˚C temperature increase (Atkin & Tjoelker, 2003):

$$Q_{10} = \left(\frac{R_{shoot-35}}{R_{shoot-25}}\right). \qquad \textit{Eq. 2.1}$$

Using the Q_{10} and $R_{shoot-25}$ values, shoot respiration at the growth temperature ($R_{shoot-growth}$) was calculated for each seedling. Shoot growth temperatures were based on the average daytime air temperature in the treatments at the beginning of the measurements. Once gas exchange measurements were complete, needles in the cuvette were removed and photographed to determine projected leaf area (LA) using ImageJ (US National Institutes of Health, Bestheda, MD, USA). The needles were then dried at 65 °C for 48 h and weighed for biomass to determine leaf mass area (LMA) (i.e. needle biomass divided by LA).

2.2.3 Biomass

After gas exchange measurements were completed, the remaining seedlings in the experiment were harvested and dried to a constant mass at 65 ˚C. Seedlings were divided into roots, shoots, and leaves, and each tissue was weighed individually.

2.2.4 Carbon and Nitrogen Analysis

A subset of the dried leaf tissue was ground using a Wiley mill (Thomas Scientific, Swedesboro, NJ, USA) and analyzed for C and N concentrations using an elemental analyzer (NCS 2500, Carlo Ebra, Peypin, France).

2.2.5 Modelling

Whole plant C fluxes of the seedlings were modelled at their respective growth temperatures. The calculated LMA was first used to extrapolate total LA for each seedling based on total leaf biomass. Seedling-level A_{net} under growth temperature and CO_2 concentrations ($A_{seedling}$) was then calculated for each seedling using:

$$A_{seedling} = A_{growth} \times LA_{seedling}, \quad \textit{Eq. 2.2}$$

where A_{growth} is A_{net} measured at the growth CO_2 and temperature.

Seedling-level shoot respiration rates ($R_{shoot\text{-}seedling}$) were calculated for each seedling as:

$$R_{shoot\text{-}seedling} = R_{shoot\text{-}growth} \times LA_{seedling}. \quad \textit{Eq. 2.3}$$

Seedling-level root respiration rates ($R_{root\text{-}seedling}$) were calculated as:

$$R_{root\text{-}seedling} = R_{root\text{-}growth} \times biomass_{root}, \quad \textit{Eq. 2.4}$$

where $biomass_{root}$ is dry root biomass and $R_{root\text{-}growth}$ is the root respiration rate at the growth temperature. Values of $R_{root\text{-}growth}$ were taken from Tjoelker, Oleksyn, & Reich (1999), who measured root respiration rates of tamarack seedlings grown at three night-time growth temperatures (12, 18 and 24 ˚C) and two CO_2 treatments (370 and 580 ppm). I plotted measured respiration rates from each temperature treatment against soil growth temperature to extrapolate $R_{root\text{-}growth}$ using the line of best fit (R^2=0.988). There was no effect of growth CO_2 on root respiration in Tjoelker et al. (1999), so root respiration rates from Tjoelker et al. (1999) were averaged across their two CO_2 treatments and a single value was used for a given growth temperature for both my AC and EC modelling. In another experiment in my thesis, I found that soil temperature was 6.8 ˚C cooler than air temperature (refer to Chapter Three). The temperatures used to calculate root respiration were therefore set at 18.2˚C for 0T, 22.2 ˚C for 4T, and 26.2˚C for 8T.

At the time of C flux measurements in August 2017, the photoperiod was 15 hours. Assuming saturating light, whole plant C uptake ($C_{seedling}$) was estimated by scaling $A_{seedling}$ up to 15 h ($A_{seedling\text{-}day}$) and R_{shoot} and R_{root} to 24 h ($R_{shoot\text{-}seedling\text{-}day}$ and $R_{root\text{-}seedling\text{-}day}$, respectively). Once all of these parameters were obtained, daily $C_{seedling}$ was calculated using:

$$C_{seedling} = A_{seedling\text{-}day} - R_{shoot\text{-}seedling\text{-}day} - R_{root\text{-}seedling\text{-}day}. \quad \textit{Eq. 2.5}$$

2.2.6 Statistics

R software (R Foundation for Statistical Computing, Vienna, Austria, EU) was used for modelling and statistical analyses. The R package 'plantecophys' was used to estimate J_{max} and V_{cmax} (Duursma, 2018). The R package 'tidyverse' was used for all statistical analyses (Wickham, 2017). Response variables of healthy seedlings from all six treatments were analyzed using two-way ANOVAs, considering growth temperature, growth CO_2 and their interaction. A post-hoc Tukey test was used when significant treatment effects were found. The comparison of variables between healthy and dying 8TAC seedlings was analyzed using a two-sample t-test.

2.3 Results

2.3.1 Carbon Fluxes and Photosynthetic Capacity in Healthy Seedlings

When comparing A_{net} under common conditions of 400 ppm CO_2 and 25 °C (A_{25}), there was no difference in A_{25} across the treatments (Table 2.1, Figure 2.4A). Under these common measurement conditions, there was also no treatment effect on stomatal conductance (g_{s25}), the ratio of intracellular CO_2 to ambient CO_2 (C_i/C_{a25}), or transpiration (E_{25}; Tables 2.1 and 2.2). The $R_{shoot\text{-}25}$ decreased by ~32% with increasing growth temperature, but the Q_{10} of shoot respiration was not altered by the treatments (Tables 2.1 and 2.2, Figure 2.4B). The ratio of A_{25} to $R_{shoot\text{-}25}$ (A/R_{25}), an index of shoot-level C balance, therefore increased by ~36% with increasing growth temperature, but there was no CO_2 effect (Table 2.1, Figure 2.4C).

In contrast, A_{net} measured at the growth CO_2 and temperature (A_{growth}) was 49-69% higher in EC seedlings compared to AC plants, but A_{growth} showed no response to growth temperature (Table 2.1, Figure 2.4D). Stomatal conductance at growth conditions ($g_{s\text{-}growth}$) was unaffected by the treatments, while transpiration measured at growth

Table 2.1. Summary of ANOVA statistics for response of gas exchange parameters as well as leaf biochemistry and growth, to the experimental treatments. Gas exchange parameters were measured at 25 ˚C and 400 ppm CO_2 (denoted by "25") and at growth conditions (denoted by "growth"). Parameters include: net CO_2 assimilation rate (A_{25}, A_{growth}); shoot dark respiration rate ($R_{shoot\text{-}25}$, $R_{shoot\text{-}growth}$); the ratio of net CO_2 assimilation rate to shoot dark respiration rate (A/R_{25}, A/R_{growth}); the Q_{10} of shoot respiration ($Q_{10\text{-}Rshoot}$); stomatal conductance (g_{s25}, $g_{s\text{-}growth}$); the ratio of intracellular to ambient CO_2 (C_i/C_{a25}, $C_i/C_{a\text{-}growth}$); transpiration rate (E_{25}, E_{growth}); the maximum rate of Rubisco carboxylation ($V_{cmax\text{-}25}$, $V_{cmax\text{-}growth}$); the maximum rate of electron transport ($J_{max\text{-}25}$, $J_{max\text{-}growth}$); and the ratio of J_{max} to V_{cmax} ($J_{max\text{-}25}/V_{cmax\text{-}25}$, $J_{max\text{-}growth}/V_{cmax\text{-}growth}$); needle percent carbon (%C); needle percent nitrogen (%N); the ratio of C/N; total biomass ($Biomass_{total}$); the root/shoot ratio ($Biomass_{root/shoot}$); tree height; and whole plant carbon (C) flux. T = growth temperature, CO_2 = growth CO_2 concentration, and DF = within-group degrees of freedom. P-values that are statistically significant ($p \leq 0.05$) are bolded.

	T			**CO_2**			**CO_2 x T**		
	DF	F-stat	P-value	DF	F-stat	P-value	DF	F-stat	P-value
(A) Gas Exchange Parameters									
A_{25}	30	0.05	0.95	30	0.05	0.83	30	0.21	0.81
$R_{shoot\text{-}25}$	30	7.09	**<0.05**	30	1.27	0.27	30	0.11	0.89
A/R_{25}	30	3.81	**<0.05**	30	1.47	0.24	30	0.05	0.95
A_{growth}	30	2.86	0.07	30	52.41	**<0.0001**	30	1.29	0.29
$R_{shoot\text{-}growth}$	30	0.04	0.96	30	1.22	0.28	30	0.15	0.86
A/R_{growth}	30	1.17	0.32	30	11.22	**<0.01**	30	0.61	0.55
$Q_{10\text{-}Rshoot}$	30	1.38	0.27	30	0.001	0.98	30	3.18	0.06
g_{s25}	30	0.03	0.97	30	0.89	0.35	30	0.85	0.44
$g_{s\text{-}growth}$	30	0.37	0.70	30	0.09	0.77	30	1.78	0.19
C_i/C_{a25}	30	0.07	0.93	30	1.57	0.22	30	0.35	0.71
$C_i/C_{a\text{-}growth}$	30	0.50	0.61	30	6.33	**<0.05**	30	0.03	0.97
E_{25}	30	0.05	0.95	30	0.07	0.95	30	0.25	0.78
E_{growth}	30	6.01	**<0.01**	30	0.04	0.84	30	1.16	0.33
(B) Photosynthetic Capacity									
$V_{cmax\text{-}25}$	30	0.10	0.90	30	0.12	0.73	30	0.09	0.92
$J_{max\text{-}25}$	30	0.52	0.60	30	0.86	0.36	30	0.07	0.93
$J_{max\text{-}25}/V_{cmax\text{-}25}$	30	4.65	**<0.05**	30	29.85	**<0.0001**	30	0.07	0.93
$V_{cmax\text{-}growth}$	30	14.67	**<0.0001**	30	3.51	0.07	30	1.74	0.19
$J_{max\text{-}growth}$	30	0.90	0.42	30	0.97	0.33	30	3.30	0.05

$J_{max\text{-}growth}/V_{cmax\text{-}growth}$	30	322.76	**<0.0001**	30	14.91	**<0.001**	30	16.82	**<0.0001**
(C) Leaf biochemistry									
%N	30	2.44	0.10	30	7.56	**<0.05**	30	2.00	0.15
%C	30	3.91	**<0.05**	30	2.88	0.10	30	0.61	0.55
C/N	30	8.87	0.29	30	1.42	**<0.01**	30	2.06	0.15
(D) Growth									
$Biomass_{total}$	234	12.97	**<0.0001**	234	19.15	**<0.0001**	234	1.67	0.19
$Biomass_{root/shoot}$	234	0.27	0.76	234	8.31	**<0.01**	234	8.53	**<0.001**
Tree Height	234	41.24	**<0.0001**	234	14.32	**<0.001**	234	5.88	**<0.05**
(E) Modelling									
Whole Plant C	30	3.20	**0.05**	30	12.89	**<0.01**	30	0.76	0.47

Table 2.2. Response of gas exchange parameters to the growth treatments. Gas exchange parameters were measured at 25 ˚C and 400 ppm CO_2 (denoted by "25") and at growth conditions (denoted by "growth). Parameters include: stomatal conductance (g_{s25}, $g_{s\text{-}growth}$; mmol H_2O m^{-2} s^{-1}); the ratio of intracellular to atmospheric CO_2 (C_i/C_{a25}, $C_i/C_{a\text{-}growth}$); transpiration rate (E_{25}, E_{growth}; mmol H_2O m^{-2} s^{-1}); and Q_{10} values of shoot respiration (R_{shoot}) of seedlings from different growth treatments. Means ± SE, n = 6. There were no differences between groups across all six growth treatments, so letters were not used to denote significance.

	0TAC	4TAC	8TAC	0TEC	4TEC	8TEC
g_{s25}	0.16±0.02	0.15±0.01	0.15±0.02	0.15±0.01	0.16±0.01	0.17±0.01
$g_{s\text{-}growth}$	0.16±0.02	0.15±0.01	0.14±0.02	0.14±0.01	0.15±0.01	0.17±0.01
C_i/C_{a25}	0.76±0.01	0.76±0.01	0.75±0.02	0.76±0.02	0.77±0.01	0.77±0.02
$C_i/C_{a\text{-}growth}$	0.76±0.01	0.74±0.01	0.74±0.02	0.78±0.02	0.78±0.01	0.77±0.02
E_{25}	1.97±0.24	1.81±0.17	1.86±0.26	1.89±0.07	2.00±0.13	1.88±0.19
E_{growth}	1.97±0.24	2.34±0.15	2.76±0.25	2.02±0.12	2.65±0.17	2.47±0.16
Q_{10}	1.70±0.06	1.71±0.02	1.70±0.02	1.63±0.02	1.71±0.05	1.81±0.04

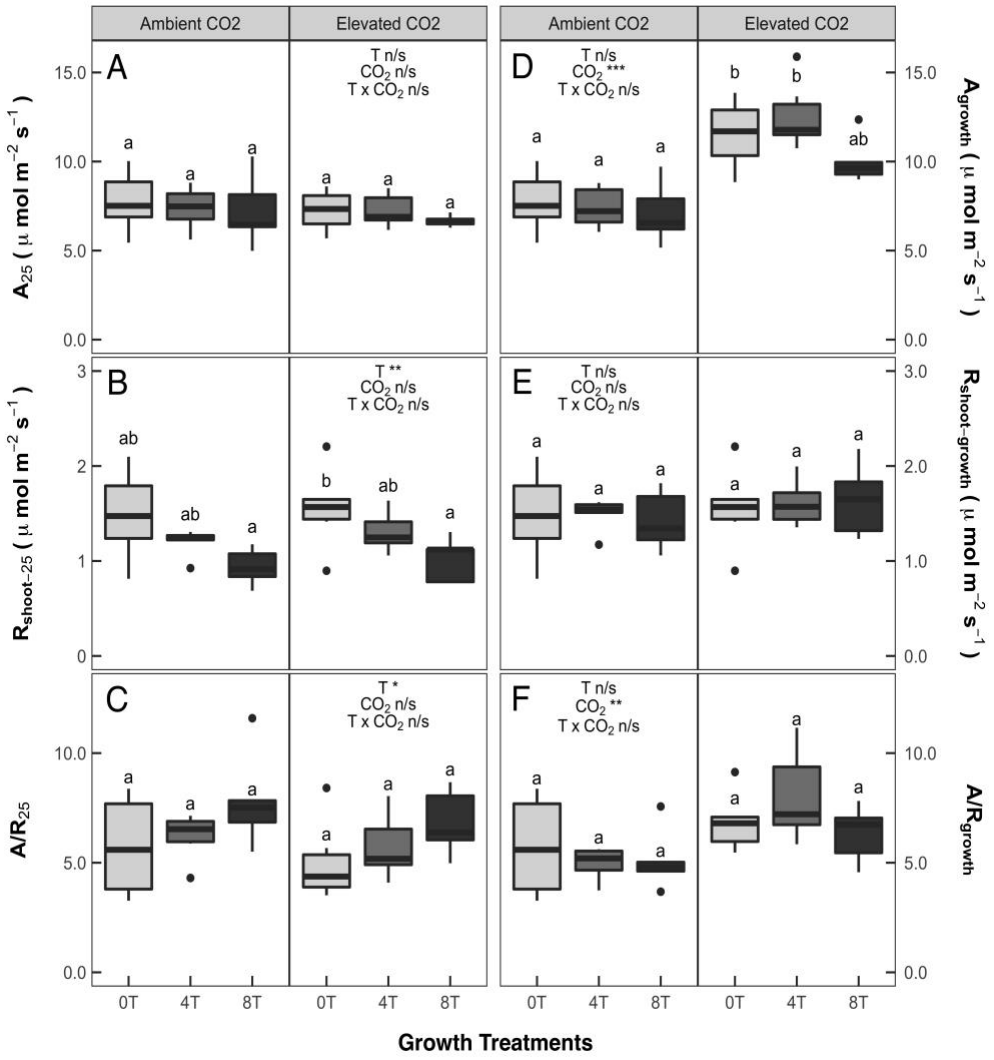

Figure 2.4. Photosynthetic and respiratory responses to elevated CO_2 and temperature treatments. Carbon fluxes were measured at 25 ˚C and 400 ppm (A,B,C) and growth conditions (25 ˚C for 0T, 29 ˚C for 4T, 33 ˚C for 8T; 400 ppm CO_2 for AC, 750 ppm CO_2 for EC) (D,E,F). A, D) net CO_2 assimilation rate ($A_{25˚C}$, A_{growth}); B, E) shoot dark respiration rate ($R_{shoot\text{-}25˚C}$, $R_{shoot\text{-}growth}$); C, F) the ratio of net CO_2 assimilation rate to respiration rate ($A/R_{25˚C}$, A/R_{growth}). Light grey, 0T; medium grey, 4T; dark grey, 8T. Horizontal lines in boxplots indicate means; whiskers display minimum and maximum values; dots indicate outliers; n = 6. Different letters above boxplots denote a significant difference across all six treatments ($p \leq 0.05$). T = growth temperature, CO_2 = growth CO_2 concentration, n/s = non-significant, * = $p \leq 0.05$, ** = $p<0.01$, and *** = $p<0.001$.

conditions (E_{growth}) increased by ~34% with warming and therefore higher measurement vapour pressure deficit (VPD; Tables 2.1 and 2.2). The ratio of intracellular CO_2 to ambient CO_2 at growth conditions ($C_i/C_{a\text{-}growth}$) was higher in EC than AC seedlings (Tables 2.1 and 2.2). Shoot dark respiration rates at growth temperature ($R_{shoot\text{-}growth}$) were unaffected by either growth temperature or CO_2 (Table 2.1, Figure 2.4E). The ratio of A_{growth} to R_{growth} (A/R_{growth}) was stimulated by EC (Table 2.1, Figure 2.4F).

When measured at 25 °C, the maximum rate of Rubisco carboxylation ($V_{cmax\text{-}25}$) and the maximum rate of electron transport ($J_{max\text{-}25}$) were unaffected by the treatments (Table 2.1, Figures 2.5A and B). The ratio of $J_{max\text{-}25}/V_{cmax\text{-}25}$ decreased from 0T to 8T, and increased with EC (Table 2.1, Figure 2.5C). When measured at the growth conditions, the maximum rate of Rubisco carboxylation ($V_{cmax\text{-}growth}$) was increased by warming (Table 2.1, Figure 2.5D), but the maximum rate of electron transport ($J_{max\text{-}growth}$) was unaffected by the treatments (Table 2.1, Figure 2.5E). The ratio of $J_{max\text{-}growth}/V_{cmax\text{-}growth}$ therefore decreased with warming and also increased with EC (Table 2.1, Figure 2.5F).

2.3.2 Growth Responses of Healthy Seedlings

Seedling growth was affected by both growth temperature and CO_2 (Table 2.1, Figure 2.6). As growth temperature increased from 0T to 4T, total seedling biomass was constant, but biomass decreased by ~73% at 8T (Table 2.1, Figure 2.6A). There was also greater biomass in EC compared to AC seedlings. The ratio of root/shoot biomass was similar across the warming treatments in AC seedlings, but higher in 8T than 0T in EC seedlings (Table 2.1, Figure 2.6B). Tree height was increased by EC only in the 0T seedlings, and 8T seedlings were shorter than 0T and 4T plants in both CO_2 treatments (Table 2.1, Figure 2.6C).

2.3.3 Needle Biochemical Responses of Healthy Seedlings

Leaf %N was lower in EC than AC trees, but there was no effect of growth temperature (Table 2.1, Figure 2.7A,). In contrast, as growth temperature increased, needle %C declined by ~4%, with no effect of growth CO_2 (Table 2.1, Figure 2.7B). The ratio of C/N was increased by EC but did not respond to growth temperature (Table 2.1, Figure 2.7C).

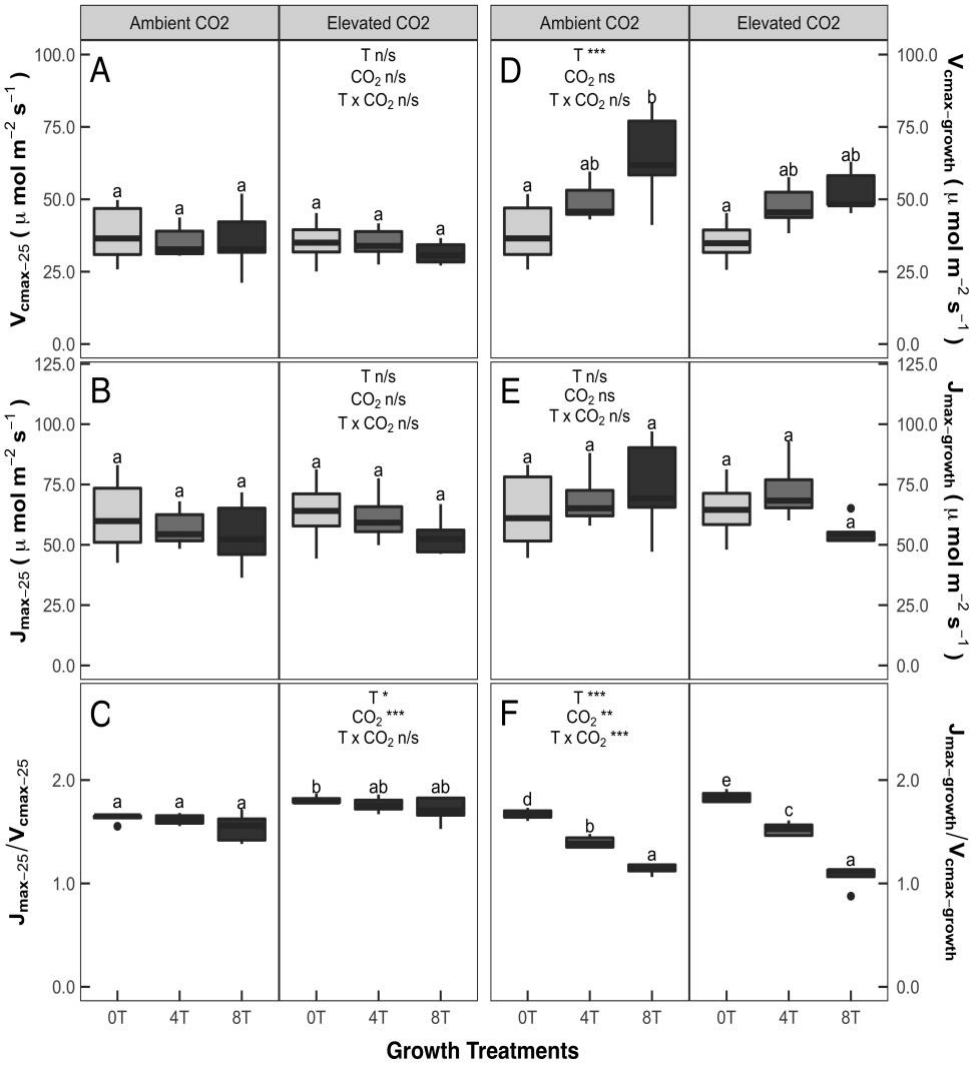

Figure 2.5. Responses of photosynthetic capacity to elevated CO_2 and temperature treatments. Photosynthetic capacity was measured at 25 ˚C and 400 ppm (A,B,C) and growth conditions (25 ˚C for 0T, 29 ˚C for 4T, 33 ˚C for 8T; 400 ppm CO_2 for AC, 750 ppm CO_2 for EC) (D,E,F). A, D) maximum rate of Rubisco carboxylation ($V_{cmax-25}$, $V_{cmax-growth}$); B, E) maximum rate of electron transport (J_{max-25}, $J_{max-growth}$); C, F) the ratio of J_{max} to V_{cmax} ($J_{max-25}/V_{cmax-25}$, $J_{max-growth}/V_{cmax-growth}$). Light grey, 0T; medium grey, 4T; dark grey, 8T. Horizontal lines in boxplots indicate means; whiskers display minimum and maximum values; dots indicate outliers; n = 6. Different letters above boxplots denote significant differences across all six treatments ($p \leq 0.05$). T = growth temperature, CO_2 = growth CO_2 concentration, n/s = non-significant, * = $p \leq 0.05$, ** = $p<0.01$, and *** = $p<0.001$.

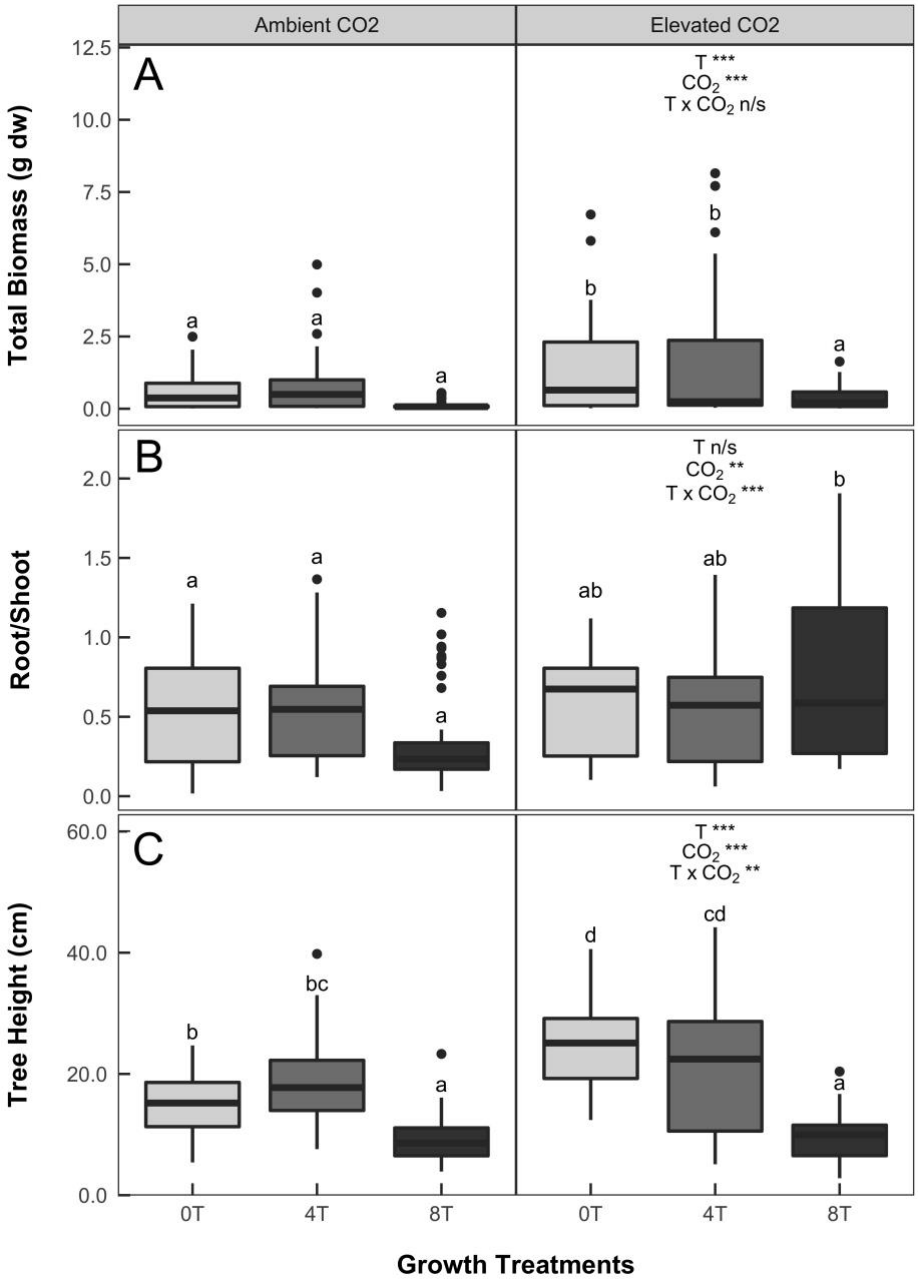

Figure 2.6. Growth responses to CO_2 and temperature treatments. A) Total biomass; B) the root/shoot ratio; and C) tree height. Light grey, 0T; medium grey, 4T; dark grey, 8T. Horizontal lines in boxplots indicate means; whiskers display minimum and maximum values; dots indicate outliers; n = 40. Different letters above boxplot denote significant differences across all six treatments ($p \leq 0.05$). T = growth temperature, CO_2 = growth CO_2 concentration, n/s = non-significant, * = $p \leq 0.05$, ** = $p < 0.01$, and *** = $p < 0.001$.

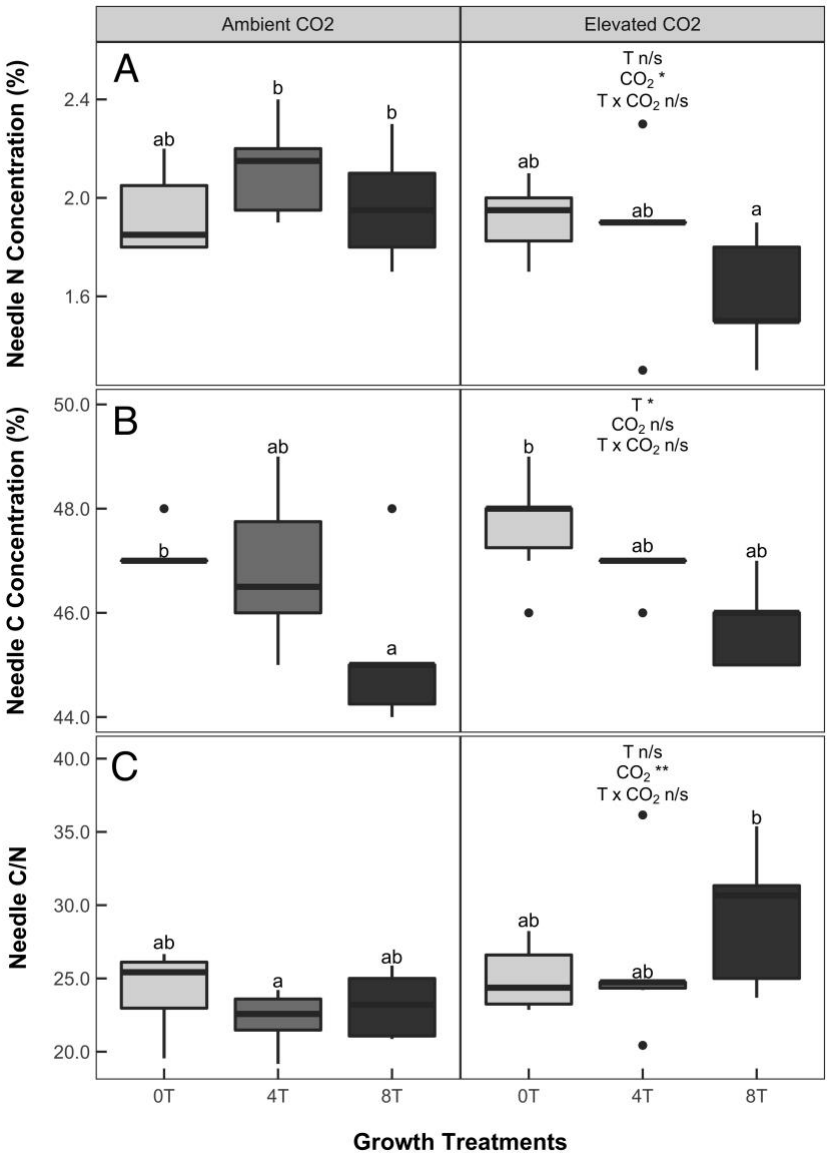

Figure 2.7. Needle biochemical responses to growth treatments. A) Needle nitrogen (N) concentrations; and B) carbon (C) concentrations; and C) the C/N ratio of needles. Light grey, 0T; medium grey, 4T; dark grey, 8T. Horizontal lines in boxplots indicate means; whiskers display minimum and maximum values; dots indicate outliers; n = 6. Different letters above boxplots denote significant differences across six treatments ($p \leq 0.05$). T = growth temperature, CO_2 = growth CO_2 concentration, n/s = non-significant, * = $p \leq 0.05$, ** = $p < 0.01$, and *** = $p < 0.001$.

2.3.4 Whole Carbon Modelling of Healthy Seedlings

When comparing whole plant daily C uptake, EC seedlings had ~2× higher daily plant C uptake than AC plants (Table 2.1, Figure 2.8). There was a weak overall temperature effect, with a trend of decreasing daily C uptake from 4T to 8T warming ($p=0.078$), but no interactive effects of growth CO_2 by temperature.

2.3.5 Comparison of Dying vs. Healthy Seedlings in the 8TAC Treatment

Overall, 8TAC seedlings had 40% mortality, characterized by complete needle browning, compared to 0% mortality in all other treatments. Similar to the quantification of C fluxes of healthy seedlings across all treatments, the same traits were examined in 8TAC dying and healthy seedlings at their growth temperature of 33 ˚C. There was no significant difference in A_{growth}, $R_{shoot\text{-}growth}$, $J_{max\text{-}growth}$, $V_{cmax\text{-}growth}$ or $J_{max}/V_{cmax\text{-}growth}$ between healthy and dying seedlings, nor was there any significant difference in the ratio of A_{growth} to $R_{shoot\text{-}growth}$ (A/R_{growth}) (Table 2.3, Figures 2.9A-F). Needle %C was 3% lower in the dying seedlings, although the needle %N and the ratio of C/N were similar between all 8TAC seedlings (Table 2.3, Figures 2.10A-C). There were also negative correlations between seedling health and their needle %C and A/R_{growth} (Figures 2.11A and B).

2.4 Discussion

2.4.1 Carbon Balance and Photosynthetic Capacity

There was surprisingly little evidence for photosynthetic acclimation (i.e., no change in photosynthetic capacity) across 8 °C of warming and a 350 ppm increase in growth CO_2, indicating that tamarack has considerable capacity for maintaining C uptake under future climates. Many studies have shown that plants grown at elevated CO_2 tend to have reduced photosynthetic capacity (Ainsworth & Long, 2005; Albert et al., 2011; Moore et al., 1999), but my work supports the idea that conifers may be less sensitive to rising CO_2 than are other plant functional types (Ainsworth & Rogers, 2007; Medlyn et al., 2001). While less is known about how deciduous conifers will respond to elevated CO_2, a study by Dusenge et al. (2020) found that photosynthetic capacity was unresponsive to

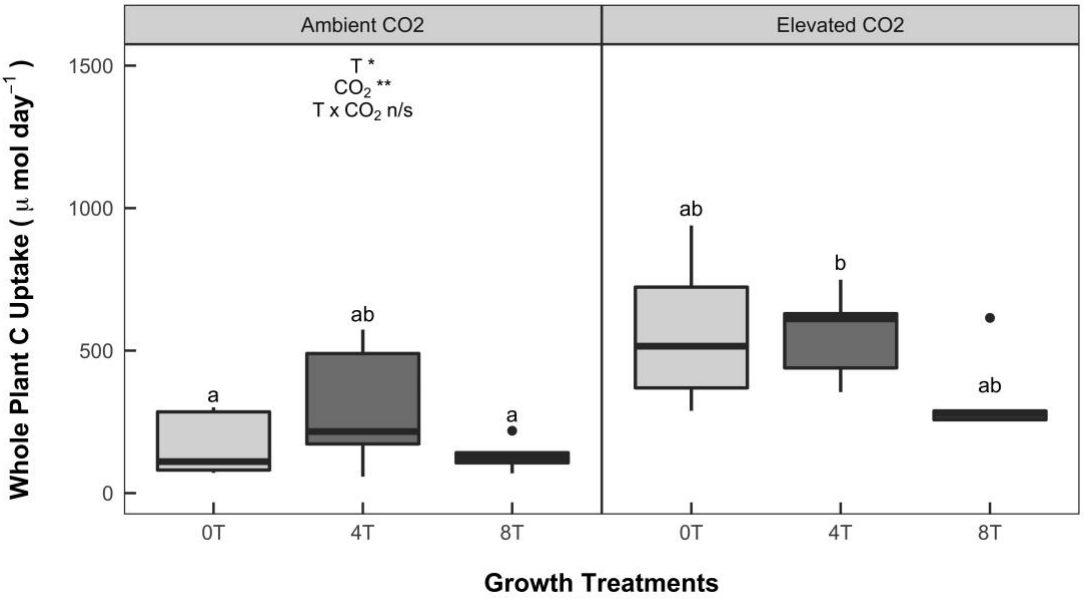

Figure 2.8. Whole plant daily C uptake of seedlings across the growth treatments. Light grey, 0T; medium grey, 4T; dark grey, 8T. Horizontal lines in boxplots indicate means; whiskers display minimum and maximum values; dots indicate outliers; n = 6. Different letters above boxplots denote significant differences across six treatments ($p \leq 0.05$). T = growth temperature, CO_2 = growth CO_2 concentration, n/s = non-significant, * = $p \leq 0.05$, ** = $p < 0.01$, and *** = $p < 0.001$.

Table 2.3. Summary of two-sample t-test statistics for parameters comparing dying and healthy 8TAC seedlings. Parameters include: net photosynthesis at growth conditions (A_{growth}); shoot dark respiration at growth conditions ($R_{shoot\text{-}growth}$); ratio between A_{growth} and $R_{shoot\text{-}growth}$ (A/R_{growth}); maximum rate of electron transport (J_{max}); maximum rate of Rubisco carboxylation (V_{cmax}); ratio between $J_{max\text{-}growth}$ and $V_{cmax\text{-}growth}$ ($J_{max}/V_{cmax\text{-}growth}$); percent needle carbon (%C); percent needle nitrogen (%N); and the ratio of needle C/N. DF = within-group degrees of freedom. P-values that are statistically significant ($p \leq 0.05$) are bolded.

	Healthy vs. Dying		
	DF	T-stat	P-value
A_{growth}	10	0.35	0.73
$R_{shoot\text{-}growth}$	10	0.64	0.54
A/R_{growth}	10	1.87	0.09
V_{cmax}	10	0.60	0.56
J_{max}	10	1.11	0.30
J_{max}/V_{cmax}	10	0.62	0.55
% Nitrogen	10	1.30	0.22
% Carbon	10	2.45	**<0.05**
C/N	10	0.91	0.38

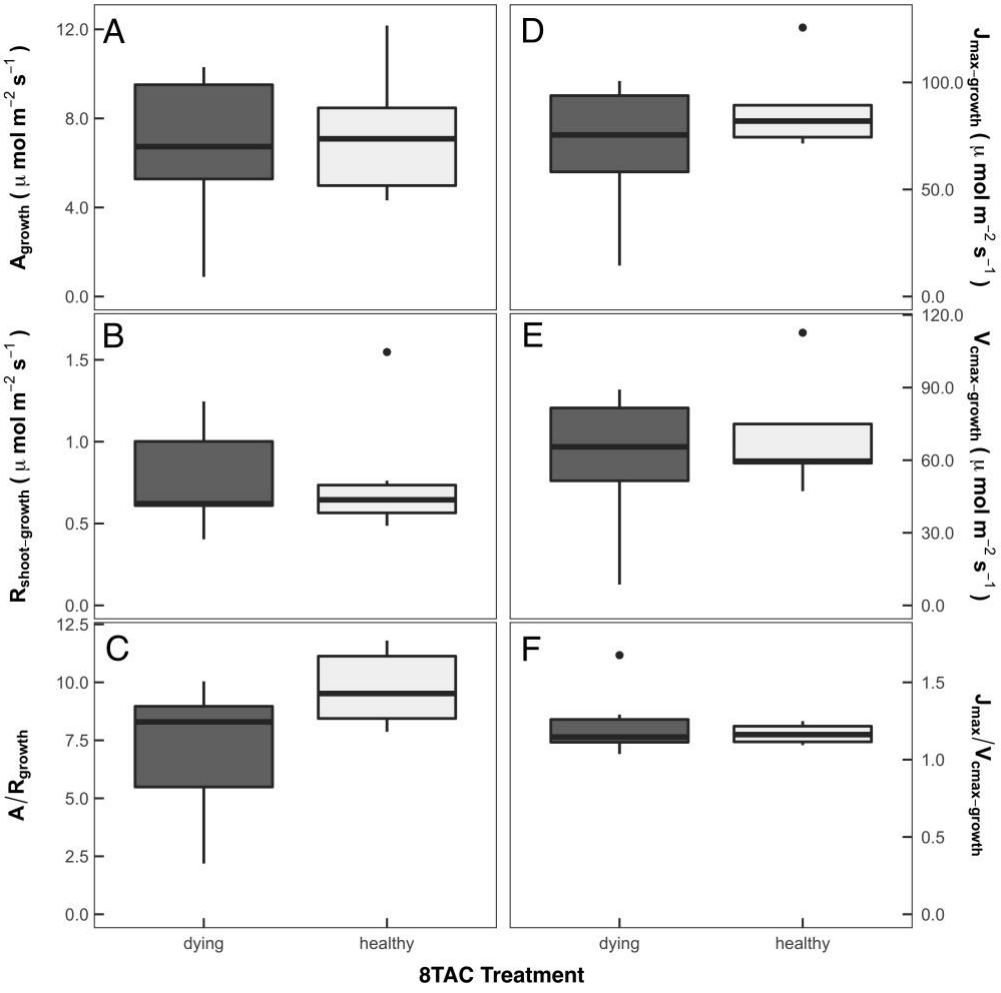

Figure 2.9. Comparison of carbon fluxes and photosynthetic capacity parameters between dying and healthy seedlings grown in the 8TAC treatment. A) Net CO_2 assimilation rate (A_{growth}), B) shoot dark respiration rate ($R_{shoot-growth}$), C) the ratio of A_{growth} to $R_{shoot-growth}$ (A/R_{growth}), D) maximum rate of electron transport ($J_{max-growth}$), E) maximum rate of Rubisco carboxylation ($V_{cmax-growth}$), and F) the ratio of $J_{max-growth}$ to $V_{cmax-growth}$ ($J_{max}/V_{cmax-growth}$). Grey, dying seedlings; white, healthy seedlings. Horizontal lines of boxplots indicate means; whiskers display minimum and maximum values; dots indicate outliers; n = 6. Different letters above boxplots denote significant differences between groups ($p \leq 0.05$).

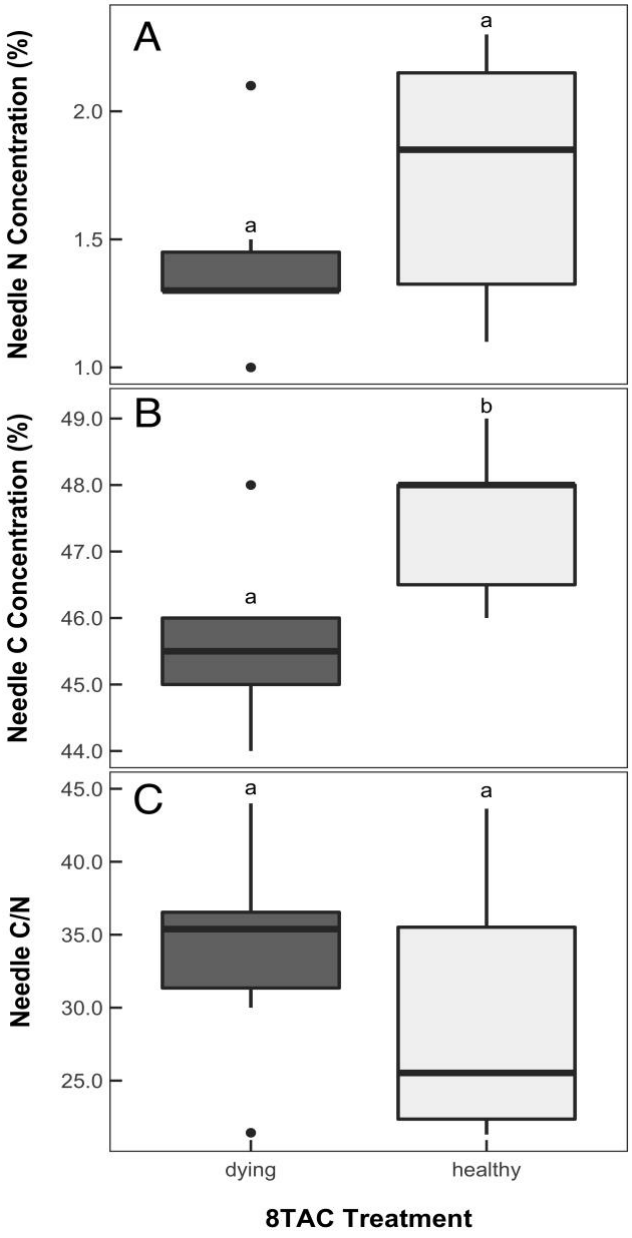

Figure 2.10. Comparison of leaf biochemical responses between dying and healthy seedlings grown in the 8TAC treatment. A) Percent carbon, B) percent nitrogen, and C) the ratio of needle percent carbon to nitrogen (C/N). Grey, dying seedlings; white, healthy seedlings. Horizontal lines of boxplots indicate means; whiskers display minimum and maximum values; dots indicate outliers; n = 6. Different letters above boxplots denote significant differences between groups ($p \leq 0.05$).

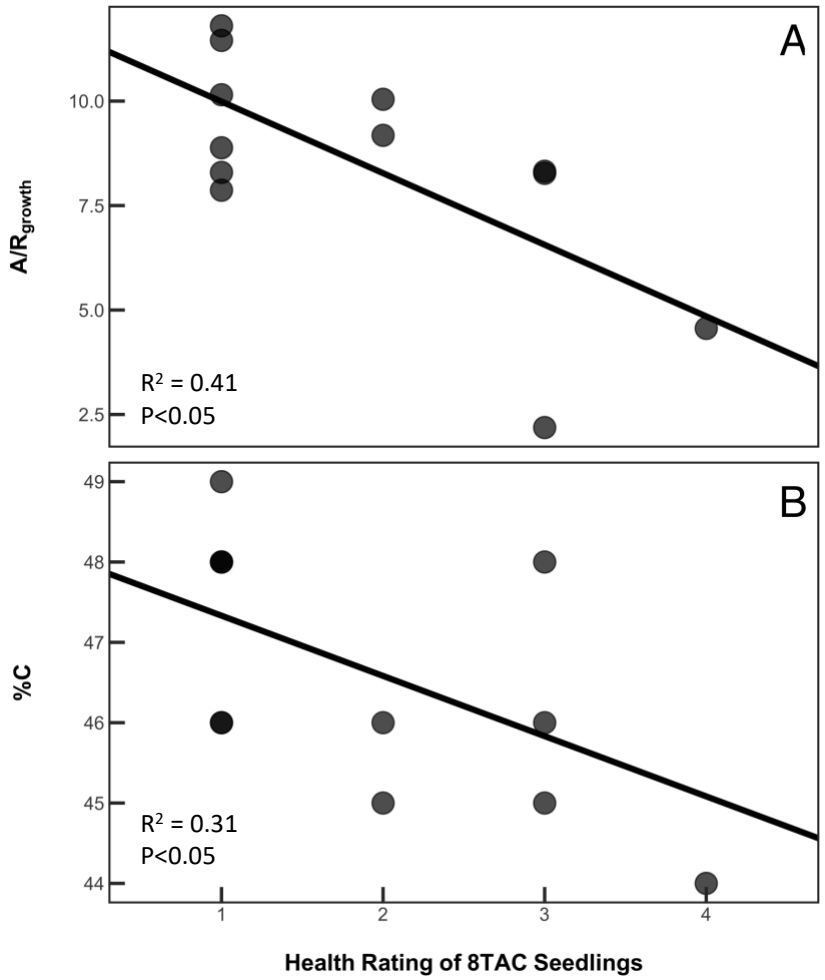

Figure 2.11. Relationship between seedling health rating and leaf C balance and foliar C. A) The ratio of net CO_2 assimilation rate to shoot dark respiration rate at growth conditions (A/R_{growth}) and B) the percent needle carbon (%C). Points represent individual seedlings, n = 12. Solid line, linear regression.

changing CO_2 in tamarack seedlings. Photosynthetic acclimation to temperature has been well documented in the literature (Kroner & Way, 2016; Tjoelker et al., 1998; Way & Oren, 2010; Yamori, Hikosaka, & Way, 2014; Yamori, Noguchi, & Terashima, 2005). However, the response of boreal tree species to warming (as indicated by A_{net}) is variable. For example, *Pinus sylvestrius* seedlings increase A_{growth} with warming, whereas *Picea abies* seedlings decrease A_{growth} with warming (Kurepin et al., 2018). *Abies faxoniana* and *Picea asperata* seedlings also increase A_{growth} with warming (Yin, Lui, & Lai, 2008), while *Picea mariana* seedlings decrease A_{growth} (Tjoelker et al. 1998). While it is unusual to find such photosynthetic stability across such a broad range of growth temperatures, thermal acclimation can result in a similar A_{growth} (Way & Yamori, 2014). Instead, the thermal optimum of photosynthetic rates (T_{opt}) is considered the most sensitive indicator of thermal acclimation (Berry & Bjorkman, 1980; Yamori et al., 2014), but it was not measured in this study. The lack of photosynthetic acclimation was correlated with the maintenance of relatively similar concentrations of needle N, indicating that warming had little effect on photosynthetic enzymes and protein concentrations across the treatments.

Since g_s was also relatively insensitive to warming and CO_2, there was higher $C_i/C_{a\text{-}growth}$ under EC, and therefore ~60% higher A_{growth} in the EC seedlings. At current CO_2 concentrations, Rubisco is substrate-limited; by increasing intracellular CO_2 concentrations, photosynthetic rates increase and photorespiration is suppressed (Sage & Kubien, 2007). Stimulation of photosynthesis by EC in mature conifers is common in the absence of sink limitations (Ainsworth & Rogers, 2007; DeLucia et al., 1999; Ryan, 2013; Dusenge, 2019) as these limitations can feed back to instigate a down-regulation of photosynthesis (Ainsworth & Long, 2005; Leakey et al., 2009). Dusenge et al. (2020) and Tjoelker et al. (1999) also found that warming led to a constant A_{growth}, but that EC stimulated A_{growth}, indicating that these results are robust. My findings add to the literature indicating that photosynthetic rates of tamarack are highly responsive to changes in elevated CO_2, even when stomatal conductance is not.

While photosynthetic capacity at 25 °C was unaffected by the treatments, the ratio of $J_{max\text{-}25}/V_{cmax\text{-}25}$ was reduced with warming. Meta-analyses have revealed that the effect of

warming on photosynthetic capacity measured at 25 °C is variable (Way and Oren, 2010; Way & Yamori, 2014), and we still lack a general understanding of how $V_{cmax\text{-}25}$ and $J_{max\text{-}25}$ will be affected by a warming world. Tamarack seedlings in the studies by Dusenge et al. (2020) had decreased photosynthetic capacity with warming and associated decreases in foliar N concentrations (%N), indicative of a lower investment into photosynthetic enzymes (Reich et al., 1998). In my study, photosynthetic capacity did not acclimate to warming, supported by similar %N across temperature treatments indicating there was no change in the relative amounts of Rubisco. But a decline in $J_{max\text{-}25}/V_{cmax\text{-}25}$ in warm-grown plants is common (Kattge & Knorr, 2007; Yamori et al., 2005; Dusenge, 2019), and is thought to indicate a shift in N partitioning within the photosynthetic apparatus from RuBP carboxylation to RuBP regeneration (Hikosaka, Ishikawa, Borjigidai, Muller, & Onoda, 2006). Under low temperatures, plants invest more N into RuBP regeneration, which is less efficient under cool temperatures, resulting in a higher ratio of cytochrome *f* to Rubisco and subsequently a higher ratio of $J_{max\text{-}25}/V_{cmax\text{-}25}$.

When measured at growth conditions, $J_{max\text{-}growth}$ was constant across the treatments, while $V_{cmax\text{-}growth}$ increased across 0T to 8T treatments. Rising leaf temperatures generally stimulate both V_{cmax} and J_{max}, (Kattge & Knorr, 2007; Way & Oren, 2010), which makes the J_{max} data somewhat surprising. However, the "coordination hypothesis" predicts that V_{cmax} and J_{max} should be co-limiting (Hikosaka et al., 2006; Maire et al., 2012; Togashi et al., 2018). Given this, the stimulation of $V_{cmax\text{-}growth}$ with warming may allow plants to match higher Rubisco activity with higher photosynthetic rates (Togashi et al., 2018). Higher rates of RuBP carboxylation by Rubisco would maintain A_{growth} across the warming treatments despite the greater photorespiratory losses expected with increased temperatures. Both $J_{max\text{-}25}/V_{cmax\text{-}25}$ and $J_{max\text{-}growth}/V_{cmax\text{-}growth}$ decreased in EC seedlings, a result linked to increased efficiency of Rubisco carboxylation under high CO_2 and a resultant rebalancing of allocation towards J_{max}.

Thermal acclimation of respiration mitigated C losses across the warming treatments. Reductions in respiration rates in response to long-term warming is common (Atkin & Tjoelker, 2003; Loveys et al., 2003; Reich et al., 1998; Slot & Kitajima, 2015; Tjoelker et al., 1999; Dusenge et al., 2020). Overall, thermal acclimation of respiration led to similar

rates of R_{growth} and similar A/R_{growth} across 0T to 8T treatments. In comparison, photosynthetic stimulation by EC increased A/R_{growth}. By acclimating respiration, tamarack was able to effectively minimize C losses under +8 ˚C and maintain similar modelled C balances across all warming treatments.

2.4.2 Growth, Biomass Allocation, and C/N Dynamics

While the C flux data are not indicative of warming stress, seedling biomass and height were 51-73% smaller at 8T compared to 0T and 4T treatments. These growth reductions were largely offset by EC, implying that the decline is growth is related to plant C dynamics. In support of this hypothesis, 8TAC seedlings had 50% lower root/shoot ratios than 8TEC seedlings, indicating increased allocation to aboveground tissues (i.e. photosynthetic tissue) to compensate for limited C availability (Poorter et al., 2012). The biomass allocation patterns of different conifer species to warming and EC are variable (Yin et al., 2008). But other work has confirmed that tamarack increases allocation to leaf tissues under warming conditions (Dusenge et al., 2020). Plants with low belowground biomass allocation prioritize C gain over water uptake and could be at a greater risk under drier climates in the future (Way & Oren, 2010). As tamarack seedlings in this study were well watered, 8TAC seedlings were able to invest in aboveground tissues to maximize C gains without experiencing water stress, but this may not be true in tamarack that experience warming in the forest over coming decades.

Warming also reduced foliar C concentrations (%C). Foliar %C has been estimated at ~50% in conifers (Ma et al., 2018), so a reduction by 5% in 8T seedlings is considerable and may indicate C limitation. Surprisingly, decreases in %C were not offset by EC, despite the increase in modelled whole plant C availability. Similarly, Tjoelker et al. (1999) found foliar %C decreased in warming treatments but was unaffected by EC. Higher C availability from stimulated A_{growth} under EC was apparently allocated to growth over storage, given the strong effect of EC on plant growth. Prioritization of growth over storage is common in conifer seedlings (Dietze et al., 2014), but the smaller C stores often found in seedlings may make them more vulnerable to C stress under this C allocation strategy.

Rising CO_2 concentrations can affect foliar nitrogen content (%N). As mentioned above, %N was unaffected by warming, but decreased in EC seedlings, possibly due to a growth dilution effect. The "dilution hypothesis" describes how N assimilation is not enhanced at the same rate as C assimilation under elevated CO_2 (Taub & Wang, 2008). In a meta-analysis of 62 plant species, Yin (2002) found that the proportional decline in %N with EC is highest in deciduous woody species, such as tamarack. Plants with higher A_{net} under EC are able to invest less in photosynthetic enzymes and still perform better than AC plants. Elevated CO_2 in future climates will likely be beneficial for tamarack C gain and growth, even when combined with moderate warming, as seen in 0TEC and 4TEC seedlings.

2.4.3 Mortality in 8TAC Seedlings

One of the objectives of this study was to investigate whether C starvation was the cause of mortality in 8TAC seedlings. The few studies that have measured tree mortality have found higher respiration in seedlings experiencing C starvation (Sevanto et al., 2014; Wiley et al., 2017). These studies also found depletions in plant C after long durations of C stress. When comparing C fluxes of dying vs. healthy seedlings, the ratio of A/R_{growth} was lowest in the 8T seedlings, but this was not significant, and there was no difference between the two groups in R_{growth}. However, across all treatments, healthy 8TAC seedlings had lower foliar %C. The comparative measurements between healthy and dying 8TAC seedlings were completed later than the measurements across all healthy treatments, and this led to overall higher %C in healthy 8TAC seedlings than initially measured. Conifers store larger amounts of C later in the season in preparation for winter, which could account for this difference in %C measured in 8TAC healthy seedlings at the two time points (Kozlowski, 1992). Regardless, the %C was lower in dying 8TAC seedlings compared to healthy seedlings, which supports the C starvation hypothesis. Additionally, both A/R_{growth} and %C were negatively correlated with the health ratings, providing evidence that C balance was slowly depleted as seedling health deteriorated. Carbon limitations were evident through decreased C availability but were not as strongly supported by leaf C balances, which may be indicative of unquantified C sinks elsewhere in the dying seedlings. While differences between the means of the healthy and dying

trees may have also been obscured by large variation in individual trees, especially because dying seedlings were measured at different health ratings, my data imply that warming, even without water stress, can lead to C stress and tree death. While my results were assessed on seedlings, old-growth trees in the forest may be better equipped than seedlings against C stress as they have larger C stores, which is one of the greatest determinants of survival against C starvation (Hartmann & Trumbore, 2016).

Despite maintaining constant air humidity and volumetric soil water content, VPD increases with air temperature, so atmospheric water stress may have occurred under +8 ˚C warming. However, the VPD would have been only ~0.7 kPa higher in the 8T glasshouses than the 0T glasshouses. Given that g_s was constant across treatments, a higher VPD in the 8T treatments would lead to higher rates of transpiration in 8T seedlings than those from 0T. This is unlikely to have led to significant water stress in the 8T plants though, since they were watered daily and had large soil volumes to hold water compared to their very small root masses. But in more realistic ecological conditions, an inability to acclimate stomatal conductance to warming may be detrimental to tamarack as droughts are predicted to become more frequent with climate change.

2.4.4 Conclusions

Whether 8TAC seedlings were experiencing C stress alone or in combination with water stress, 8T warming coupled with ambient CO_2 led to decreased growth and high mortality. Thermal acclimation of respiration minimized C losses under warming and resulted in similar C balances across temperature treatments. While moderate warming combined with EC may be beneficial to C balance, +8 ˚C warming was detrimental to growth even when supplemented with EC. To reach warming of +8 ˚C, atmospheric levels of CO_2 will likely have to rise, which would prevent the 40% mortality observed in 8TAC seedlings. However, trees may experience +8 ˚C warming without strong increases in CO_2 if other greenhouse gases, such as methane (CH_4), accumulate in the atmosphere. The melting of permafrost continues to release large amounts of CH_4, which is 84% more potent than CO_2 in terms of warming potential (Schuur et al., 2015). Therefore, CO_2 may not be able to offset C stress caused by warming in the future. Regardless, my results indicate that high temperature-induced C stress can reduce growth and increase mortality

in the absence of water stress, which may be detrimental to the future functioning of tamarack and, potentially, other boreal tree species as warming continues.

2.5 References

Adams, H. D., Zeppel, M. J. B., Anderegg, W. R. L., Hartmann, H., Landhäusser, S. M., Tissue, D. T., … McDowell, N. G. (2017). A multi-species synthesis of physiological mechanisms in drought-induced tree mortality. *Nature Ecology and Evolution*, *1*(9), 1285–1291. https://doi.org/10.1038/s41559-017-0248-x

Ainsworth, E. A., & Long, S. P. (2005). What have we learned from 15 years of free-air CO_2 enrichment (FACE)? A meta-analytic review of the responses of photosynthesis, canopy properties and plant production to rising CO_2. *New Phytologist*, *165*(2), 351–372. https://doi.org/10.1111/j.1469-8137.2004.01224.x

Ainsworth, E. A., & Rogers, A. (2007). The response of photosynthesis and stomatal conductance to rising [CO_2]: Mechanisms and environmental interactions. *Plant, Cell and Environment*, *30*(3), 258–270. https://doi.org/10.1111/j.1365-3040.2007.01641.x

Albert, K. R., Mikkelsen, T. N., Michelsen, A., Ro-Poulsen, H., & van der Linden, L. (2011). Interactive effects of drought, elevated CO_2 and warming on photosynthetic capacity and photosystem performance in temperate heath plants. *Journal of Plant Physiology*, *168*(13), 1550–1561. https://doi.org/10.1016/j.jplph.2011.02.011

Allen, C. D., Macalady, A. K., Chenchouni, H., Bachelet, D., McDowell, N., Vennetier, M., … Cobb, N. (2010). A global overview of drought and heat-induced tree mortality reveals emerging climate change risks for forests. *Forest Ecology and Management*, *259*(4), 660–684. https://doi.org/10.1016/j.foreco.2009.09.001

Allen, C. D., Breshears, D. D., & McDowell, N. G. (2015). On underestimation of global vulnerability to tree mortality and forest die-off from hotter drought in the Anthropocene. *Ecosphere*, *6*(8), 1–55. https://doi.org/10.1890/ES15-00203.1

Amthor, J. S., Koch, G. W., Willms, J. R., & Layzell, D. B. (2001). Leaf O_2 uptake in the dark is independent of coincident CO_2 partial pressure. *Journal of Experimental Botany*, *52*(364), 2235–2238. https://doi.org/10.1093/jexbot/52.364.2235

Anderegg, W. R. L., Berry, J. A., & Field, C. B. (2012). Linking definitions, mechanisms, and modeling of drought-induced tree death. *Trends in Plant Science*, *17*(12), 693–700. https://doi.org/10.1016/j.tplants.2012.09.006

Atkin, O. K., & Tjoelker, M. G. (2003). Thermal acclimation and the dynamic response of plant respiration to temperature. *Trends in Plant Science*, *8*(7), 343–351. https://doi.org/10.1016/S1360-1385(03)00136-5

Berry, J., & Bjorkman, O. (1980). Photosynthetic response and adaptation to temperature in higher plants. *Annual Review of Plant Physiology*, *31*(1), 491–543. https://doi.org/10.1146/annurev.pp.31.060180.002423

Brandt, J. P. (2009). The extent of the North American boreal zone. *Environmental Reviews, 17*, 101–161. https://doi.org/10.1139/A09-004

Cramer, W., Yohe, G. W., Auffhammer, M., Huggel, C., Molau, U., Dias, M. A. F. S., … Tibig, L. (2014). Detection and attribution of observed impacts. In C. B. Field, V. R. Barros, D. J. Dokken, K. J. Mach, M. D. Mastrandrea, T. E. Bilir, … L. L. White (Eds.), *Climate Change 2014: Impacts, Adaptation, and Vulnerability. Part A: Global and Sectoral Aspects. Contribution of Working Group II to the Fifth Assessment Report of the Intergovernmental Panel of Climate Change* (pp. 979–1037). Cambridge, United Kingdom and New York, NY, USA: Cambridge University Press.

DeLucia, E. H., Hamilton, J. G., Naidu, S. L., Thomas, R. B., Andrews, J. A., Finzi, A., … Schlesinger, W. H. (1999). Net primary production of a forest ecosystem with experimental CO_2 enrichment. *Science*, *284*(5417), 1177–1179. https://doi.org/10.1126/science.284.5417.1177

Dietze, M. C., Sala, A., Carbone, M. S., Czimczik, C. I., Mantooth, J. A., Richardson, A. D., & Vargas, R. (2014). Nonstructural carbon in woody plants. *Annual Review of Plant Biology*, *65*(1), 667–687. https://doi.org/10.1146/annurev-arplant-050213-040054

Duursma, R. (2018) Plantecophys: Modelling and analysis of leaf gas exchange data. R Package Version 1.4.4.

Dusenge, M. E., Madhavji, S., & Way, D. A. (2020). Contrasting acclimation responses to elevated CO_2 and warming between an evergreen and a deciduous boreal conifer. *Global Change Biology.* https://doi.org/10.1111/gcb.15084

Dusenge, M. E. (2019). *Effects of elevated temperature and elevated CO_2 on leaf carbon fluxes in boreal conifers: lab and field studies* (Doctoral thesis, University of Western Ontario, Ontario, Canada). Retrieved from: https://ir.lib.uwo.ca/etd/6607

Farquhar, G. D., von Caemmerer, S., & Berry, J. A. (1980). A biochemical model of photosynthetic CO_2 assimilation in leaves of C_3 species. *Planta*, *149*(1), 78–90. https://doi.org/10.1007/BF00386231

Hartmann, H., Moura, C. F., Anderegg, W. R. L., Ruehr, N. K., Salmon, Y., Allen, C. D., … O'Brien, M. (2018). Research frontiers for improving our understanding of drought-induced tree and forest mortality. *New Phytologist*, *218*(1), 15–28. https://doi.org/10.1111/nph.15048

Hartmann, H., & Trumbore, S. (2016). Understanding the roles of nonstructural carbohydrates in forest trees - from what we can measure to what we want to know. *New Phytologist*, *211*(2), 386–403. https://doi.org/10.1111/nph.13955

Hikosaka, K., Ishikawa, K., Borjigidai, A., Muller, O., & Onoda, Y. (2006). Temperature acclimation of photosynthesis: Mechanisms involved in the changes in temperature dependence of photosynthetic rate. *Journal of Experimental Botany*, *57*(2 SPEC. ISS.), 291–302. https://doi.org/10.1093/jxb/erj049

Islam, M. A., & Macdonald, S. E. (2004). Ecophysiological adaptations of black spruce (*Picea mariana*) and tamarack (*Larix laricina*) seedlings to flooding. *Trees - Structure and Function*, *18*(1), 35–42. https://doi.org/10.1007/s00468-003-0276-9

Kattge, J., & Knorr, W. (2007). Temperature acclimation in a biochemical model of photosynthesis: A reanalysis of data from 36 species. *Plant, Cell and Environment*, *30*(9), 1176–1190. https://doi.org/10.1111/j.1365-3040.2007.01690.x

Kozlowski, T. T. (1992). Carbohydrate sources and sinks in woody plants. *The Botanical Review*, *58*(2), 107–222. https://doi.org/10.1007/BF02858600

Kroner, Y., & Way, D. A. (2016). Carbon fluxes acclimate more strongly to elevated growth temperatures than to elevated CO_2 concentrations in a northern conifer. *Global Change Biology*, *22*(8), 2913–2928. https://doi.org/10.1111/gcb.13215

Kurepin, L. V., Stangl, Z. R., Ivanov, A. G., Bui, V., Mema, M., Hüner, N. P. A., … Hurry, V. (2018). Contrasting acclimation abilities of two dominant boreal conifers to elevated CO_2 and temperature. *Plant Cell and Environment*, *41*(6), 1331–1345. https://doi.org/10.1111/pce.13158

Kurz, W. A., Shaw, C. H., Boisvenue, C., Stinson, G., Metsaranta, J., Leckie, D., … Neilson, E. T. (2013). Carbon in Canada's boreal forest: A synthesis. *Environmental Reviews*. Canadian Science Publishing. https://doi.org/10.1139/er-2013-0041

Leakey, A. D. B., Ainsworth, E. A., Bernacchi, C. J., Rogers, A., Long, S. P., & Ort, D. R. (2009). Elevated CO_2 effects on plant carbon, nitrogen, and water relations: Six important lessons from FACE. *Journal of Experimental Botany*, *60*(10), 2859–2876. https://doi.org/10.1093/jxb/erp096

Loveys, B. R., Atkinson, L. J., Sherlock, D. J., Roberts, R. L., Fitter, A. H., & Atkin, O. K. (2003). Thermal acclimation of leaf and root respiration: An investigation comparing inherently fast- and slow-growing plant species. *Global Change Biology*, *9*(6), 895–910. https://doi.org/10.1046/j.1365-2486.2003.00611.x

Ma, S., He, F., Tian, D., Zou, D., Yan, Z., Yang, Y., … Fang, J. (2018). Variations and determinants of carbon content in plants: A global synthesis. *Biogeosciences*, *15*(3), 693–702. https://doi.org/10.5194/bg-15-693-2018

Maire, V., Martre, P., Kattge, J., Gastal, F., Esser, G., Fontaine, S., & Soussana, J. F. (2012). The coordination of leaf photosynthesis links C and N fluxes in C_3 plant species. *PLoS ONE*, *7*(6), 1–15. https://doi.org/10.1371/journal.pone.0038345

Mcdowell, N. G., & Sevanto, S. (2010). The mechanisms of carbon starvation: how, when, or does it even occur at all? *New Phytologist*, *186*(2), 264–266. https://doi.org/10.1111/j.1469-8137.2010.03232.x

Medlyn, B. E., Barton, C. V. M., Broadmeadow, M. S. J., Ceulemans, R., De Angelis, P., Forstreuter, M., … Jarvis, P. G. (2001). Stomatal conductance of forest species after long-term exposure to elevated CO_2 concentration: A synthesis. *New Phytologist*, *149*(2), 247–264. https://doi.org/10.1046/j.1469-8137.2001.00028.x

Moore, B. D., Cheng, S. H., Sims, D., & Seemann, J. R. (1999). The biochemical and molecular basis for photosynthetic acclimation to elevated atmospheric CO_2. *Plant, Cell and Environment*, *22*(6), 567–582. https://doi.org/10.1046/j.1365-3040.1999.00432.x

Oppenheimer, M., Campos, M., Warren, R., Birkmann, J., Luber, G., O'Neill, B. C., & Takahashi, K. (2014). Emergent risks and key vulnerabilities. In C. B. Field, V. R. Barros, D. J. Dokken, K. J. Mach, M. D. Mastrandrea, T. E. Bilir, … L. L. White (Eds.), *Climate Change 2014: Impacts, Adaptation, and Vulnerability. Part A: Global and Sectoral Aspects. Contribution of Working Group II to the Fifth Assessment Report of the Intergovernmental Panel of Climate Change* (pp. 1039–1099). Cambridge, United Kingdom and New York, NY, USA: Cambridge University Press.

Peng, C., Ma, Z., Lei, X., Zhu, Q., Chen, H., Wang, W., … Zhou, X. (2011). A drought-induced pervasive increase in tree mortality across Canada's boreal forests. *Nature Climate Change*, *1*(9), 467–471. https://doi.org/10.1038/nclimate1293

Poorter, H., Niklas, K. J., Reich, P. B., Oleksyn, J., Poot, P., & Mommer, L. (2012). Biomass allocation to leaves, stems and roots: Meta-analyses of interspecific variation and environmental control. *New Phytologist*, *193*, 30–50. https://doi.org/10.1111/j.1469-8137.2011.03952.x

Reich, P. B., Walters, M. B., Ellsworth, D. S., Vose, J. M., John, C., Gresham, C., & Bowman, W. D. (1998). Relationships of leaf dark respiration to leaf nitrogen, specific leaf area and leaf life-span: A test across biomes and functional groups. *Oecologia*, *114*(4), 471–482. https://doi.org/10.1007/s004420050471

Ryan, M. G. (2013). Three decades of research at Flakaliden advancing whole-tree physiology, forest ecosystem and global change research. *Tree Physiology*, *33*(11), 1123–1131. https://doi.org/10.1093/treephys/tpt100

Sage, R. F., & Kubien, D. S. (2007). The temperature response of C_3 and C_4 photosynthesis. *Plant, Cell and Environment*, *30*(9), 1086–1106. https://doi.org/10.1111/j.1365-3040.2007.01682.x

Schuur, E. A. G., McGuire, A. D., Schadel, C., Grosse, G., Harden, J. W., Hayes, D. J., … Vonk, J. E. (2015). Climate change and the permafrost carbon feedback. *Nature*, *520*, 171–179.

Serreze, M. C., Walsh, J. E., Chapin, F. S. I., Osterkamp, T., Dyurgerov, M., Romanovsky, V., … Barry, R. G. (2000). Observational evidence of recent change in the northern high-latitude environment. *Climatic Change*, *46*(1–2), 159–207. https://doi.org/10.1023/A:1005504031923

Sevanto, S., Mcdowell, N. G., Dickman, L. T., Pangle, R., & Pockman, W. T. (2014). How do trees die? A test of the hydraulic failure and carbon starvation hypotheses. *Plant, Cell and Environment*, *37*(1), 153–161. https://doi.org/10.1111/pce.12141

Slot, M., & Kitajima, K. (2015). General patterns of acclimation of leaf respiration to elevated temperatures across biomes and plant types. *Oecologia*, *177*(3), 885–900. https://doi.org/10.1007/s00442-014-3159-4

Taub, D. R., & Wang, X. (2008). Why are nitrogen concentrations in plant tissues lower under elevated CO_2? A critical examination of the hypotheses. *Journal of Integrative Plant Biology*, *50*(11), 1365–1374. https://doi.org/10.1111/j.1744-7909.2008.00754.x

Tjoelker, M. G., Oleksyn, J., & Reich, P. B. (1998). Seedlings of five boreal tree species differ in acclimation of net photosynthesis to elevated CO_2 and temperature. *Tree Physiology*, *18*, 715–716. https://doi.org/10.1093/treephys/18.11.715

Tjoelker, M., Oleksyn, J., & Reich, P. (1999). Acclimation of respiration to temperature and CO_2 in seedlings of boreal tree species in relation to plant size and relative growth rate. *Global Change Biology*, *49*(6), 679–691. https://doi.org/10.1046/j.1365-2486.1999.00257.x

Togashi, F. H., Prentice, C. I., Atkin, O. K., Macfarlane, C., Prober, S. M., Bloomfield, K. J., & Evans, B. J. (2018). Thermal acclimation of leaf photosynthetic traits in an evergreen woodland, consistent with the coordination hypothesis. *Biogeosciences*, *15*(11), 3461–3474. https://doi.org/10.5194/bg-15-3461-2018

Way, D. A., & Oren, R. (2010). Differential responses to changes in growth temperature between trees from different functional groups and biomes: A review and synthesis of data. *Tree Physiology*, *30*(6), 669–688. https://doi.org/10.1093/treephys/tpq015

Way, D. A., Oren, R., & Kroner, Y. (2015). The space-time continuum: The effects of elevated CO_2 and temperature on trees and the importance of scaling. *Plant Cell and Environment*, *38*(6), 991–1007. https://doi.org/10.1111/pce.12527

Way, D. A., & Yamori, W. (2014). Thermal acclimation of photosynthesis: On the importance of adjusting our definitions and accounting for thermal acclimation of respiration. *Photosynthesis Research*, *119*(1–2), 89–100. https://doi.org/10.1007/s11120-013-9873-7

Wickhan, H. (2017) Tidyverse: Easily install and load the ‘tidyverse’. R Package Version 1.2.1

Wiley, E., Hoch, G., & Landhäusser, S. M. (2017). Dying piece by piece: Carbohydrate dynamics in aspen (*Populus tremuloides*) seedlings under severe carbon stress. *Journal of Experimental Botany*, *68*(18), 5221–5232. https://doi.org/10.1093/jxb/erx342

Yamori, W., Hikosaka, K., & Way, D. A. (2014). Temperature response of photosynthesis in C_3, C_4, and CAM plants: Temperature acclimation and temperature adaptation. *Photosynthesis Research*, *119*(1–2), 101–117. https://doi.org/10.1007/s11120-013-9874-6

Yamori, W., Noguchi, K., & Terashima, I. (2005). Temperature acclimation of photosynthesis in spinach leaves: Analyses of photosynthetic components and temperature dependencies of photosynthetic partial reactions. *Plant, Cell and Environment*, *28*(4), 536–547. https://doi.org/10.1111/j.1365-3040.2004.01299.x

Yin, H. J., Liu, Q., & Lai, T. (2008). Warming effects on growth and physiology in the seedlings of the two conifers *Picea asperata* and *Abies faxoniana* under two contrasting light conditions. *Ecological Research*, *23*(2), 459–469. https://doi.org/10.1007/s11284-007-0404-x

Yin, X. (2002). Responses of leaf nitrogen concentration and specific leaf area to atmospheric CO_2 enrichment: A retrospective synthesis across 62 species. *Global Change Biology*, *8*(7), 631–642. https://doi.org/10.1046/j.1365-2486.2002.00497.x

Chapter 3

3 Do High Growth Temperatures Induce Carbon Stress in Seedlings? A Test Using Tamarack

3.1 Introduction

Since the Industrial Revolution, there has been a 45% increase in atmospheric CO_2 concentrations, and CO_2 levels will continue to increase for the foreseeable future (IPCC, 2014; Zeng et al., 2014). Rising atmospheric greenhouse gases are the main contributor to increasing global surface temperatures. Global mean surface temperatures could increase by as much as 5 °C by the year 2100 in a "business as usual" scenario (Oppenheimer et al., 2014). However, warming will be most severe in northern latitudes, with warming of up to 8 °C predicted for the end of the century in the North American boreal forest. (Serreze et al., 2000). The boreal forest is one of the largest land-based biomes in the world, accounting for ~30% of the earth's terrestrial carbon (C) pools (Gauthier et al., 2015; Pan et al., 2011). With increasing temperatures causing a decline in forest health, the ability of the boreal forest to continue to sequester C and, more importantly, to survive, will depend on the resilience of boreal tree species to warming and rising CO_2.

The resilience of boreal trees to climate change will be linked to their ability to maintain physiological processes, such as photosynthesis, in a future climate. Net CO_2 assimilation rates (A_{net}) are temperature-dependent, and the temperature at which A_{net} is highest is the photosynthetic thermal optimum (T_{opt}; Sage & Kubien 2007). With long-term increases in growth temperatures, T_{opt} shifts to higher temperatures (Berry & Bjorkman, 1980; Yamori et al., 2014). However, thermal acclimation of photosynthesis can increase, decrease, or maintain similar rates of A_{net} at the new growth temperatures, such that the impact of warming on the actual C gain of a plant is hard to predict (Way & Yamori, 2014). Under high temperatures (>30 °C for cold-tolerant species), plants may be unable to maintain a similar A_{net} to what they achieve in current climates, leading to reduced C availability for growth.

While extreme warming may lead to reductions in CO_2 assimilation, elevated CO_2 is expected to increase photosynthesis and growth. On average, elevated CO_2 causes a 30% increase in photosynthetic rates, with an associated ~10% increase in growth (Ainsworth & Long, 2005; Kirschbaum, 2011). Rubisco is substrate-limited under current CO_2 concentrations, so rates of carboxylation are higher under elevated CO_2. Higher intracellular CO_2 concentrations also reduce C losses by suppressing photorespiration in C_3 plants (Ainsworth & Rogers, 2007). However, due to sink limitations, often caused by low water and nitrogen (N) availability, field experiments often observe a down-regulation in net photosynthetic rates after long-term exposure to elevated CO_2 (Leakey et al., 2009). A large component of this photosynthetic down-regulation is a reduction in stomatal conductance, which reduces intracellular CO_2 concentrations and improves plant water balance, which may prove beneficial under drier future climates. Additionally, plants grown at high CO_2 often produce less Rubisco to compensate for the enzyme's increased carboxylation rates (Ainsworth & Long, 2005; Albert et al., 2011; Moore et al., 1999)

To thrive in a warmer world, it will be critical to not only acclimate photosynthesis, but also to mitigate C losses through thermal acclimation of respiration. Under short-term increases in shoot temperature (minutes to hours), respiration increases exponentially (Atkin & Tjoelker, 2003; Loveys et al., 2003; Slot & Kitajima, 2015). Most plants thermally acclimate respiration after longer-term exposure to warmer temperatures (Atkin & Tjoelker, 2003), resulting in a reduction in respiration rates. These lower respiration rates are often linked to reductions in leaf N (Atkin & Tjoelker, 2003; Loveys et al., 2003; Reich, Oleksyn, & Wright, 2009; Tjoelker et al., 1999). Conifers generally have a positive linear relationship between leaf N and respiration (Reich et al., 1998), the result of higher metabolic costs associated with greater concentrations of N-rich enzymes. When grown from seed at warmer temperatures, boreal conifers have less decreased leaf N, indicative of an overall decrease in enzyme and protein content, and also to show a subsequent decrease in respiration rates (Atkin & Tjoelker, 2003; Dusenge et al., 2020; Kroner & Way, 2016; Loveys et al., 2003; Reich et al., 1998; Way & Sage, 2008; Way, Sage, & Kubien, 2008)

Quantifying the acclimation of C fluxes in boreal conifers will be useful in understanding the response and future health of the boreal trees to climate change. In Chapter Two, I reported the C fluxes and mortality of tamarack seedlings under increasing warming treatments with and without CO_2 enrichment when grown in glasshouses. Only seedlings grown under +8 ˚C warming with ambient CO_2 displayed needle browning and eventual mortality. Carbon flux measurements across healthy seedlings were not indicative of C stress, but in comparing dying and healthy seedlings in the +8 ˚C warming with ambient CO_2 treatment, there was a trend of decreasing A_{net}/R_{dark} ($P = 0.09$). The experiment in this Chapter was designed as a follow-up to the experiment in Chapter Two to increase the number of seedlings measured and standardize a specific health rating for when dying seedlings would be measured. Beyond measurements related to mortality, the purpose of this study was also to understand C fluxes in tamarack responding to an 8 ˚C increase in temperature with and without elevated CO_2. Growth chambers were used to minimize confounding variables (such as variation in irradiance) and focus on the effects of temperature and CO_2 to compare to previous work in glasshouses (i.e. Chapter Two).

I combined a +8 ˚C warming treatment with ambient (400 ppm) or elevated CO_2 concentrations (750 ppm). I predicted that seedlings grown with elevated CO_2 compared to ambient CO_2 would have higher photosynthetic rates at their growth CO_2 and greater overall productivity (as seen in Ainsworth & Rogers, 2007; Aranda, Cadahía, & Fernández de Simón, 2020; Chavan et al., 2019). I also predicted that warming would result in an increase in the photosynthetic thermal optima of the seedlings. Lastly, I predicted that shoot and root dark respiration would thermally acclimate to reduce C losses at elevated growth temperatures. Overall, I also predicted that seedlings exposed to a combination of +8˚C warming and ambient CO_2 would display C stress through needle browning, mortality and the slowest growth of the three treatments.

3.2 Methods

3.2.1 Experimental Design

Tamarack seeds were sown in 11.3 L grow bags filled with Promix HP mycorrhizal growing medium (Premier Tech Horticulture, Rivieire-du-Loup, QC, Canada) with slow-

release fertilizer (Slow Release Plant Food, 12-4-8, Miracle Grow, The Scotts Company, Mississauga, ON, Canada). Seeds were ordered from the Canadian National Seed Tree Center and the provenance (Robertson Lake, Ontario [45 °N, 76.6 °W]) was selected to be geographically similar to the seed collection site used in Chapter Two (Finch Township, ON [45.133 °N, 75.083 °W]).

Twenty-four pots with five seeds per pot were assigned to one of three CO_2-controlled reach-in plant growth chambers (Conviron, Controlled Environments Ltd., Winnipeg, MN) for a total of 72 pots. After establishment, seedlings were thinned to one per pot. Seedlings were grown under diurnal environmental conditions based on a five-year historical average from May to September in Drummond, ON, the closest Environmental Canada climate data available for the seed lot. The chamber irradiance was 300 μmol photons m^{-2} s^{-1} (the highest irradiance the chambers could achieve) and the photoperiod was set to 14 h. Each growth chamber had a different temperature by CO_2 treatment: 1) ambient temperature (0T, 24/11 ˚C day/night temperatures) with ambient CO_2 (400 ppm; AC); 2) ambient temperature +8 ˚C (8T, 32/19 ˚C) with AC; and 3) 8T with elevated CO_2 (EC, 750 ppm). Carbon dioxide concentrations were measured every second in each growth chamber using a CO_2 analyzer (WMA-4, PP Systems, Amesbury, MA, USA) and controlled by injecting pure CO_2 as needed to maintain the EC treatment. Humidity was controlled at 60% in all chambers and seedlings were watered as needed to maintain a moist growth medium (Figure 3.1). Volumetric soil moisture measurements were measured in all pots biweekly (HH2 Moisture Meter, Delta-T Devices, Cambridge, UK). Average soil temperatures under the different treatments were measured continuously using dataloggers (LogTag TRIX-8, Microdaq Ltd., Contoocook, NH, USA). The experiment was replicated once, with the first replicate running from January to June 2018 and the second replicate running from June to October 2018. Treatments were rotated between chambers between the replicates.

3.2.2 Gas Exchange Measurements

Gas exchange measurements were made in the last month of each replicate. Measurements were made on fully-expanded needles using a portable photosynthesis

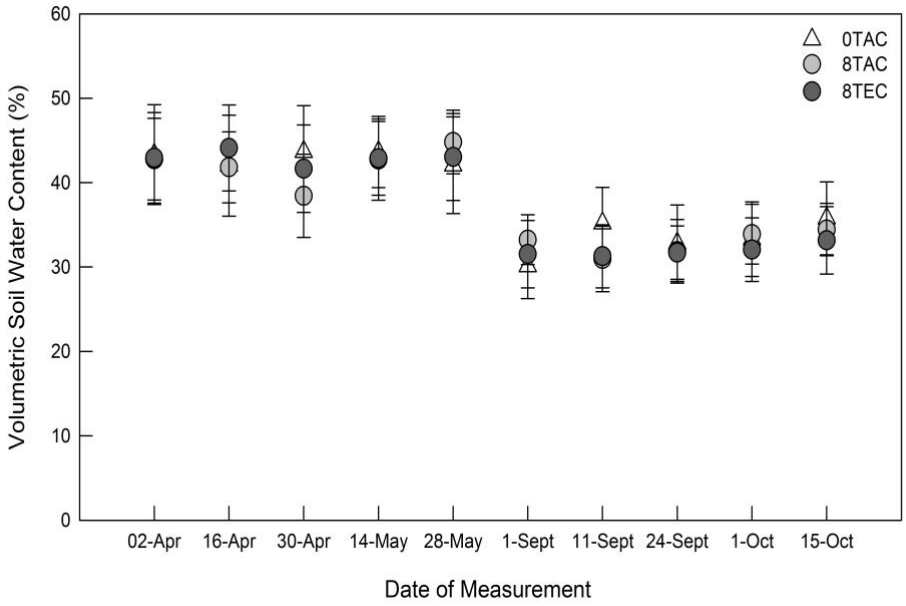

Figure 3.1. Volumetric soil water content (%) of tamarack seedlings grown under three climate treatments. Data are means ± SD, n = 24. White circles, 0TAC; light grey circles, 8TAC; dark grey circles, 8TEC.

system (Li-cor 6400 XT, Li-cor Biosciences, Lincoln, NE). Six healthy seedlings from each treatment were measured to establish treatment effects (N=36). Seedlings were sampled across the treatments to avoid phenological effects as measurements took approximately three weeks to complete. Despite the low irradiance growth conditions, light saturation for tamarack was 1200 μmol photons m^{-2} s^{-1} (Figure 3.2). Measurements were made in a reach-in growth chamber to allow seedlings and the photosynthetic system to reach a full range of temperatures. Net CO_2 assimilation rates (A_{net}) at both 400 ppm and 750 ppm were taken at a range of temperatures (20 ˚C, 24 ˚C, 28 ˚C, 32 ˚C and 36 ˚C), at an irradiance of 1200 μmol photons m^{-2} s^{-1}. Relative humidity was held at 50-65% from 20 ˚C to 32˚C, but dropped to ~35% at 36 ˚C. The thermal optimum of A_{net} (T_{opt}) was calculated by fitting a second-order polynomial to each temperature response curve at each CO_2 concentration. After the last point was measured at 36 °C, the sample was dark-acclimated for 20 minutes at 0 μmol photons m^{-2} s^{-1}. Shoot dark respiration (R_{shoot}) was then measured at the same temperatures as A_{net}, but in descending order back

down to 20 ˚C. The R_{shoot} was measured at 400 ppm, as there is no short-term effect of CO_2 on R_{dark} measurements (Amthor et al., 2001).

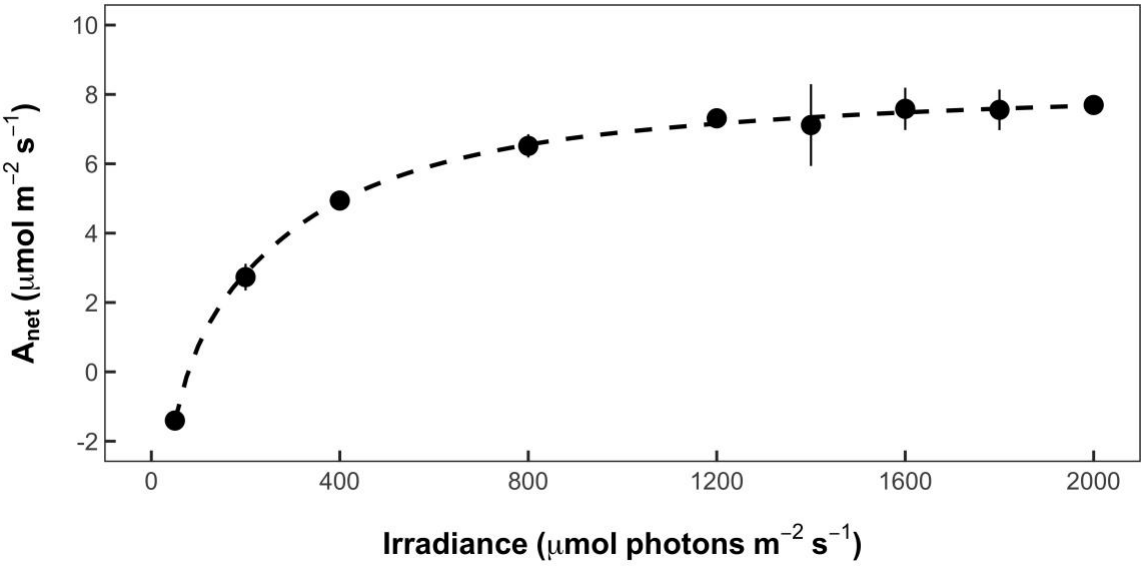

Figure 3.2. Photosynthetic light response curve for 0TAC tamarack seedlings. Net CO_2 assimilation (A_{net}) was measured at 0TAC growth conditions (400 ppm CO_2 and 25 ˚C). Points represent mean ± SE, N = 5.

Once gas exchange measurements were complete, the needles measured in the cuvette were removed and photographed to determine projected leaf area (LA) using ImageJ software (US National Institutes of Health, Bestheda, MD, USA). The needles were then dried at 65 °C and weighed to determine leaf mass area (LMA) (i.e. needle biomass divided by LA).

3.2.3 Root Respiration

Root dark respiration (R_{root}) measurements were also made in June and October 2018 using the same photosynthesis system. The seedlings used to assess A_{net} and R_{shoot} were also used to measure R_{root} (N=36). Entire seedlings were carefully removed from pots, then the roots were rinsed of the growth medium and placed in water to maintain hydration for five minutes before measurements. Roots were gently blotted dry before being put into the cuvettes. R_{root} was measured at the respective soil growth temperatures

as indicated by the dataloggers (18.5 ˚C for 0T and 24.8 ˚C for 8T). Once R_{root} was measured, the roots within the cuvette were severed from the seedling, dried at 65 ˚C, weighed and used to standardize respiration rates on a root mass basis.

3.2.4 Biomass

After gas exchange measurements were completed, the remaining seedlings in the experiment were harvested and dried to a constant mass at 65 ˚C. Seedlings were divided into roots, shoots and leaves, and each tissue was weighed individually.

3.2.5 Carbon and Nitrogen Analysis

A subset of the dried leaf tissue was ground using a Wiley mill (Thomas Scientific, Swedesboro, NJ, USA) and analyzed for C and N concentrations using an elemental analyzer (NCS 2500, Carlo Ebra, Peypin, France).

3.2.6 Statistics

R software (R Foundation for Statistical Computing, Vienna, Austria, EU) was used for statistical analyses. The R package ‘tidyverse’ was used for statistical analyses, specifically three-way ANOVAs (Wickham, 2017), and the R package ‘nlme’ was used for repeated measures ANOVAs (Pinheiro et al., 2019). Response variables of seedlings from all three treatments were analyzed using three-way ANOVAs, considering growth temperature, growth CO_2 and replication effects. Additionally, repeated measure multi-way ANOVAs were used to analyze the temperature response curves for A_{net} and R_{dark}, considering growth CO_2, growth temperature, measurement temperature, and replicate. Data from parameters with a significant replicate effect have been relativized or, where no replicate effect existed, pooled. The maximum value of a parameter (e.g., the rate of photosynthesis) from all treatments was used to relativize the other data within the replicate and then the relativized data across both replicates were pooled. Relativized values were used in some figures to better visualize the results, but all statistical analyses and results description were based on raw data values. Type III tests were conducted to account for the unbalanced design of the experiment (i.e., no 0TEC treatment).

3.3 Results

3.3.1 Temperature Curves Measured at 400 ppm and Growth CO_2

Comparing temperature response curves measured at 400 ppm (A_{400}), there was an increase in A_{400} in the 8T treatments compared to the 0T treatment (Table 3.1, Figure 3.3A). However, there was no effect of growth CO_2 on the temperature response of A_{400}. Under growth CO_2, A_{growth} was enhanced by both the 8T treatment and EC (Table 3.1, Figure 3.3B). There was also a significant replicate effect for A_{400}. For A_{growth} there was a replicate effect, and also significant interaction effects between measurement temperature and replicate, and measurement temperature and growth temperature.

The thermal optimum for both A_{400} ($T_{opt-400}$) and A_{growth} ($T_{opt-growth}$) increased in the 8T seedlings compared to the 0T seedlings (Table 3.2, Figures 3.4A and B). For $T_{opt-400}$, there was no effect of growth CO_2, but there was a significant replicate effect, whereby $T_{opt-400}$ increased by ~2.5 ˚C (for replicate one) and ~3.9 ˚C (for replicate two) from AT to 8T seedlings (Figure 3.4A). In contrast, there was an effect of growth CO_2 on $T_{opt-growth}$, but no replicate effect (Figure 3.4B). Overall, the $T_{opt-growth}$ was highest for the 8TEC seedlings, indicating an additive effect of elevated CO_2 and temperature.

3.3.2 Response of Stomatal Conductance to Growth CO_2 and Temperature

There was a growth temperature effect on stomatal conductance (g_s) when measured at both 400 ppm CO_2 (g_{s-400}) and growth CO_2 ($g_{s-growth}$; Table 3.1, Figures 3.5A and B). Stomatal conductance was lower in the 0T seedlings than the 8T plants, a difference that was more pronounced at higher measurement temperatures (Table 3.1). In contrast, there was no effect of growth CO_2 or measurement temperature (T_m) on g_s. From replicate one to replicate two, there was a decrease in both g_{s-400} and $g_{s-growth}$ (Table 3.1).

3.3.3 Shoot and Root Respiration

There was no effect of growth temperature or CO_2 on R_{shoot}, although there was a decrease in R_{shoot} from replicate one to replicate two (Table 3.1, Figure 3.6). The R_{shoot} increased with increasing measurement temperature (Figure 3.6). Similar to R_{shoot}, there

Table 3.1. Summary of repeated ANOVA statistics for the temperature responses of gas exchange parameters. Gas exchange parameters were measured at 25 ˚C and 400 ppm CO_2 (denoted by "25") and at growth conditions (denoted by "growth). Parameters include temperature response curves of: net CO_2 assimilation rate (A_{400}, A_{growth}); stomatal conductance measured at 400 ppm ($g_{s\text{-}400}$, $g_{s\text{-}growth}$); and shoot respiration measured at 400 ppm CO_2 (R_{shoot}). Bolded p-values are statistically significant ($P<0.05$). T = growth temperature treatment, CO_2 = growth CO_2 treatment, T_m = measurement temperature, R = Replicate, and DF = within-group degrees of freedom.

	DF	*F*-ratio	*P*-value
A_{400}			
T	165	14.55	**<0.001**
CO_2	165	0.94	0.33
T_M	3	1.90	0.26
R	165	29.11	**<0.0001**
T x R	165	2.20	0.14
CO_2 x R	165	2.69	0.10
T_M x R	165	1.90	0.17
T x T_M	165	3.04	0.08
CO_2 x T_M	165	0.14	0.71
T x T_M x R	165	0.01	0.92
CO_2 x T_M x R	165	0.03	0.86
A_{growth}			
T	165	52.12	**<0.0001**
CO_2	165	45.34	**<0.0001**
T_M	3	0.03	0.89
R	165	26.35	**<0.0001**
T x R	165	4.91	**<0.05**
CO_2 x R	165	0.76	0.38
T_M x R	165	3.92	**<0.05**
T x T_M	165	5.22	**<0.05**
CO_2 x T_M	165	3.58	0.06
T x T_M x R	165	0.49	0.49
CO_2 x T_M x R	165	1.16	0.28
$g_{s\text{-}400}$			
T	165	19.82	**<0.0001**
CO_2	165	0.001	0.98
T_M	3	0.42	0.56
R	165	9.91	**<0.01**
T x R	165	1.68	0.20

CO_2 x R	165	2.50	0.17
T_M x R	165	0.06	0.80
T x T_M	165	1.18	0.28
CO_2 x T_M	165	0.01	0.91
T x T_M x R	165	1.45	0.23
CO_2 x T_M x R	165	0.17	0.68
$g_{s\text{-growth}}$			
T	165	16.363	**<0.0001**
CO_2	165	0.04	0.85
T_M	3	0.54	0.51
R	165	8.52	**<0.01**
T x R	165	1.55	0.22
CO_2 x R	165	3.01	0.08
T_M x R	165	0.42	0.52
T x T_M	165	1.38	0.24
CO_2 x T_M	165	0.12	0.73
T x T_M x R	165	2.16	0.14
CO_2 x T_M x R	165	0.04	0.85
R_{shoot}			
T	165	1.02	0.31
CO_2	165	2.64	0.11
T_M	3	42.45	**<0.01**
R	165	49.52	**<0.0001**
T x R	165	1.97	0.16
CO_2 x R	165	0.72	0.40
T_M x R	165	1.98	0.16
T x T_M	165	0.04	0.84
CO_2 x T_M	165	0.002	0.96
T x T_M x R	165	0.34	0.56
CO_2 x T_M x R	165	1.17	0.28

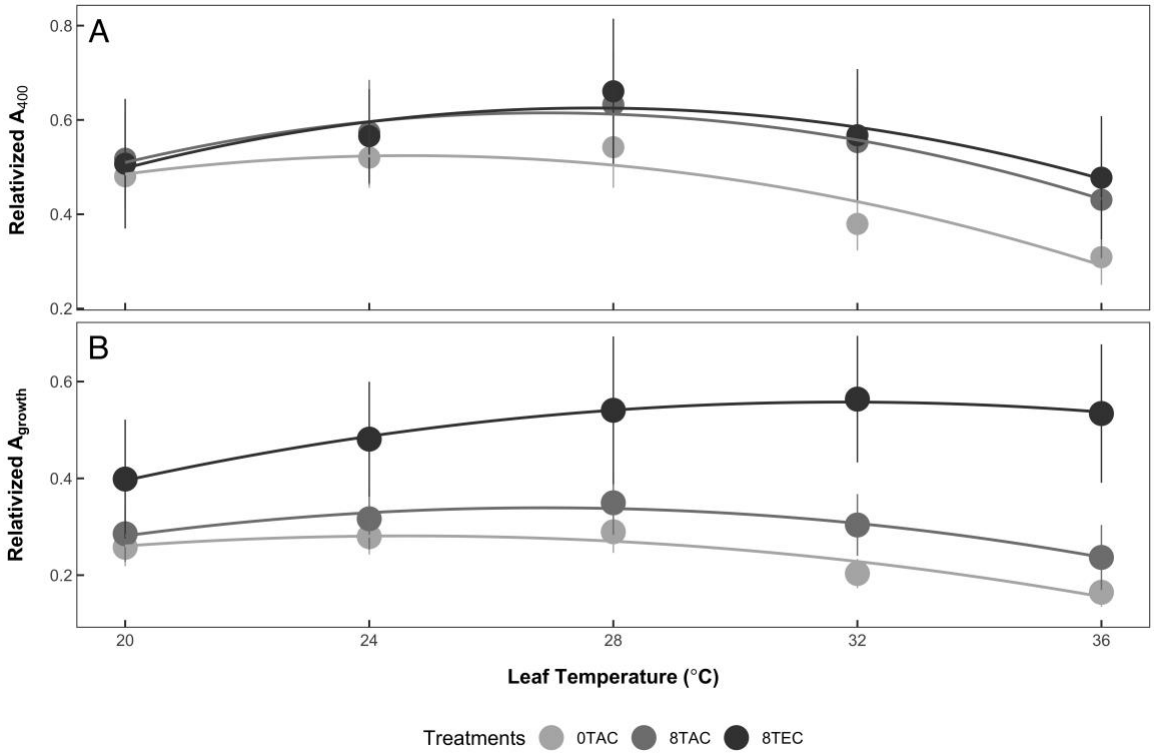

Figure 3.3. Relativized temperature response curves of net CO_2 assimilation rates. Net photosynthetic rates were measured at: A) a common CO_2 of 400 ppm (A_{400}) and B) growth CO_2 (A_{growth}). Points represent means ± SE; n = 6. Curves were relativized by the maximum rate of net CO_2 assimilation per replicate. Light grey, 0TAC; medium grey, 8TAC; dark grey, 8TEC.

Table 3.2. Summary of ANOVA statistics for the responses of gas exchange parameters, growth and leaf biochemistry to the treatments. Parameters include: thermal optima of net photosynthesis at 400 ppm ($T_{opt-400}$) and growth CO_2 ($T_{opt-growth}$); total biomass ($Biomass_{Total}$); the root/shoot ratio; tree height; root dark respiration at growth temperature (R_{root}); needle percent nitrogen (%N); needle percent carbon (%C); the ratio of C/N. Bolded p-values are significant ($P<0.05$). T = growth temperature treatment, CO_2 = growth CO_2 treatment, R = Replicate, and DF = within-group degrees of freedom.

	DF	*F*-ratio	*P*-value
$T_{opt-400}$			
T	30	41.39	**<0.0001**
CO_2	30	1.68	0.21
R	30	5.00	**<0.05**
T x R	30	2.08	0.16
CO_2 x R	30	0.40	0.53
$T_{opt-growth}$			
T	30	29.47	**<0.0001**
CO_2	30	10.54	**<0.01**
R	30	2.63	0.17
T x R	30	1.20	0.28
CO_2 x R	30	0.54	0.47
$Biomass_{Total}$			
T	138	0.02	0.90
CO_2	138	0.61	0.44
R	138	43.04	**<0.0001**
T x R	138	0.15	0.70
CO_2 x R	138	0.01	0.93
Root/Shoot			
T	138	0.09	0.76
CO_2	138	2.45	0.12
R	138	12.44	**<0.001**
T x R	138	0.92	0.34
CO_2 x R	138	1.92	0.17
Tree Height			
T	138	1.08	0.30
CO_2	138	4.97	**<0.05**
R	138	114.22	**<0.0001**
T x R	138	0.48	0.49

CO_2 x R	138	2.50	0.12
R_{root}			
T	30	3.13	0.09
CO_2	30	0.36	0.55
R	30	48.61	**<0.0001**
T x R	30	0.59	0.45
CO_2 x R	30	0.20	0.65
%N			
T	30	3.89	0.06
CO_2	30	0.14	0.71
R	30	3.33	0.08
T x R	30	0.24	0.62
CO_2 x R	30	1.24	0.27
%C			
T	30	0.05	0.83
CO_2	30	1.82	0.19
R	30	2.69	0.11
T x R	30	0.31	0.58
CO_2 x R	30	0.02	0.88

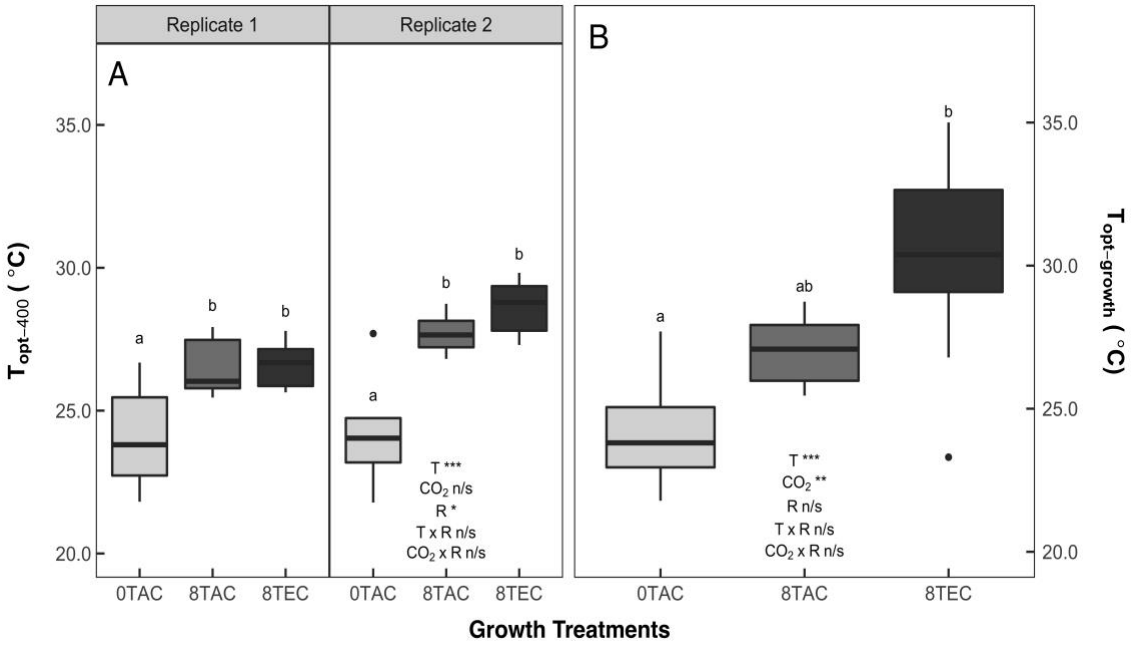

Figure 3.4. Changes in thermal optima of net CO_2 assimilation rate in response to temperature and CO_2 treatments. Temperature optima were measured at: A) a common CO_2 of 400 ppm ($T_{opt-400}$) and B) growth CO_2 ($T_{opt-growth}$). The horizontal line of the boxplot represents the mean; the box edges indicate the 25th and 75th percentiles; the whiskers display the minimum and maximum values; dots indicate outliers; n = 6. Light grey, ambient temperature with ambient CO_2 (0TAC); medium grey, +8 ˚C warming with AC (8TAC); dark grey, 8T with elevated CO_2 (8TEC). Different letters above boxplots denote a significant difference across all growth treatments and/or replicates ($p < 0.05$). T = growth temperature, CO_2 = growth CO_2 concentration, R = replicate, n/s = non-significant, * = $p<0.05$, ** = $p<0.01$, and *** = $p<0.001$.

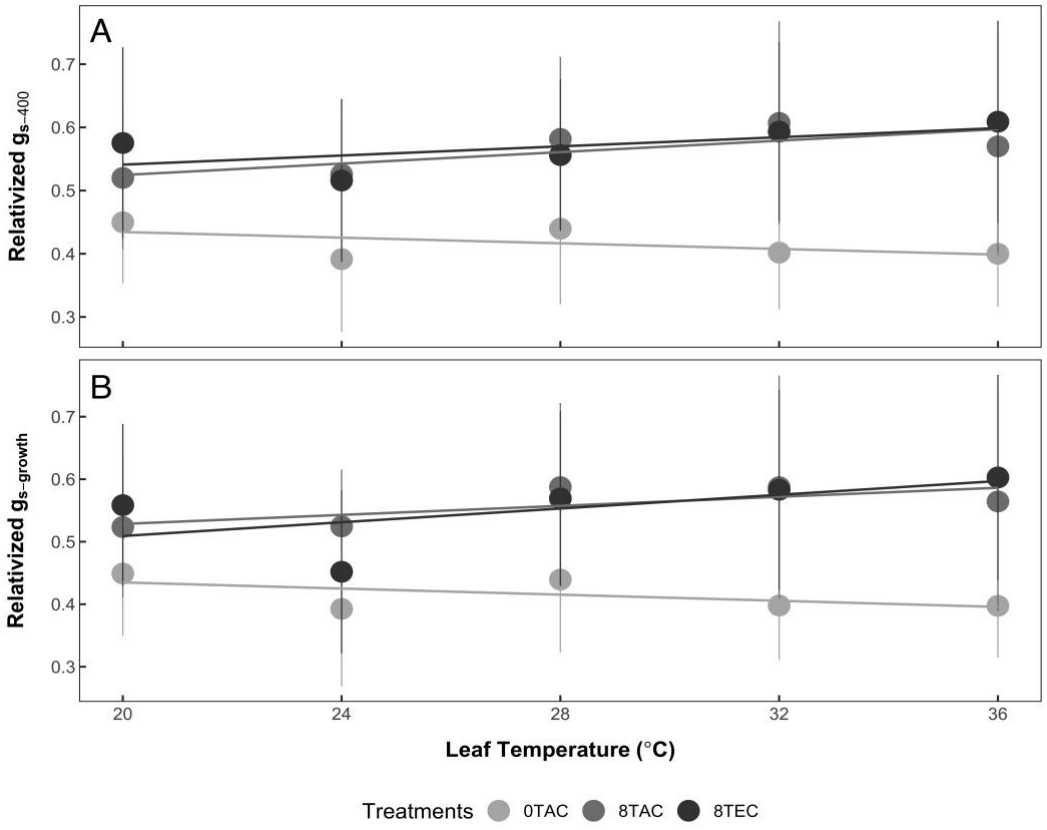

Figure 3.5. Relativized stomatal conductance of temperature curves. Stomatal conductance was measured at: A) a common CO_2 of 400 ppm ($g_{s\text{-}400}$) and B) growth CO_2 ($g_{s\text{-}growth}$). Curves were relativized by the maximum rate of stomatal conductance per replicate. Points represent means $\pm$ SE; n = 6. Light grey, ambient temperature with ambient CO_2 (0TAC); medium grey, +8 ˚C warming with AC (8TAC); dark grey, 8T with elevated CO_2 (8TEC).

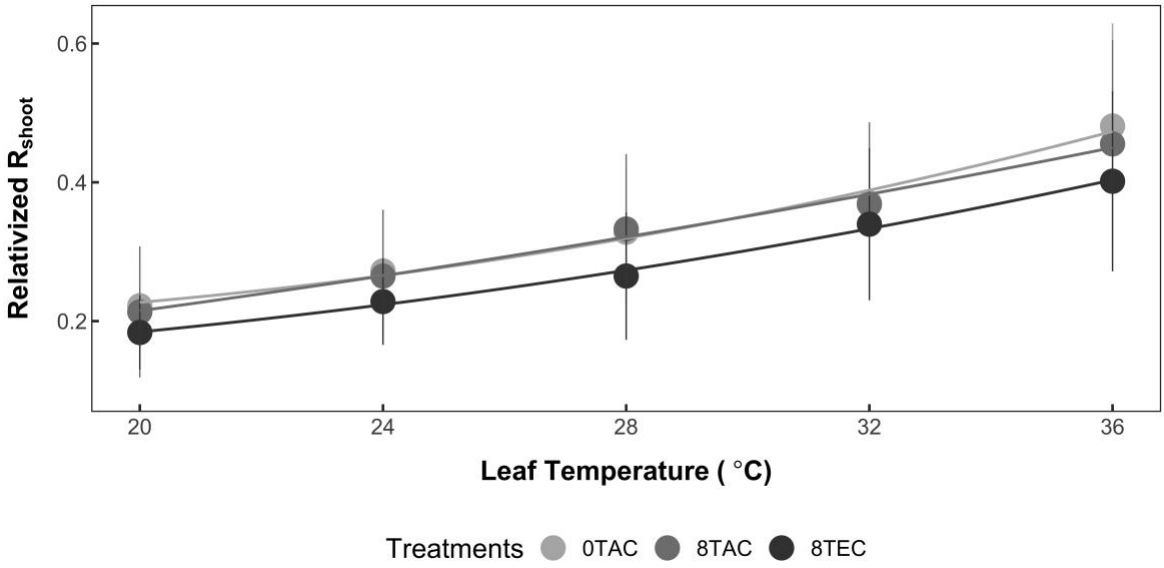

Figure 3.6. Relativized temperature response curves of shoot dark respiration measured at 400 ppm CO_2. Curves were relativized by the maximum rate of shoot dark respiration (R_{shoot}) per replicate. Points represent means ± SE; n = 12. Light grey, ambient temperature with ambient CO_2 (0TAC); medium grey, +8 ˚C warming with AC (8TAC); dark grey, 8T with elevated CO_2 (8TEC).

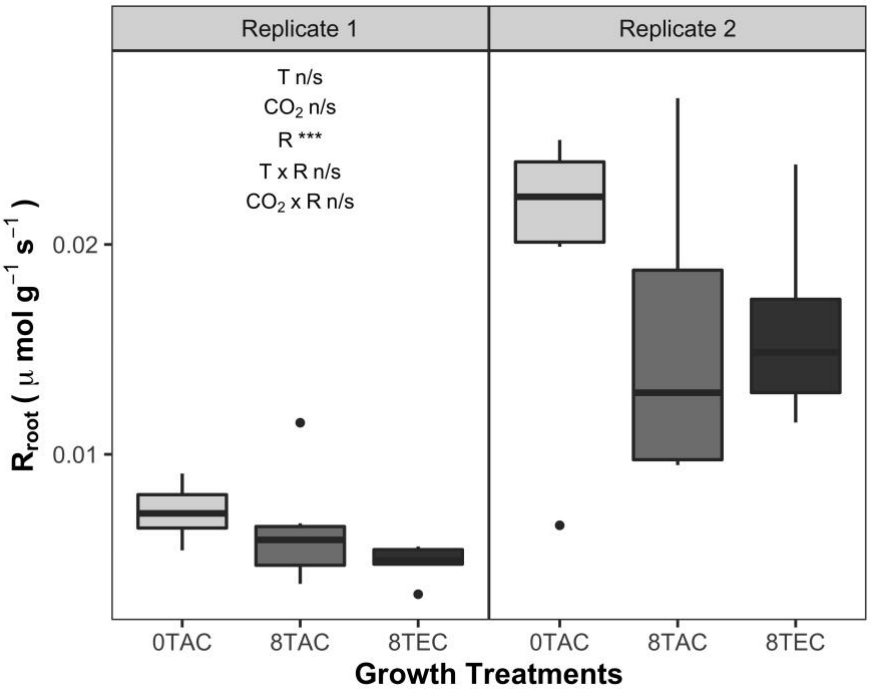

Figure 3.7. Root dark respiration (R_{root}) measured at 400 ppm CO_2 and growth soil temperature. 0T soil was 18.5 ˚C and the 8T soil was 24.5 ˚C. Data are displayed for both replicates, separately. The horizontal line of the boxplot represents the mean; the box edges indicate the 25th and 75th percentiles; the whiskers display the minimum and maximum values; dots indicate outliers; n = 6. Light grey, ambient temperature with ambient CO_2 (0TAC); medium grey, +8 ˚C warming with AC (8TAC); dark grey, 8T with elevated CO_2 (8TEC). Different letters above boxplots denote a significant difference across growth treatments and replicates ($p < 0.05$). T = growth temperature, CO_2 = growth CO_2 concentration, R = replicate, n/s = non-significant, * = $p<0.05$, ** = $p<0.01$, and *** = $p<0.001$.

was no effect of growth temperature or CO_2 on R_{root} but there was an ~2× increase in R_{root} from replicate one to replicate two.

3.3.4 Growth Response

Total seedling biomass and the ratio of root to shoot biomass (root/shoot) were similar across all growth treatments (Table 3.2; Figures 3.8A and B). There was a sharp decline in biomass and tree height from replicate one to replicate two. Comparatively, root/shoot allocation of biomass increased from replicate one to replicate two. Tree height was unaffected by growth temperature but increased with EC (Table 3.2; Figure 3.8C).

3.3.5 Leaf Biochemistry

Needle C and N concentrations were not affected by growth temperature or CO_2 (Table 3.2; Figures 3.9A and B). There was also no replicate effect on leaf %C or %N.

3.4 Discussion

3.4.1 Acclimation of Carbon Fluxes to Warming and High CO_2

With +8 ˚C warming, tamarack seedlings had significant thermal acclimation of photosynthesis, as indicated by an increase in $T_{opt,}$ along with an increase in A_{400} and $g_{s\text{-}400}$. Yamori et al. (2014) found that for every 1 ˚C shift in the growth temperature of C_3 plants, T_{opt} would subsequently shift by 0.55 ˚C, similar to the shift in T_{opt} seen in the 8T tamarack. However, unlike my findings on a deciduous conifer, a meta-analysis by Dusenge et al. (2018) found that warming resulted in similar A_{growth} compared to control plants in deciduous broad-leaved woody species. In previous studies on tamarack seedlings, Dusenge et al. (2020) and Tjoelker et al. (1998) supported this result, as these two studies also reported similar A_{growth} across warming treatments. In my study, higher $g_{s\text{-}growth}$ in the 8T seedlings may have reduced stomatal limitations for CO_2 diffusion, increasing the rate of carboxylation by Rubisco and therefore increasing A_{growth}. While warming treatments did stimulate g_s in tamarack seedlings in Tjoelker et al. (1998), the effect was less pronounced ($P=0.03$) than my observations ($P<0.001$). Dusenge et al. (2020) also argued for a trend in higher $g_{s\text{-}growth}$ in their paper, though they found no

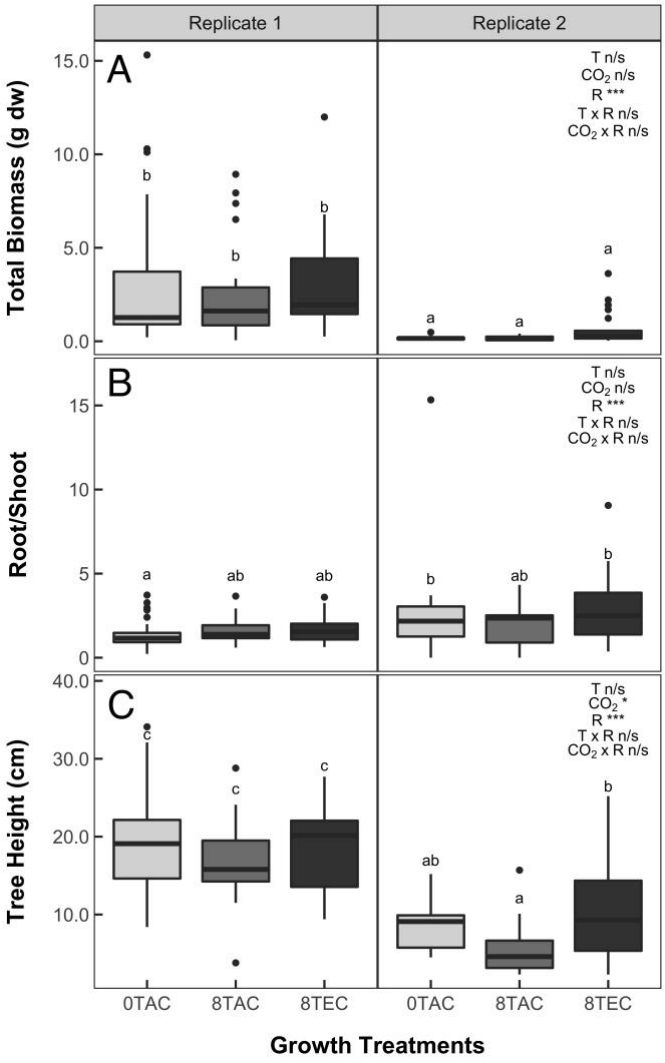

Figure 3.8. Growth responses to temperature and CO_2 treatments. A) total biomass; B) root/shoot ratio; and C) tree height. Data are displayed for both replicates, separately. The horizontal line of the boxplot represents the mean; the box edges indicate the 25th and 75th percentiles; the whiskers display the minimum and maximum values; dots indicate outliers; n = 6. Light grey, ambient temperature with ambient CO_2 (0TAC); medium grey, +8 ˚C warming with AC (8TAC); dark grey, 8T with elevated CO_2 (8TEC). Different letters above boxplots denote a significant difference across growth treatments and replicates ($p < 0.05$). T = growth temperature, CO_2 = growth CO_2 concentration, R = replicate, ns = non-significant, * = $p<0.05$, ** = $p<0.01$, and *** = $p<0.001$.

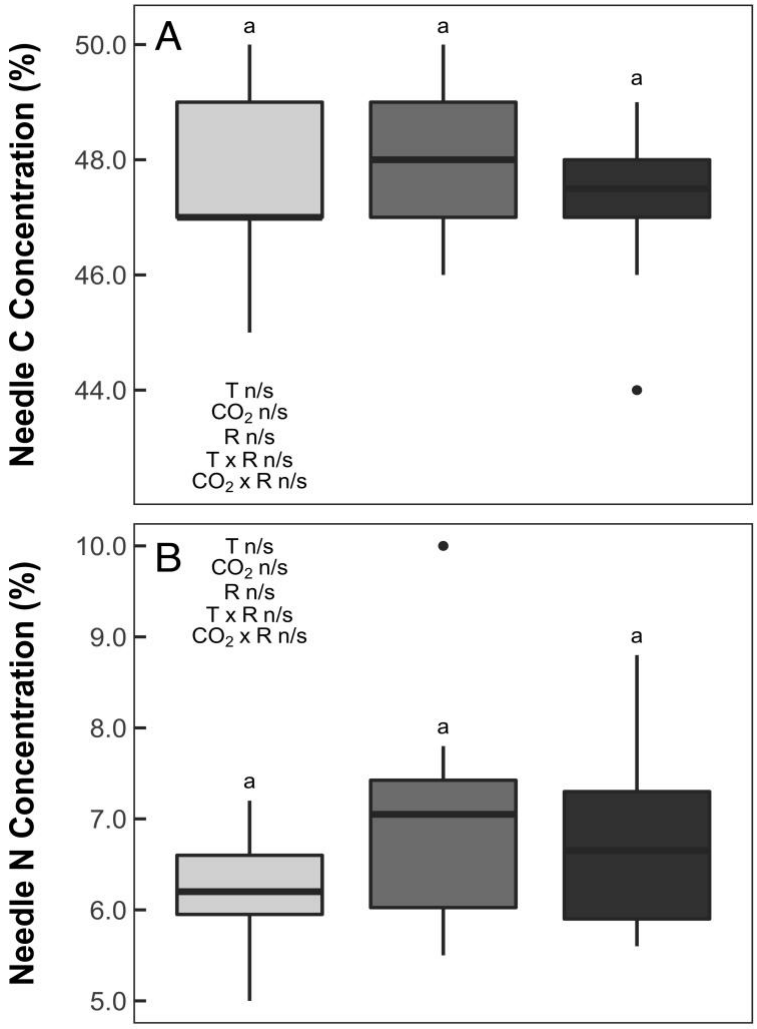

Figure 3.9. Needle biochemical responses to temperature and CO_2 treatments. A) Needle carbon (C) concentrations and B) needle nitrogen (N) concentrations. Data are pooled for both parameters as there were no replicate effects. The horizontal line of the boxplot represents the mean; the box edges indicate the 25th and 75th percentiles; the whiskers display the minimum and maximum values; dots indicate outliers; n = 6. Light grey, ambient temperature with ambient CO_2 (0TAC); medium grey, +8 ˚C warming with AC (8TAC); dark grey, 8T with elevated CO_2 (8TEC). Different letters above boxplots denote a significant difference between growth treatments ($p < 0.05$). T = growth temperature, CO_2 = growth CO_2 concentration, R = replicate, n/s = non-significant, * = $p<0.05$, ** = $p<0.01$, and *** = $p<0.001$.

significant difference in g_s (P=0.09) with warming treatments. Given these similarities, it appears that warming may enhance $g_{s\text{-growth}}$ in tamarack, which can lead to greater A_{growth}, a result which would have positive effects on the C balance, growth and survival of the species in a warmer world, provided water supplies are non-limiting.

In contrast to the effects of warming, there was no acclimation of photosynthesis to EC. Given this, A_{growth} was increased by the EC treatment. However, none of the other gas exchange parameters showed a CO_2 effect, indicating a general insensitivity of both photosynthetic processes and stomatal conductance to elevated CO_2 conditions. Similar to my findings, Dusenge et al. (2020) also found A_{growth} increased with EC despite stomatal conductance being unresponsive to growth CO_2. With similar g_s but higher CO_2 across the EC treatments, seedlings have a higher ratio of intracellular CO_2 to atmospheric CO_2 (C_i/C_a) and subsequently higher rates of photosynthesis. In the literature, it is hypothesized that plants will acclimate to elevated CO_2 by down-regulating g_s to decrease transpiration (Ainsworth & Rogers, 2007). While this may be true for some plant functional types, in a meta-analysis, Medlyn et al. (2001) found that overall there was no evidence of acclimation of g_s to EC in forest tree species, and conifers had the lowest responsiveness of g_s to changing CO_2 compared other plant functional types. In addition, under experimental designs where plants were well-watered, stomatal conductance was higher in plants grown at EC, indicating a priority for CO_2 assimilation over water conservation in non-stressed plants (Medlyn et al., 2001). Overall, my results add to the growing set of data emphasizing that stomatal conductance is insensitive to EC in some species or plant functional types, and that broad generalities about how stomata will respond to rising CO_2 derived from crop species and temperate trees may not be appropriate for all vegetation types.

Similar to the response of T_{opt} to warming, T_{opt} increased in response to EC treatments. With increasing CO_2 concentrations, photorespiration is suppressed at high temperatures, leading to a higher T_{opt} with EC (Sage & Kubien, 2007). Increased T_{opt} with elevated CO_2 has been found in different C_3 plant studies, including experiments with tamarack, but this does not mean that there is always an additive response on the shift in T_{opt} with EC and warming (Dusenge, 2019; Ghannoum et al., 2010). The stimulation of photosynthesis

by EC combined with warming also lead to higher A_{growth} in 8TEC seedlings. I predicted that the 8TAC trees would have the worst photosynthetic performance, as they would experience heat stress and high photorespiration rates without the offsetting benefits of elevated CO_2. While 8TAC seedlings did have lower A_{growth} compared to 8TEC, they did not appear to experience C stress, but instead benefitted from thermal acclimation of photosynthesis.

When comparing the temperature responses of R_{shoot}, there was no acclimation to temperature or CO_2. This is an unusual finding, as most plants show strong respiratory acclimation to warming (Atkin & Tjoelker, 2003; Tjoelker et al., 1999; Reich et al., 1998; Loveys et al., 2003; Slot & Kitajima, 2015). The lack of shoot respiratory acclimation seen here may be correlated with the similar foliar %N values found across the temperature and CO_2 growth treatments, which implies that the treatments had little effect on enzyme and protein concentrations in seedlings. Similarly, in a study on *Eucalyptus globulus*, Crous et al. (2017) found no thermal acclimation of shoot respiration which was correlated with higher %N in the warm-grown plants. There is a relationship that exists between %N and respiratory capacity, as well as the photosynthetic capacity of the plant, as Rubisco is a N-rich enzyme (Tjoelker et al., 1999). Under warming, plants may invest more in photosynthetic enzymes to maintain C gain, but this increase in photosynthetic capacity can lead to greater respiratory losses (Reich et al., 1998), partly linked to increased protein turnover rates and high metabolic rates. In my study, tamarack appear to prioritize maximizing C gains over minimizing C losses, and this allowed 8T seedlings to maintain similar growth to 0T trees.

Without thermal acclimation of respiration, shoots experienced greater respiratory losses under warming treatments. In contrast, the lack of a temperature effect on R_{root} measured under growth temperatures indicates that thermal acclimation led to homeostasis. Tjoelker et al. (1999) found thermal acclimation of root respiration resulted in lower root respiration rates than those predicted with instantaneous temperature response models in tamarack and other boreal conifer seedlings. Even with acclimation of both shoot and root respiration in their study, total daily respiratory losses for tamarack were still 14% higher in warming conditions than in cooler temperatures. Even in the best-case scenario

of homeostatic plant respiratory acclimation, plants still contend with respiratory losses and need thermal acclimation of photosynthesis to ensure a positive C balance in the future.

3.4.2 Performance and Biomass in Growth Treatments

While photosynthetic rates increased with the EC treatment, EC seedlings had similar biomass as AC trees, though EC did stimulate tree height. Similarly, while warming resulted in increased photosynthesis, it had little effect on growth. While enhanced C gain can stimulate growth, photosynthesis and growth are not always positively correlated. Increased photosynthesis may result in greater C availability, but there are limiting factors that determine how much of this C can be utilized for growth. Two of the main limiting factors on sink strength in growth chamber studies are nutrient availability and pot size (Kirschbaum, 2011). For plants with high photosynthetic rates, any limitation on nutrient availability, most often N, can dampen growth and the ability to build new tissues with available C due to stoichiometric imbalances. However, low nutrient availability is unlikely in my experiment as all plants were well fertilized. Small pots (defined as <10 L) can also be limiting for growth, specifically by reducing rooting potential (Drake, Gonzàlez-Meler, & Long, 1997; Kirschbaum, 2011). The pot size used in this experiment was ~11 L, thus higher biomass accumulation associated with higher A_{growth} in 8TEC seedlings may have been limited by root growth. In terms of C balance, growth is not the only sink for photosynthates: C is predominantly used for plant maintenance. Despite the fact that conifers are slow-growing, they have greater respiratory losses compared to broad-leaved trees (Wang & Curtis, 2002), and tamarack has been found to have higher total respiratory losses compared to other boreal conifers, e.g. *Picea mariana* and *Pinus banksiana* (Tjoelker et al., 1999). Given that I saw no thermal acclimation of respiration, higher C losses in the 8TEC seedlings most likely offset the higher photosynthetic rates observed with warming and EC, leading to similar total growth.

3.4.3 Differences Across Replicates

There were significant differences between replicates for almost all parameters that were measured. Arguably, the largest difference between the replicates was the drastic reduction in growth from replicate one to replicate two. While I cannot definitively determine what caused the replicate effect, a few non-mutually exclusive explanations are possible.

First, the difference may be related to soil moisture. The second replicate had 10-15% lower volumetric soil water content compared to the first replicate, which likely contributed to the lower $g_{s\text{-}growth}$ in the second replicate. While this may seem like a small difference in water availability, tamarack favours wetter sites and generally has low water use efficiency compared to other boreal conifers (Gower & Richards, 1990). Additionally, plants may have experienced some water stress due to higher VPD with warming despite the 40-45% volumetric soil water content in Chapter Two, therefore a 10-15% drop below that could be detrimental to growth. Plants can decrease g_s to conserve water, but lower g_s negatively impacts CO_2 assimilation and growth (Jones, 1998). The seedlings in replicate two did indeed have lower $g_{s\text{-}400}$ and $g_{s\text{-}growth}$ than the seedlings in replicate one, which supports this interpretation. Additionally, seedlings from replicate two also had a higher root/shoot ratio than those from replicate one. Allocation to larger root systems could be another response to low water availability (Van Den Boogaard, Alewijnse, Veneklaas, & Lambers, 1997). Larger roots also require greater construction costs and respiratory demands, such that the bigger root systems, combined with higher measured root respiration rates, in replicate two would have resulted in greater C losses and could have negatively impacted seedling growth.

Secondly, while growth chambers have many benefits for controlling abiotic factors, they do not produce truly uniform conditions and can introduce variability in experimental results (Porter, Evans-Fitz.Gerald, McElwain, Yiotis, & Elliott-Kingston, 2015; Weintraub, 2019). Porter et al. (2015) found that when using eight “identical” growth chambers, chamber effects resulted in significantly different rates of photosynthesis in 2/8 chambers, stomatal conductance in 1/8 chambers, and wet fresh weight in 3/8 chambers for *Vicia faba* (broad bean) plants, despite using identical CO_2, temperature,

humidity, and light settings. While the treatments in my experiment were rotated between the replicates to minimize chamber effects, the lights were variable between the chambers and were set at different heights to achieve a similar irradiance. Though I did not track irradiance in the chambers over the experiment, the light conditions may have deteriorated over time, reducing the irradiance available for growth in replicate two. The use of growth chambers therefore requires meticulous measurements of parameter settings, such as irradiance, throughout the experiment to account for any changes over time.

3.4.4 Conclusions

Thermal acclimation of photosynthesis, but no acclimation of respiration, resulted in similar foliar %C and growth across treatments. Photosynthetic acclimation was evident, as measured by changes in T_{opt} and A_{growth}. However, higher R_{shoot} under elevated temperatures may have limited growth in warm-grown tamarack seedlings, while homeostasis of R_{root} likely reduced overall total respiratory losses in warm-grown tamarack. Overall, tamarack was highly responsive to both warming and CO_2 in terms of photosynthetic performance and this may be an asset if water and nutrients are non-limiting under future climate change. The positive effects of increased growth temperature and CO_2 on photosynthetic rates and the thermal optima of tamarack seedlings may prove to be beneficial to the boreal forest's role in C sequestration if mature trees are able to maximize C uptake under global warming.

3.5 References

Ainsworth, E. A., & Long, S. P. (2005). What have we learned from 15 years of free-air CO_2 enrichment (FACE)? A meta-analytic review of the responses of photosynthesis, canopy properties and plant production to rising CO_2. *New Phytologist*, *165*(2), 351–372. https://doi.org/10.1111/j.1469-8137.2004.01224.x

Ainsworth, E. A., & Rogers, A. (2007). The response of photosynthesis and stomatal conductance to rising [CO_2]: Mechanisms and environmental interactions. *Plant, Cell and Environment*, *30*(3), 258–270. https://doi.org/10.1111/j.1365-3040.2007.01641.x

Albert, K. R., Mikkelsen, T. N., Michelsen, A., Ro-Poulsen, H., & van der Linden, L. (2011). Interactive effects of drought, elevated CO_2 and warming on photosynthetic capacity and photosystem performance in temperate heath plants. *Journal of Plant Physiology*, *168*(13), 1550–1561. https://doi.org/10.1016/j.jplph.2011.02.011

Amthor, J. S., Koch, G. W., Willms, J. R., & Layzell, D. B. (2001). Leaf O_2 uptake in the dark is independent of coincident CO_2 partial pressure. *Journal of Experimental Botany*, *52*(364), 2235–2238. https://doi.org/10.1093/jexbot/52.364.2235

Aranda, I., Cadahía, E., & Fernández de Simón, B. (2020). Leaf ecophysiological and metabolic response in *Quercus pyrenaica* Willd seedlings to moderate drought under enriched CO_2 atmosphere. *Journal of Plant Physiology*, *244*, 153083. https://doi.org/10.1016/j.jplph.2019.153083

Atkin, O. K., & Tjoelker, M. G. (2003). Thermal acclimation and the dynamic response of plant respiration to temperature. *Trends in Plant Science*, *8*(7), 343–351. https://doi.org/10.1016/S1360-1385(03)00136-5

Berry, J., & Bjorkman, O. (1980). Photosynthetic response and adaptation to temperature in higher plants. *Annual Review of Plant Physiology*, *31*(1), 491–543. https://doi.org/10.1146/annurev.pp.31.060180.002423

Chavan, S. G., Duursma, R. A., Tausz, M., & Ghannoum, O. (2019). Elevated CO_2 alleviates the negative impact of heat stress on wheat physiology but not on grain yield. *Journal of Experimental Botany*, *70*(21), 6447–6459. https://doi.org/10.1093/jxb/erz386

Crous, K.Y., Wallin, G., Atkin, O.K., Udding, J., & af Ekenstam, A. (2017) Acclimation of light and dark respiration to experimental and seasonal warming are mediated by changes in leaf nitrogen in *Eucalyptus globulus. Tree Physiology*, *37*(8), 1069-1083. https://doi.org/10.1093/treephys/tpx052

Drake, B. G., Gonzàlez-Meler, M. A., & Long, S. P. (1997). More efficient plants: a consequence of rising atmospheric CO_2? *Annual Review of Plant Physiology and Plant Molecular Biology*, *48*(1), 609–639. https://doi.org/10.1146/annurev.arplant.48.1.609

Dusenge, M. E. (2019). *Effects of elevated temperature and elevated CO_2 on leaf carbon fluxes in boreal conifers: lab and field studies* (Doctoral thesis, University of Western Ontario, Ontario, Canada). Retrieved from: https://ir.lib.uwo.ca/etd/6607

Dusenge, M. E., Duarte, A. G., & Way, D. A. (2019). Plant carbon metabolism and climate change: elevated CO_2 and temperature impacts on photosynthesis, photorespiration and respiration. *New Phytologist, 221*(1), 32-49. http://doi.org/10.1111/nph.15283

Dusenge, M. E., Madhavji, S., & Way, D. A. (2020). Contrasting acclimation responses to elevated CO_2 and warming between an evergreen and a deciduous boreal conifer. *Global Change Biology*. https://doi.org/10.1111/gcb.15084

Gauthier, S., Bernier, P., Kuuluvainen, T., Shvidenko, A. Z., & Schepaschenko, D. G. (2015). Boreal forest health and global change. *Science*, *349*(6250), 819–822. https://doi.org/10.1126/science.aaa9092

Ghannoum, O., Phillips, N. G., Sears, M. A., Logan, B. A., Lewis, J. D., Conroy, J. P., & Tissue, D. T. (2010). Photosynthetic responses of two eucalypts to industrial-age changes in atmospheric [CO_2] and temperature. *Plant, Cell and Environment*, *33*(10), 1671–1681. https://doi.org/10.1111/j.1365-3040.2010.02172.x

Gower, S. T., & Richards, J. H. (1990). Larches: Deciduous conifers in an evergreen world. *BioScience*, *40*(11), 818–826. https://doi.org/10.2307/1311484

IPCC. (2014). *Summary for Policy Makers*. *Climate Change 2014: Synthesis Report. Contribution of Working Groups I, II and III to the Fifth Assessment Report of the Intergovernmental Panel on Climate Change*. https://doi.org/10.1017/CBO9781107415324

Jones, H. G. (1998). Stomatal control of photosynthesis and transpiration. *Journal of Experimental Botany*, *49*, 387–398. https://doi.org/10.1093/jxb/49.special_issue.387

Kirschbaum, M. U. F. (2011). Does enhanced photosynthesis enhance growth? Lessons learned from CO_2 enrichment studies. *Plant Physiology*, *155*(1), 117–124. https://doi.org/10.1104/pp.110.166819

Kroner, Y., & Way, D. A. (2016). Carbon fluxes acclimate more strongly to elevated growth temperatures than to elevated CO_2 concentrations in a northern conifer. *Global Change Biology*, *22*(8), 2913–2928. https://doi.org/10.1111/gcb.13215

Leakey, A. D. B., Ainsworth, E. A., Bernacchi, C. J., Rogers, A., Long, S. P., & Ort, D. R. (2009). Elevated CO_2 effects on plant carbon, nitrogen, and water relations: Six important lessons from FACE. *Journal of Experimental Botany*, *60*(10), 2859–2876. https://doi.org/10.1093/jxb/erp096

Loveys, B. R., Atkinson, L. J., Sherlock, D. J., Roberts, R. L., Fitter, A. H., & Atkin, O. K. (2003). Thermal acclimation of leaf and root respiration: An investigation comparing inherently fast- and slow-growing plant species. *Global Change Biology*, *9*(6), 895–910. https://doi.org/10.1046/j.1365-2486.2003.00611.x

Medlyn, B. E., Barton, C. V. M., Broadmeadow, M. S. J., Ceulemans, R., De Angelis, P., Forstreuter, M., … Jarvis, P. G. (2001). Stomatal conductance of forest species after long-term exposure to elevated CO_2 concentration: A synthesis. *New Phytologist*, *149*(2), 247–264. https://doi.org/10.1046/j.1469-8137.2001.00028.x

Moore, B. D., Cheng, S. H., Sims, D., & Seemann, J. R. (1999). The biochemical and molecular basis for photosynthetic acclimation to elevated atmospheric CO_2. *Plant, Cell and Environment, 22*(6), 567–582. https://doi.org/10.1046/j.1365-3040.1999.00432.x

Oppenheimer, M., Campos, M., Warren, R., Birkmann, J., Luber, G., O'Neill, B. C., & Takahashi, K. (2014). Emergent risks and key vulnerabilities. In C. B. Field, V. R. Barros, D. J. Dokken, K. J. Mach, M. D. Mastrandrea, T. E. Bilir, … L. L. White (Eds.), *Climate Change 2014: Impacts, Adaptation, and Vulnerability. Part A: Global and Sectoral Aspects. Contribution of Working Group II to the Fifth Assessment Report of the Intergovernmental Panel of Climate Change* (pp. 1039–1099). Cambridge, United Kingdom and New York, NY, USA: Cambridge University Press.

Pan, Y., Birdsey, R. A., Fang, J., Houghton, R. A., Kauppi, P. E., Kurz, W. A., … Hayes, D. (2011). A large and persistent carbon sink in the world's forest. *Science, 333*(6045), 988–993. https://doi.org/10.1126/science.1201609

Pinheiro, J., Bates, D., DebRoy, S., Sarkar, D., R Core Team (2019). Nlme: Linear and nonlinear mixed effects models. R Package Version 3.1-141

Porter, A. S., Evans-Fitz.Gerald, C., McElwain, J. C., Yiotis, C., & Elliott-Kingston, C. (2015). How well do you know your growth chambers? Testing for chamber effect using plant traits. *Plant Methods, 11*(1), 1–10. https://doi.org/10.1186/s13007-015-0088-0

Reich, P. B., Oleksyn, J., & Wright, I. (2009) Leaf phosphorus influences the photosynthesis-nitrogen relation: A cross-biome analysis of 314 species. *Oecologia,* 160(2), 207-212. https://doi.org/10.1007/s00442-009-1291-3

Reich, P. B., Walters, M. B., Ellsworth, D. S., Vose, J. M., John, C., Gresham, C., & Bowman, W. D. (1998). Relationships of leaf dark respiration to leaf nitrogen, specific leaf area and leaf life-span: A test across biomes and functional groups. *Oecologia, 114*(4), 471–482. https://doi.org/10.1007/s004420050471

Sage, R. F., & Kubien, D. S. (2007). The temperature response of C_3 and C_4 photosynthesis. *Plant, Cell and Environment, 30*(9), 1086–1106. https://doi.org/10.1111/j.1365-3040.2007.01682.x

Serreze, M. C., Walsh, J. E., Chapin, F. S. I., Osterkamp, T., Dyurgerov, M., Romanovsky, V., … Barry, R. G. (2000). Observational evidence of recent change in the northern high-latitude environment. *Climatic Change, 46*(1–2), 159–207. https://doi.org/10.1023/A:1005504031923

Slot, M., & Kitajima, K. (2015). General patterns of acclimation of leaf respiration to elevated temperatures across biomes and plant types. *Oecologia, 177*(3), 885–900. https://doi.org/10.1007/s00442-014-3159-4

Tjoelker, M. G., Oleksyn, J., & Reich, P. B. (1998). Seedlings of five boreal tree species differ in acclimation of net photosynthesis to elevated CO_2 and temperature. *Tree Physiology, 18,* 715–716. https://doi.org/10.1093/treephys/18.11.715

Tjoelker, M. G., Oleksyn, J., & Reich, P. (1999a). Acclimation of respiration to temperature and CO_2 in seedlings of boreal tree species in relation to plant size and relative growth rate. *Global Change Biology*, *49*(6), 679–691. https://doi.org/10.1046/j.1365-2486.1999.00257.x

Tjoelker, M. G., Reich, P. B., & Oleksyn, J. (1999b). Changes in leaf nitrogen and carbohydrates underlie temperature and CO_2 acclimation of dark respiration in five boreal tree species. *Plant, Cell and Environment*, *22*(7), 767–778. https://doi.org/10.1046/j.1365-3040.1999.00435.x

Van Den Boogaard, R., Alewijnse, D., Veneklaas, E. J., & Lambers, H. (1997). Growth and water-use efficiency of 10 *Triticum aestivum* cultivars at different water availability in relation to allocation of biomass. *Plant, Cell and Environment*, *20*(2), 200–210. https://doi.org/10.1046/j.1365-3040.1997.d01-60.x

Wang, X., & Curtis, P. (2002). A meta-analytical test of elevated CO_2 effects on plant respiration. *Plant Ecology, 161*(2), 251–261. https://doi.org/10.1023/A:1020305006949

Way, D. A., & Sage, R. F. (2008). Elevated growth temperatures reduce the carbon gain of black spruce [*Picea mariana* (Mill.) B.S.P.]. *Global Change Biology, 14*(3), 624–636. https://doi.org/10.1111/j.1365-2486.2007.01513.x

Way, D. A., Sage, R. F., & Kubien, D. S. (2008). Rubisco, Rubisco activase, and global climate change. *Journal of Experimental Botany*, *59*(7), 1581–1595. https://doi.org/10.1093/jxb/ern053

Way, D. A., & Yamori, W. (2014). Thermal acclimation of photosynthesis: On the importance of adjusting our definitions and accounting for thermal acclimation of respiration. *Photosynthesis Research*, *119*(1–2), 89–100. https://doi.org/10.1007/s11120-013-9873-7

Weintraub, P. G. (2019). Growth chamber data should not be used to predict invasive *liriomyza huidobrensis* (Diptera: Agromyzidae) establishment. *Environmental Entomology*, *48*(2), 271–273. https://doi.org/10.1093/ee/nvz003

Wickhan, H. (2017) Tidyverse: Easily install and load the ‘tidyverse’. R Package Version 1.2.1

Yamori, W., Hikosaka, K., & Way, D. A. (2014). Temperature response of photosynthesis in C_3, C_4, and CAM plants: Temperature acclimation and temperature adaptation. *Photosynthesis Research*, *119*(1–2), 101–117. https://doi.org/10.1007/s11120-013-9874-6

Zeng, N., Zhao, F., Collatz, G. J., Kalnay, E., Salawitch, R. J., West, T. O., & Guanter, L. (2014). Agricultural Green Revolution as a driver of increasing atmospheric CO_2 seasonal amplitude. *Nature*, *515*(7527), 394–397. https://doi.org/10.1038/nature13893

Chapter 4

4 General Discussion

4.1 Glasshouse vs. Growth Chamber

The goal of my thesis was to investigate the cause of mortality of tamarack seedlings under +8 ˚C warming paired with ambient CO_2 (8TAC), as originally found by Dusenge et al. (2020). Similar to the original experiment, tamarack grown from seed in glasshouses displayed high mortality in the 8TAC treatment. High mortality in 8TAC seedlings correlated with lower needle C concentrations and decreased ratios of A_{net}/R_{dark}. I designed a growth chamber experiment as a follow-up to measure a greater number of dying seedlings at a standardized health rating, but no seedlings died. Overall, the contrasting acclimation responses of photosynthesis and respiration of tamarack seedlings led to different leaf C dynamics, growth and mortality across the two experimental designs.

Despite similar potting, fertilization, and water regimes, the glasshouse seedlings (Chapter Two) and growth chamber seedlings (Chapter Three) had vastly different acclimation responses to +8 ˚C warming with and without CO_2 enrichment. Glasshouse seedlings had thermal acclimation of respiration, but no response to temperature or CO_2 measured via photosynthetic parameters, whereas growth chamber seedlings displayed thermal acclimation of photosynthesis, but no response of respiration to temperature. While the growth chamber experiment did have large differences between replicates, the directions of the treatment effects were consistent between replicate one and two. Arguably the largest difference was that 8TAC seedlings had 40% mortality in glasshouses compared to 0% mortality in growth chambers. While there was no mortality in the growth chambers, there were symptoms of stress in +8 ˚C warming seedlings, similar to the stress observed in the glasshouses (Figure 4.1). Some growth chamber 8TAC and 8TEC seedlings displayed needle browning; however, this browning never reached 100% of the leaf tissue as it did in the glasshouse experiment. Unique to the growth chamber seedlings was the visible needle curling that occurred in the larger plants. Needle or leaf curling is a phenomenon that has been observed in plants

experiencing environmental stress, such as low water and high salinity (Bussotti, Bottacci, Bartolesi, Grossoni, & Tani, 1995; Pääkkönen, Vahala, Pohjolal, Holopainen, & Kärenlampi, 1998; Stone, 1993). Studies by Stone (1993) found that needle curling in *Pinus taeda* (loblolly pine) seedlings experiencing low soil moisture from minimal watering, but similar stress occurs under high VPD from extreme warming treatments. Interestingly, Stone (1993) found the needle curling was not detrimental to growth nor did it lead to mortality. As the seedlings in growth chambers were well-watered, needle curling was most likely caused by some combination of high VPD and heat stress, as relative humidity was maintained at 60% despite the higher temperatures in +8 ˚C.

The seedlings in the glasshouses experienced natural light variation and changing photoperiods over the summer. Comparatively, the seedlings in the growth chambers experienced a lower light intensity of 300 μmol photons m^{-2} s^{-1} for 14 h photoperiods. High light can impose additional stress on plants and may help to explain the differences in C stress and mortality observed between the two experiments. Seedlings in the glasshouse would have experienced irradiance of up to 2000 μmol photons m^{-2} s^{-1} on sunny days, which would have put them at greater risk of photoinhibition. Photoinhibition occurs when there is a reduction of photosynthetic activity due to light-induced decreases in CO_2 assimilation caused by rapid saturation, and eventual closure, of photosynthetic reaction centers (Muller, Li, & Niyogi, 2001). To avoid photoinhibition, plants will employ photoprotective measures such as the use of non-photochemical quenching, which dissipates excess absorbed light as heat (Gilmore, 2006). Unfortunately, non-photochemical quenching increases leaf temperatures and thus can further heat stress plants (Kulasek et al., 2016). Glasshouse seedlings also likely experienced higher leaf temperatures and thus heat stress compared to the growth chamber seedlings due to the higher light intensity and the greater radiative heat load this imposes on leaves, despite experiencing similar air temperatures. Overall, seedlings clearly experienced greater climatic stress under more ecologically relevant light conditions.

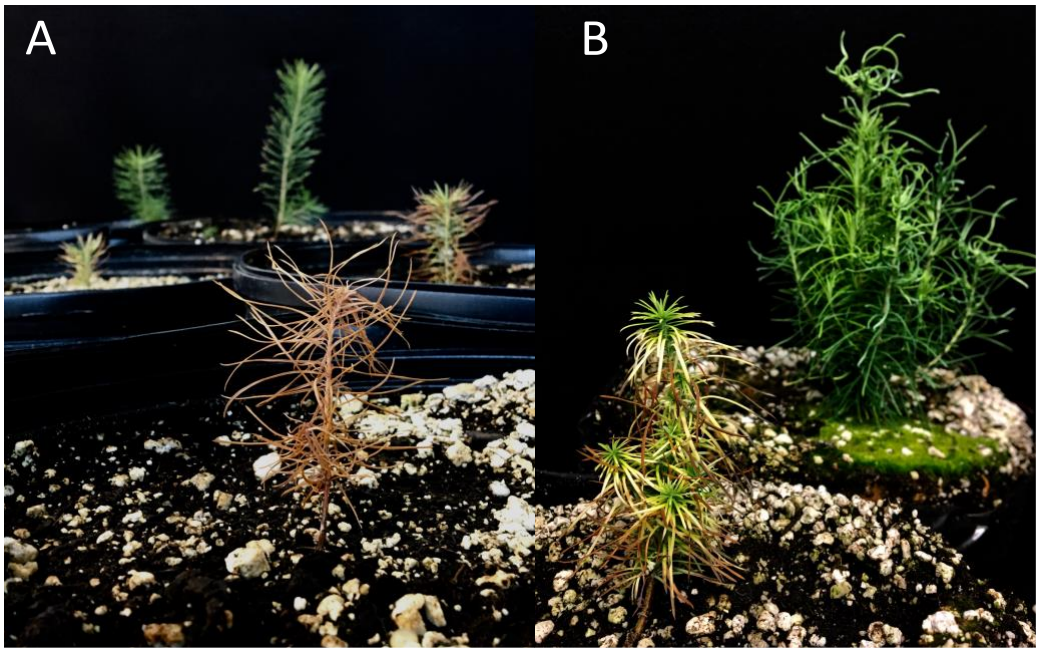

Figure 4.1. Comparative symptoms of stress in tamarack seedlings under +8 ˚C warming. A) Glasshouse experiment and B) growth chamber experiment. Browning of the tissue is indicative of necrotic tissue, whereas needle curling is often related to water and salinity stress.

4.2 Ecological Relevance of Experimental Designs

The experimental designs used in this thesis exposed seedlings to different temperature and light environments. The environmental conditions in the glasshouse experiment were much more similar to what boreal conifers experience in the field. Ironically, the main limitation of the glasshouse experimental design is that seedlings did not experience other environmental conditions that can induce sink limitations in nature—i.e., low nitrogen or water availability.

Free air CO_2 enrichment (FACE) and free air temperature enhancement (FATE) studies are considered the highest calibre of experimental design for climate change as they study plants in their natural environment but supplemented with CO_2 and warming. The second-best approach is to use open top chambers in the field, so that plants experience natural soils, climate and biotic interactions while the treatment is applied. The best evidence that my glasshouse experiments are more ecologically relevant than my growth

chamber experiments is that many of the results from the glasshouse-grown tamarack seedlings have also been found in mature tamarack grown at the SPRUCE (Spruce and Peatland Responses Under Changing Environments) experiment (Figure 4.2; Dusenge, 2019). The SPRUCE experiment is a whole-ecosystem warming experiment in a boreal forest peatland in Minnesota that is comprised of 10 octagonal open-top enclosures with warming of up to 9 ˚C and CO_2 enrichment up to 750 ppm. The enclosures were built around the existing plant community, which included mature tamarack and black spruce trees and four shrub species. Dusenge et al. (2019) measured the C fluxes of large, mature tamarack under warming and CO_2 enrichment treatments in these open-top enclosures. Similar to my glasshouse work, Dusenge et al. (2019) found a lack of photosynthetic acclimation, measured as no change in A_{25} and $g_{s\text{-}25}$ resulted in similar A_{growth} across the different growth temperatures, and also found that EC stimulated A_{growth}. Despite finding no acclimation of respiration to warming (in contrast to my results here), the tamarack at the SPRUCE site still had similar R_{growth} across the treatments, as did my glasshouse seedlings. The most notable difference between my findings and Dusenge et al. (2019) was that growth of mature trees was unaffected by warming. Mature trees have greater C stores than seedlings (Dietze et al., 2014) and would not experience the same C stress after one year of warming as the seedlings in the glasshouses did after being grown their entire life at high temperatures, which could explain the difference in growth patterns under +8 ˚C warming. Comparatively, growth chamber seedlings displayed photosynthetic acclimation to both warming and CO_2, but no acclimation of shoot respiration. The contrasting acclimation responses of photosynthesis and respiration to growth chamber conditions resulted in both higher carbon gains and losses with warming, and similar growth across all treatments. Overall, leaf C balances between seedlings grown in glasshouses were more similar than those from the growth chambers to the mature tamarack studied at SPRUCE, providing strong evidence that the glasshouse work produced ecologically relevant data.

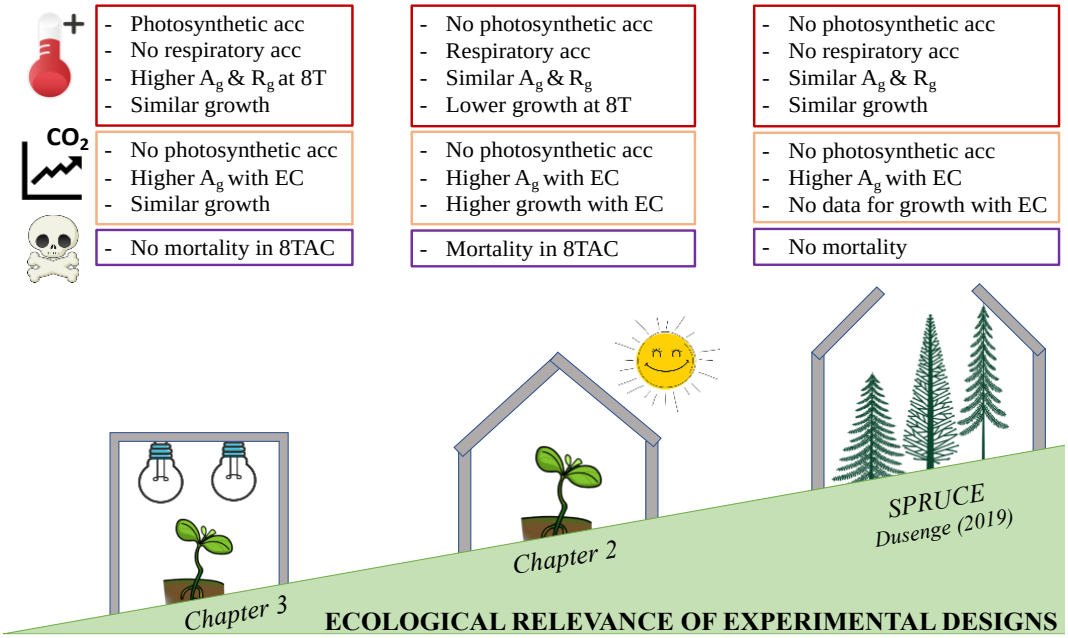

Figure 4.2. The ecological relevance of different experimental designs: growth chambers, glasshouses, and open top chambers. The responses of C fluxes and growth to warming and CO_2 in tamarack in Chapter 2 (using glasshouses) were more similar than those from Chapter 3 (using growth chambers) to the work by Dusenge (2019) (using open top chambers at the SPRUCE site). Acclimation, acc; net photosynthetic rates measured at growth conditions, A_g; respiration rates measured at growth conditions, R_g; +8˚C warming, 8T; elevated CO_2, EC; Spruce and Peatland Responses Under Changing Environments, SPRUCE.

4.3 Future Directions

My glasshouse work was novel in examining C starvation under natural light conditions and in the absence of water stress; however, there is still much to learn about how tamarack, along with other boreal conifers, will respond to climate change in terms of mortality. One important consideration is that while growth temperatures will increase gradually over time, extreme heat events will also become more frequent and trees could experience acute heat stress on top of moderate warming (Della-Marta et al., 2007). Studying the response of seedlings to both acute heat stress and more gradual warming in a laboratory setting could be beneficial in understanding plant C balance and thermotolerance without the confounding factors of water stress and competition. On the

other hand, studying seedlings in the field allows for a more realistic interpretation of results as these seedlings are experiencing conditions associated with natural boreal soils and variable precipitation, on top of heat stress. Whether in a lab or in a field, a molecular approach to studying heat stress (such as quantification of heat stress proteins and protective phytohormones), in addition to physiological measurements, may help us understand species-specific thermotolerance and ultimately why some conifer species survive, and some species die, under similar climatic stress.

While I studied seedlings from a single population, there is also genetic variation across populations within a species. Genetic variation can determine the vulnerability of populations from different geographic origins to similar abiotic stress (Badyaev, 2005). This will be important in the future as differential warming will occur, with high latitudes projected to see the most severe warming (IPCC, 2014; Serreze et al., 2000). While population variation in tamarack in response to drought or heat stress has not been well studied, mature white spruce (*Picea glauca*) has increased resilience to drought in populations from drier geographical locations compared to those from more humid locations (Depardieu et al., 2020). In my thesis, a population of tamarack from southern latitudes in Canada were subjected to ambient +8 ˚C warming. In reality, it is much more likely that northern populations will experience such extreme warming. As northern populations generally experience cooler annual temperatures compared to southern populations, they may lack the necessary adaptations associated with thermotolerance and drought stress resilience and may be at a greater risk of mortality. Alternatively, this extreme warming may be well within their ability to acclimate to, given that their thermal regime is much cooler than that of London, ON. Adaptive genetic variation could be a strong determinant for survival and therefore it would be useful to compare the responses of different tamarack genotypes to warming and CO_2 in the future.

Abiotic stress increases plant susceptibility to insect outbreaks and forest fires, which is most often the final cause of death in mature trees (Adams et al., 2017). Hydraulic failure and C starvation prevent the production and translocation of carbohydrates necessary for plant defence against biotic attacks (Allen et al., 2010). Hydraulic failure also results in tissue desiccation, providing more flammable fuel for forest fires, which have become

more frequent with climate change (Westerling, Hidalgo, Cayan, & Swetnam, 2006). It is also important to consider the vulnerability of different boreal conifers to biotic stress and how community composition may be affected in the future. Tamarack is easily killed by fire but is not considered to be at high risk from forest fires because it preferentially inhabits wetter areas of the boreal region, such as bogs and peatlands, where hydraulic failure is less common (Gower & Richards, 1990). However, tamarack is already experiencing defoliation by the larch casebearer (*Coleophora laricella)* and this could worsen with climate change if mature trees undergo similar C stress as the seedlings in the glasshouse experiment and are unable to synthesize and transport defence compounds such as those found in resin (Habermann, 2000).

4.4 Conclusions

Outside of the work by Dusenge (2019), there is little known about the acclimation responses of C fluxes in mature tamarack to climate change drivers. Based on dendrochronological analyses, tamarack has experienced enhanced radial and vertical growth since the 1990s, associated with warming (Dufour-Tremblay, Lévesque, & Boudreau, 2012). Tamarack appears to be phenotypically plastic to environmental changes, such that moderate warming may be advantageous for the growth of mature trees. Based on the assumption that the glasshouse experimental work is of greater ecological relevance than the growth chamber work, tamarack will likely have stronger acclimation of respiration than photosynthesis and will minimize C losses associated with warming in the future. Photosynthetic rates in conifers are highly responsive to elevated CO_2 (Ainsworth & Long, 2005) and work thus far, including my own, on tamarack supports this finding (Dusenge, 2019; Dusenge et al., 2020). With that in mind, C gain associated with future elevated CO_2 will likely offset any C stress caused solely by moderate warming, unless increased temperatures are driven by other, more potent greenhouse gases like methane. The greater likelihood is that mortality in mature conifers will be caused by water stress and associated C limitations imposed by decreased stomatal conductance or the extreme temperature increases predicted for the end of this century.

4.5 References

Adams, H. D., Zeppel, M. J. B., Anderegg, W. R. L., Hartmann, H., Landhäusser, S. M., Tissue, D. T., … McDowell, N. G. (2017). A multi-species synthesis of physiological mechanisms in drought-induced tree mortality. *Nature Ecology and Evolution*, *1*(9), 1285–1291. https://doi.org/10.1038/s41559-017-0248-x

Allen, C. D., Macalady, A. K., Chenchouni, H., Bachelet, D., McDowell, N., Vennetier, M., … Cobb, N. (2010). A global overview of drought and heat-induced tree mortality reveals emerging climate change risks for forests. *Forest Ecology and Management*, *259*(4), 660–684. https://doi.org/10.1016/j.foreco.2009.09.001

Ainsworth, E. A., & Long, S. P. (2005). What have we learned from 15 years of free-air CO_2 enrichment (FACE)? A meta-analytic review of the responses of photosynthesis, canopy properties and plant production to rising CO_2. *New Phytologist*, *165*(2), 351–372. https://doi.org/10.1111/j.1469-8137.2004.01224.x

Badyaev, A. V. (2005). Stress-induced variation in evolution: from behavioural plasticity to genetic assimilation. *Proceedings of the Royal Society Biological Sciences*, *272*, 877–886. https://doi.org/1098/rspb.2004.3045

Bussotti, F., Bottacci, A., Bartolesi, A., Grossoni, P., & Tani, C. (1995). Morpho-anatomical alterations in leaves collected from beech trees (*Fagus sylvatica L.*) in conditions of natural water stress. *Environmental and Experimental Botany*, *35*(2), 201–213. https://doi.org/10.1016/0098-8472(94)00040-C

Della-Marta, P. M., Haylock, M. R., Luterbacher, J., and Wanner, H. (2007). Doubled length of western European summer heat waves since 1880. *Journal of Geophysical Research, 25*, 369-375.

Depardieu, C., Girardin, M. P., Nadeau, S., Lenz, P., Bousquet, J., & Isabel, N. (2020). Adaptive genetic variation to drought in a widely distributed conifer suggests a potential for increasing forest resilience in a drying climate. *New Phytologist.* https://doi.org/10.1111/nph.16551

Dietze, M. C., Sala, A., Carbone, M. S., Czimczik, C. I., Mantooth, J. A., Richardson, A. D., & Vargas, R. (2014). Nonstructural carbon in woody plants. *Annual Review of Plant Biology*, *65*(1), 667–687. https://doi.org/10.1146/annurev-arplant-050213-040054

Dufour-Tremblay, G., Lévesque, E., & Boudreau, S. (2012). Dynamics at the treeline: Differential responses of *Picea mariana* and *Larix laricina* to climate change in eastern subarctic Québec. *Environmental Research Letters*, *7*(4). https://doi.org/10.1088/1748-9326/7/4/044038

Dusenge, M. E., Madhavji, S., & Way, D. A. (2020). Contrasting acclimation responses to elevated CO_2 and warming between an evergreen and a deciduous boreal conifer. *Global Change Biology.* https://doi.org/10.1111/gcb.15084

Dusenge, M. E. (2019). *Effects of elevated temperature and elevated CO_2 on leaf carbon fluxes in boreal conifers: lab and field studies* (Doctoral thesis, University of Western Ontario, Ontario, Canada). Retrieved from: https://ir.lib.uwo.ca/etd/6607

Gilmore, A. M. (2006). Mechanistic aspects of the xanophyll cycle-dependent photoprotection in higher plant chloroplasts and leaves. *Physiologia Plantarum, 99*(1), 197-209.

Gower, S. T., & Richards, J. H. (1990). Larches: Deciduous conifers in an evergreen world. *BioScience, 40*(11), 818–826. https://doi.org/10.2307/1311484

Habermann, M. (2000). The larch casebearer and its host tree: II. Changes in needle physiology of the infested trees, *136*, 23–34. https://doi.org/10.1016/S0378-1127(99)00267-4

IPCC. (2014). *Summary for Policy Makers*. *Climate Change 2014: Synthesis Report. Contribution of Working Groups I, II and III to the Fifth Assessment Report of the Intergovernmental Panel on Climate Change*. https://doi.org/10.1017/CBO9781107415324

Kulasek, M., Bernacki, M. J., Ciszak, K., Witon, K., & Karpinski, S. (2016). Contribution of PsbS function and stomatal conductance to foliar temperature in higher plants. *Plant and Cell Physiology, 57(*7), 1495–1509. https://doi.org/10.1093/pcp/pcw083

Muller, P., Li, X., & Niyogi, K. K. (2001). Non-photochemical quenching: A response to excess light energy. *Plant Physiology, 125*, 1558–1566. https://doi.org/10.1104/pp.125.4.1558

Pääkkönen, E., Vahala, J., Pohjolal, M., Holopainen, T., & Kärenlampi, L. (1998). Physiological, stomatal and ultrastructural ozone responses in birch (*Betula pendula* Roth.) are modified by water stress. *Plant, Cell and Environment, 21*(7), 671–684.

Serreze, M. C., Walsh, J. E., Chapin, F. S. I., Osterkamp, T., Dyurgerov, M., Romanovsky, V., … Barry, R. G. (2000). Observational evidence of recent change in the northern high-latitude environment. *Climatic Change, 46*(1–2), 159–207. https://doi.org/10.1023/A:1005504031923

Stone, D. M. (1993). Curly needle syndrome of loblolly pine seedlings. *Canadian Journal of Forest Research, 23*, 1810–1814.

Westerling, A. L., Hidalgo, H. G., Cayan, D. R., & Swetnam, T. W. (2005). Warming and earlier spring increase Western U.S. forest wildfire activity. *Science, 313(*5789), 940–943.

Curriculum Vitae

Name: Bridget Kathleen Murphy

Post-secondary Education and Degrees:
University of Western Ontario
London, Ontario, Canada
2013-2017 Hons. B.Sc.

Honours and Awards:

Faculty of Arts and Science Top Doctoral Fellowship at the University of Toronto
2020

Queen Elizabeth II Graduate Scholarship for Science and Technology
2018-2019

Global Award Winner of Earth and Environmental Science Category of the Undergraduate Awards
2017

Florence Bucke Graduate Scholarship Award from the University of Western Ontario
2017

NSERC Undergraduate Student Research Award
2017

Dean's Honors List
2014, 2016, 2017

Christina A. MacKerracher Admission Scholarship
2013

Related Work Experience
Teaching Assistant
University of Western Ontario
2017-2020

Publications:

Murphy BK and Stinziano JR. (in review). A derivation error exists in the current implantation of the Johnson et al. (1942) modified Arrhenius function that affects leaf carbon balance models

- Pre-print manuscript ID# BIORXIV/2020/921973